STUDIES

OF THE UNIVERSITY OF ŽILINA

Volume 27 Number 1

March 2015

MATHEMATICAL SERIES

Editorial Board

Studies of the University of Žilina • Mathematical series
Faculty of Operation and Economics of Transport and Communications, University of Žilina, Univerzitná 1, 010 26 Žilina, Slovakia
phone: +42141 5133250, fax: +42141 5651499, e-mail: studies@fpedas.uniza.sk,
electronic edition: `http://fpedas.uniza.sk` or `http://frcatel.fri.uniza.sk/studies`
Typeset using LaTeX, Printed by: EDIS – Žilina University publisher

ISSN 1336–149X

Editorial

The subject of the papers in the present issue is geometry, and the guiding principle in them is visualization. The authors present their results either in theory or application or education by illustrating them with well designed figures in order to help the reader to understand also the abstract ideas.

In the theory of non-Euclidean and higher dimensional geometry visualization is based on an appropriate model, in which the reader can rely on his or her understanding of three dimensional Euclidean space. That helps to imagine the abstract structures. In the applications everyday objects are shown in order to illustrate the ideas of the authors about the presented subject. Visualization has a particularly important role in education either in geometry or in other fields of science. It is not only a technique in the presentation of disciplines, but also the task of the teaching process. Electronic teaching materials help to develop the ability of the students in spatial imagination and thinking. The authors dealing with education show a rich collection of the used techniques and a number of nice examples from their teaching material.

These articles were presented at the conference held in October 21–22, 2014 in Sopron, Hungary with the title “Visual methods in engineer and teacher education in science”. The conference and the printing of this issue was supported by the International Visegrad Fund Small Grants No. 11420082. We thank for this financial support and also the authors for their cooperation in editing this issue.

Visegrad Fund
www.visegradfund.org

Guest Editors
M. Szilvási-Nagy and J. Szirmai

Studies of the University of Žilina
Mathematical Series
Vol. 27/2015, 3–10

EXPERIENCES IN THE DEVELOPMENT OF DIGITAL LEARNING ENVIRONMENT

A. BÖLCSKEI and J. KATONA

Abstract. In this article our experiences on the development and usage of some e-learning materials are reported. We formulate seven statements about the requirements a useful digital content should fulfil.

Introduction

Usually it is difficult to predict the success of a movie or a book. It is also often the case that the critics and the public have basically different opinion about the same artworks. Similarly, it is also difficult to estimate the acceptance of a textbook or an e-learning content among students and teachers.

In this article our experiences on the development and usage of some e-learning materials are reported. We formulate seven statements about the requirements a useful digital content should fulfil. However, we are aware that no curriculum can be universal and can be optimal for all types of learners. The statements therefore characterize such learning environments that may be suitable for the vast majority of students. (For exact proof of the above instructions a comparative survey would be necessary. Till that our comments may be better called conjectures or experiences.)

The digital contents we developed were related to the subjects "Descriptive Geometry" and "Information Technology for Engineers", both for engineer students. However, these teaching materials not only provided specialized knowledge, but aimed also general goals, such as the development of spatial abilities. The statements in this article are general. We hope that our experiences will be useful not only in teaching geometry and 3D modeling, but also in teaching mathematics and information technology.

Received December 22, 2014.
2000 *Mathematics Subject Classification.* Primary 97C50, 97D20, 97C80; Secondary 97U50, 97U70, 97U80.
Key words and phrases. spatial ability, e-learning, maths didactics.
This work was supported by the Visegrad Fund, small grant 11420082.

1. Background

The main motivation for our development was provided by the experienced difficulties of teaching and illustrating the traditional descriptive geometry and 3D geometric modeling. If a figure with the complete construction is given, then the consecutive steps are hardly seen and difficult to follow, the description however is long and wordy:

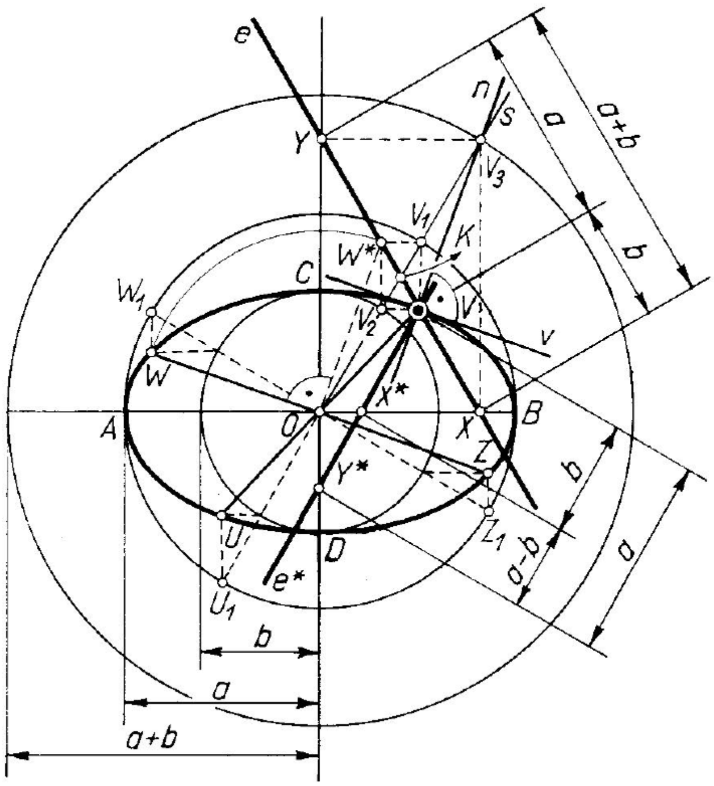

Figure 1. Rytz's construction from the book Szabó Ferdinánd: Műszaki Ábrázolás II. Győr, 2006, p. 17.

Considering the figure it is not easy to see what was given initially, what is the final result, and what are the consecutive steps leading to the result. To avoid this problem we made sequences of figures, animations and movies for each teaching material that showed the process of construction step by step.

A further advantage of e-learning materials is that we can add interactive 3D models to them. This greatly facilitates the understanding that can otherwise be similarly effective giving specific models in hands. The relationship between the spatial position and the views becomes understandable in virtual space. In this respect the change of viewpoints, moving, rotating the models and to vary the display modes (changing the rendering, the transparency of bodies; using lights and shadows) play a big role. In addition to these advantages many other benefits of e-learning materials will be given in Chapter 2.

1.1. Specifics

Motivated by the difficulties listed in the previous paragraph, in the past 10 years, we developed several digital learning materials at the Szent István University, Ybl Miklós Faculty of Architecture and Civil Engineering. These all were criticized by reviewers and our colleagues. Based on the feedbacks we revised the materials. The products are repeatedly used in the education and their effects were investigated [12, 13, 14, 15].

Among the teaching materials there were plain text files, charts and tables. These were used for setting the tasks, for example, or to summarize, systematize things, also make reminders. It was important to provide the easy distribution, and the colorful and aesthetic appearance of the documents.

Another well-known type of electronic learning materials is the presentation. This can be considered as a complete curriculum. Its application is vulgar, we also took some advantages, e.g. animated images, videos, and links were inserted. Beside all that we created interactive web sites, and a large amount of teaching videos. These videos can be considered as successors of the previously used educational films. Compared to them our videos are much easier to handle, think on the storage, sharing, playback, etc. From the teacher's point of view it has great advantages too, because it is easier to update, to reconstruct and to correct the errors.

We collected also the students' feedback. These were the following: spontaneous conversations, interviews (with 12 students), specific questionnaires (the number of subjects were 106). In addition, we asked the students about a possible continuation of the content. We conducted a comparative educational survey with app. 50 subjects, where the progress of those 25 who used the digital content was referred to the control group of 25 people.

Based on all that we formulated the requirements of an „ideal" digital teaching content. Our own developments do not fulfil all the criteria, they will be taken into account in the next revision.

2. Comparison of paper-based and digital learning materials

The computer is a versatile, universal tool. Using this excellent machine, however, does not mean automatically that any digital curriculum has good quality. It could even be said that despite the widened possibilities, there are much more way to slip up.

Consequently, there is a unity in the literature, that it is not enough to digitize the traditional curriculum [1, 2, 3], and that we need the same basic principles in the development of e-learning materials as for the traditional curricula. We have to try for being visual; to show the hidden connections, to connect to precognition, and we must stabilize what the students learned, by repetitions and exercises [4, 11].

A possible model for the progress of the development of digital learning materials is shown below:

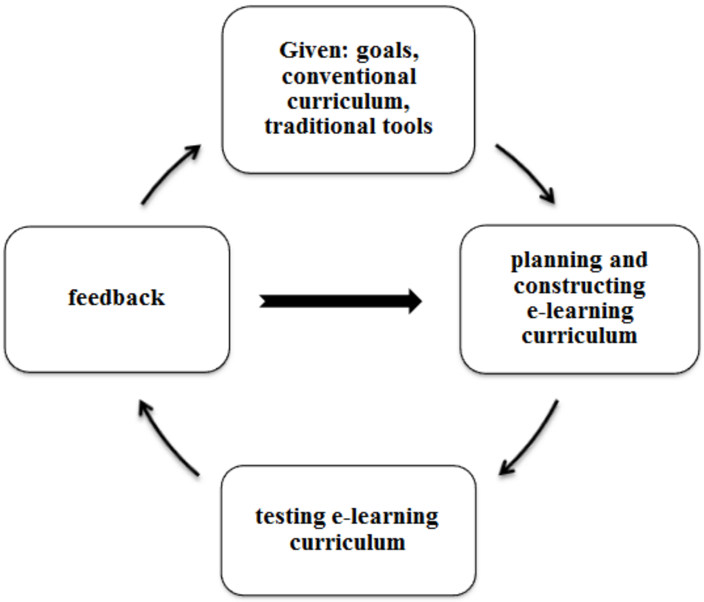

Figure 2. Model for the progress of the development of digital learning materials.

The aims of teaching and traditional instruments are considered to be given. The development of digital curriculum is based also on them. The completed digital contents will be then reviewed, published and tried out. Then the feedback comes: based on experiences one can change the targets; or what much more often happens: we revise the digital curriculum. Curriculum published in electronic form has a huge advantage in this regard: it can be changed much easier and faster. The teacher may open the source file every time, can modify (for example, correct typos, add a paragraph, update, etc,) and upload to the Internet. The students download the best possible version all the time.

A further advantage of e-learning contents is the usage of multimedia materials, space-saving storage and easy sharing. However, the computer can not be used only as content provider. It allows you to experiment with, for example, you can run your simulation models. It may improve the appearance of our work, or the accuracy of our constructions and planes. In the digital learning environment, using social networks permit cooperative learning [5, 6]; and interactive test. The teacher can generate thousands of similar problems by computer [7].

The downside of digital learning materials is addiction on technology, lack of manual activities and the decline of personal pedagogical influence. For all these reasons do not use it instead of the traditional tools, but parallel to them.

3. Students' criteria

Based on the feedback mentioned in Section 1.1, students set the following seven characteristics for a good curriculum. The requirements we have to meet are then:

3.1. Digital

It seems that all students can come at a computer with Internet access. Registration to the university networks, as e.g. applications for exams; information about the description and requirements of subjects, homework; sharing teaching materials and other information – these happen all electronically nowadays. It does not cause any problem for the students to submit their tasks digitally. They can install without a problem even such resource-intensive softwares as CAD systems. We can conclude, therefore, that there are no fundamental technical barriers.

The computer and the media lost their motivation effect, it is obvious for the students to use the computer for learning. However, digital learning materials are expected, because they do not want to carry paper-based media, whose purchase, storage and sharing is more difficult.

3.2. Free for the students

There is probably no need to justify it long. The social status of many students does not allow purchasing expensive books. Besides, many of the students download films and music for free, they are not willing to give money for any textbook. (We should add that the majority of free films, music and teaching material are legal. But we know that there exist and spread the black, but at least the gray copies, too.) Free electronic contents may refer to works published by other authors, a simple link can point to external materials.

If a curriculum is free of charge for the students, it does not imply that the extra work of the authors can not be rewarded. There are examples that in this case the author is paid by the higher education institution from public or private project resources. Since the author receives the money independently from the number of copies sold; therefore the higher education institution, the tenderer and the referees are responsible for the quality.

3.3. Full but moderate

The students do not like to collect the necessary knowledge from many sources. The information collected from several locations may not be uniform concerning notions, level and order. In addition, the students also often complain, if the selected bibliography is deeper and want to teach them more. Many students seek after the minimum, and reject to learn more than needed.

In contrast, a good curriculum can be found at a specific location, is consistent, complete, and teaches you exactly that the requirements of the subject contain.

3.4. Independent from the platform

Today, the boundaries among television, different type of computers (desktop, laptop, notebook, netbook, tablet) and smartphone are dissolved. Smart TVs will play movies and music from a memory stick, display photographs, and are also suitable for Internet browsing. In addition, smartphones can be used for recording audio files, images, videos and have GPS, too. The camera, microphone and speaker of a simple PC are suitable for videotelephony.

A large number of platforms and operating systems are around us. Students want to display the e-learning materials on a variety of devices, without installing special softwares and plug-ins. Therefore, we must adhere to the most commonly used format: hypertext (HTML) for the browsers, and the almost standardized video, image and document types, as e.g. PDF, JPEG, MPEG, AVI.

3.5. Suitable for single study

The digital material should not only complement the lectures and exercises, but it must also include them. This is especially true for correspondent students who often are not able to attend the lectures; or are not fresh enough to understand what they learn for instance on Saturday night classes. For ordinary students it is often the case that they could not participate the classes for various reasons: illness, two classes at the same time, other tasks that can not be postponed, examination, or simply laziness.

In our institution often happens that the daily load is 8 classes (45 minutes each) or possibly even more. However, mathematics has a strict structure, even a moment's inattention threatens the understanding. The digital teaching materials can be replayed, so student can follow the train of thought. Another advantage is that no need to take notes, because the teacher publishes the lecture notes electronically. The student can focus on understanding, instead.

3.6. Visual, colorful, practical, interesting, playful and funny

It seems that merely a new material is not absorbing enough. But we have good experiences with useful and practical problems, which are closely related to everyday life and have the potential to teach the new materials while solving them.

The success of the online game „Honfoglaló" shows that even the dead descriptive geography, or the years of historical events can also be amusing to deal with, when they are processed in a playful manner. („Honfoglaló" is an online game where quiz questions on history or geography must be answered, and better perform imply to conquer regions from the opponents on a virtual map.)

Another secret of success was probably the development of race condition. For instance, we found very useful the games that develop the spatial abilities [8, 9]. There are many traditional ones, as building blocks, metal building, Babylon, Java, Lego, Geomag, Polidron, Rubik's cube, etc, but also digital games: 3D tetris, Welltris, Tubis, spatial tic-tac-toe, etc.

The curriculum should be visual in the sense that it helps to understand the complicated terminology by vision. All illustration must be aesthetic and colorful. (In geometry it is much easier to show and to hint to the red segment instead of the segment AB. In a crowded figure it is sometimes difficult to mark the corresponding letter close to the point in question. Colored segments are much easier to notice.) Of course, these findings are well-known, and are valid not only for the electronic, but equally to the traditional curriculum. Colorful graphics are, however, cheaper to perform electronically, than printed.

3.7. Consist of distinct, small parts

The vast majority of students do not read the entire chapter of the textbook before solving the problems. Very commonly, having received the task they start to collect the necessary knowledge in the book. Therefore, a detailed table of contents and index is very important in the traditional teaching, while the searching function in digital contents makes the navigation more effective.

Therefore, for curricula, the students expect that kind of structure that do not cite previous chapters; or does not matter if they are repeated. More study also concludes that the members of Z-generation expect immediate and rapid results, even if the curriculum is processed not linearly, but in parallel, or in random order [8, 10]. The findings of these papers were reconfirmed by the completed questionnaires of our students: many of them found our teaching materials slow and expected more dynamic, faster and shorter videos.

4. Conclusion

The criteria of teachers and those of students are not incompatible at all. The teachers' intention is to transmit useful knowledge and quality, within a given time, and want to improve the effectiveness of teaching. Most students, however, want to learn using the least possible time, so they want to increase the effectiveness of learning. We believe that e-learning curricula that fulfil the principles of mathematics-didactics, and the seven properties listed above, can satisfy both requirements.

We also need to realize that there is no best textbook, there is no best digital curriculum. It is impossible to compile a curriculum that would be perfect for all types of learners at all level. Therefore it is important to provide the choice: the same chapter should be worked up in different ways, using different approaches, with more or less details.

References

[1] Joyes G., Frize P., *Valuing Individual Differences Within Learning: From Face-to-Face to Online Experience*, International Journal of Teaching and Learning in Higher Education **17** (2005), 33–41.

[2] Sorden S. D., *A Cognitive Approach to Instructional Design for Multimedia Learning*, Informing Science Journal **8** (2005), 263–279.
[3] Tempelman-Kluit N., *Multimedia Learning Theories and Online instruction*, College & Research Librarie **67** (2006), 364–369.
[4] Shrestha C. H., May, S., Edirisingha P., *From Face-to-Face to e-Mentoring: Does the "e" Add Any Value for Mentors?*, International Journal of Teaching and Learning in Higher Education **2062** (2009), 116–124.
[5] McLoughlin C., Lee M. J., *The Three P's of Pedagogy for the Networked Society: Personalization, Participation, and Productivity*, International Journal of Teaching and Learning in Higher Education **20/1** (2008), 10–27.
[6] Molnár P., *Számítógéppel támogatott együttműködő tanulás online közösségi hálózatos környezetben* (Hungarian), Magyar Pedagógia **109/3** (2009), 261–285.
[7] Katona J., *One programm – more than a million exercises*, Proceedings of the 3rd International Conference on Applied Informatics ICAI, Eger, Eszterházy Károly Főiskola Kiadó (1997), 391–394.
[8] Prensky M., *Digital Game-Based Learning*, New York, McGraw-Hill, 2007.
[9] Gee J. P., *Good video games and good learning*, Frankfurt am Main, Peter Lang Publishing, 2007.
[10] Oblinger D. G., Oblinger J. L. (editors), *Educating the Net Generation*, USA, Educause, 2005.
[11] Ambrus A., *Bevezetés a matematika-didaktikába* (Hungarian), Budapest, ELTE Kiadó, 2004.
[12] Bölcskei A., Szoboszlai M., *A középiskolai geometria oktatásról a mérnök képzés és tehetséggondozás szemüvegén keresztül* (Hungarian), A matematika tanítása **2** (2012), 36–38.
[13] Bölcskei A., Katona J., *Efforts in Descriptive Geometry Education and Their Result*, Proceedings of the International Scientific Conference moNGeometrija, Novi Sad, University of Nis (2012), 381–389.
[14] Bölcskei A., Katona J., *Ábrázoló geometria példákon keresztül, (egyetemi jegyzet)* (Hungarian), 2011,`http://www.asz.ymmf.hu/geometria/`.
[15] Bölcskei A., Katona J., *Ábrázoló geometria példákon keresztül II., (egyetemi jegyzet)* (Hungarian), 2013, `http://www.asz.ymmf.hu/geometria2/`.

A. Bölcskei, Szent István University, Ybl Miklós Faculty of Architecture and Civil Engineering, Thököly út 74., 1147 Budapest, Hungary,
E-mail address: `bolcskei.attila@ybl.szie.hu`

J. Katona, Szent István University, Ybl Miklós Faculty of Architecture and Civil Engineering, Thököly út 74., 1147 Budapest, Hungary,
E-mail address: `katona.janos@ybl.szie.hu`

Studies of the University of Žilina
Mathematical Series
Vol. 27/2015, 11–34

ON THE HYPERBOLIC TRIANGLE CENTERS

ÁKOS G. HORVÁTH

Abstract. Using the method of C. Vörös, we establish results on hyperbolic plane geometry, related to triangles. In this note we investigate the orthocenter, the concept of isogonal conjugate and some further center as of the symmedian of a triangle. We also investigate the role of the "Euler line" and the pseudo-centers of a triangle.

1. Introduction and preliminaries

In an earlier work of the author [9, 10]), the concept of distance extracted from the work of Cyrill Vörös was investigated. By translating the standard methods of Euclidean plane geometry into the hyperbolic plane, he applied these methods for various configurations. We gave a model independent construction for the famous problem of Malfatti (discussed in [8]) and gave some interesting formulas connected with the geometry of hyperbolic triangles. In this paper we follow the investigations above for some other concept of the hyperbolic triangle.

1.1. Well-known formulas on hyperbolic trigonometry

The points A, B, C denote the vertices of a triangle. The lengths of the edges opposite to these vertices are a, b, c, respectively. The angles at A, B, C are denoted by α, β, γ, respectively. If the triangle has a right angle, it is always at C.

The symbol δ denotes half of the area of the triangle; more precisely, we have $2\delta = \pi - (\alpha + \beta + \gamma)$.

- **Connections between the trigonometric and hyperbolic trigonometric functions:**

$$\sinh a = \frac{1}{\mathrm{i}}\sin(\mathrm{i}\, a), \quad \cosh a = \cos(\mathrm{i}\, a), \quad \tanh a = \frac{1}{\mathrm{i}}\tan(\mathrm{i}\, a).$$

- **Law of sines:**

$$\sinh a : \sinh b : \sinh c = \sin\alpha : \sin\beta : \sin\gamma. \tag{1}$$

Received August 28, 2014, and in revised form January 29, 2015.
2000 *Mathematics Subject Classification.* Primary 51M10, 51M15.
Key words and phrases. cycle, hyperbolic plane, triangle centers.
This work was supported by the Visegrad Fund, small grant 11420082.

- **Law of cosines:**
$$\cosh c = \cosh a \cosh b - \sinh a \sinh b \cos \gamma. \tag{2}$$
- **Law of cosines on the angles:**
$$\cos \gamma = -\cos \alpha \cos \beta + \sin \alpha \sin \beta \cosh c.$$
- **The area of the triangle:**
$$T := 2\delta = \pi - (\alpha + \beta + \gamma), \qquad \tan \tfrac{T}{2} = \left(\tanh \tfrac{a_1}{2} + \tanh \tfrac{a_2}{2}\right) \tanh \tfrac{m_a}{2},$$
where m_a is the height of the triangle corresponding to A and a_1, a_2 are the signed lengths of the segments into which the foot point of the height divides the side BC.
- **Heron's formula:**
$$\tan \tfrac{T}{4} = \sqrt{\tanh \tfrac{s}{2} \tanh \tfrac{s-a}{2} \tanh \tfrac{s-b}{2} \tanh \tfrac{s-c}{2}}.$$
- **Formulas on Lambert's quadrangle:** The vertices of the quadrangle are A, B, C, D and the lengths of the edges are $AB = a$, $BC = b$, $CD = c$ and $DA = d$, respectively. The only angle which is not right-angle is $BCD\measuredangle = \varphi$. Then, for the sides, we have:
$$\tanh b = \tanh d \cosh a, \qquad \tanh c = \tanh a \cosh d,$$
and
$$\sinh b = \sinh d \cosh c, \qquad \sinh c = \sinh a \cosh b,$$
moreover, for the angles, we have:
$$\cos \varphi = \tanh b \tanh c = \sinh a \sinh d, \qquad \sin \varphi = \tfrac{\cosh d}{\cosh b} = \tfrac{\cosh a}{\cosh c},$$
and
$$\tan \varphi = \tfrac{1}{\tanh a \sinh b} = \tfrac{1}{\tanh d \sinh c}.$$

1.2. The distance of the points and the lengths of the segments

In [9] we extracted the concepts of the distance of real points following the method of the book of Cyrill Vörös [18]. We extend the plane with two types of points, one type of the points at infinity and the other one the type of ideal points. In a projective model these are the boundary and external points of a model with respect to the embedding real projective plane. Two parallel lines determine a point at infinity and two ultraparallel lines an ideal point which is the pole of their common transversal. Now the concept of the line can be extended; a line is real if it has real points (in this case it also has two points at infinity and the other points on it are ideal points being the poles of the real lines orthogonal to the mentioned one). The extended real line is a closed compact set with finite length. We also distinguish the line at infinity which contains precisely one point at infinity and the so-called ideal line which contains only ideal points. By definition the common lengths of these lines are $\pi k\,\mathrm{i}$, where k is a constant of the hyperbolic plane and i is the imaginary unit. In this paper we assume that $k = 1$. Two points on a line determine two segments AB and BA. The sum of the lengths of these segments is $AB + BA = \pi\,\mathrm{i}$. We define the length of a segment as an element of the linearly ordered set $\bar{\mathbb{C}} := \overline{\mathbb{R}} + \mathbb{R} \cdot \mathrm{i}$. Here $\overline{\mathbb{R}} = \mathbb{R} \cup \{\pm\infty\}$ is the linearly ordered set of real numbers extracted with two new numbers with the "real infinity" ∞ and its additive inverse $-\infty$. The infinities can be considered as new "numbers" having the properties that either "there is no real number greater or equal to ∞" or "there is no real number less or equal to $-\infty$". We also introduce the following operational rules: $\infty + \infty = \infty$, $-\infty + (-\infty) = -\infty$, $\infty + (-\infty) = 0$ and $\pm\infty + a = \pm\infty$ for real a. It is obvious that $\overline{\mathbb{R}}$ is not a group, the rule of associativity holds only such expressions which contain at most two new objects. In fact, $0 = \infty + (-\infty) = (\infty + \infty) + (-\infty) = \infty + (\infty + (-\infty)) = \infty$ is a contradiction. We also require that the equality $\pm\infty + b\,\mathrm{i} = \pm\infty + 0\,\mathrm{i}$ holds for every real number b and for brevity we introduce the respective notations $\infty := \infty + 0\,\mathrm{i}$ and $-\infty := -\infty + 0\,\mathrm{i}$. We extract the usual definition of hyperbolic function based on the complex exponential function by the following formulas

$$\cosh(\pm\infty) := \infty, \quad \sinh(\pm\infty) := \pm\infty, \text{ and } \quad \tanh(\pm\infty) := \pm 1.$$

We also assume that $\infty \cdot \infty = (-\infty) \cdot (-\infty) = \infty$, $\infty \cdot (-\infty) = -\infty$ and $\alpha \cdot (\pm\infty) = \pm\infty$.

Assuming that the trigonometric formulas of hyperbolic triangles are also valid with ideal vertices the definition of the mentioned lengths of the complementary segments of a line are given. We defined all of the possible lengths of a segment on the basis of the type of the line contains them.

The definitions of the respective cases can be found in Table 1. We abbreviate the words real, infinite and ideal by symbols $\mathcal{R}$, $\mathcal{I}n$ and $\mathcal{I}d$, respectively. d means a real (positive) distance of the corresponding usual real elements which are a real point or the real polar line of an ideal point, respectively. Every box in the table contains two numbers which are the lengths of the two segments determined by the two points. For example, the distance of a real and an ideal point is a complex number. Its real part is the distance of the real point to the polar of the ideal point with a sign, this sign is positive in the case when the polar line intersects the segment between the real and ideal points, and is negative otherwise. The imaginary part of the length is $(\pi/2)\,\mathrm{i}$, implying that the sum of the lengths of two complementary segments of this projective line has total length $\pi\,\mathrm{i}$. Consider now an infinite point. This point can also be considered as the limit of real points or limit of ideal points of this line. By definition the distance from a point at infinity of a real line to any other real or infinite point of this line is $\pm\infty$ according to that it contains or not ideal points. If, for instance, A is an infinite point and B is a real one, then the segment AB contains only real points has length ∞. It is clear that with respect to the segments on a real line the length-function is continuous.

We can check that the length of a segment for which either A or B is an infinite point is indeterminable. On the other hand if we consider the polar of the ideal point A we get a real line through B. The length of a segment connecting the (ideal) point A and one of the points of its polar is $(\pi/2)\,\mathrm{i}$. This means that we can define the length of a segment between A and B also as this common value. Now if we want to preserve the additivity property of the lengths of segments on

		B		
		$\mathcal{R}$	$\mathcal{I}n$	$\mathcal{I}d$
A	$\mathcal{R}$	$AB = d$ $BA = -d + \pi\,\mathrm{i}$	$AB = \infty$ $BA = -\infty$	$AB = d + \frac{\pi}{2}\,\mathrm{i}$ $BA = -d + \frac{\pi}{2}\,\mathrm{i}$
	$\mathcal{I}n$		$AB = \infty$ $BA = -\infty$	$AB = \infty$ $BA = -\infty$
	$\mathcal{I}d$			$AB = d + \pi\,\mathrm{i}$ $BA = -d$

Table 1. Distances on the real line.

a line at infinity, too then we must give the pair of values 0, $\pi\,\mathrm{i}$ for the lengths of segment with ideal ends. The Table 2 collects these definitions.

		B	
		$\mathcal{I}n$	$\mathcal{I}d$
A	$\mathcal{I}n$	$AB = 0$ $BA = \pi\,\mathrm{i}$	$AB = \frac{\pi}{2}\,\mathrm{i}$ $BA = \frac{\pi}{2}\,\mathrm{i}$
	$\mathcal{I}d$		$AB = 0$ $BA = \pi\,\mathrm{i}$

Table 2. Distances on the line at infinity.

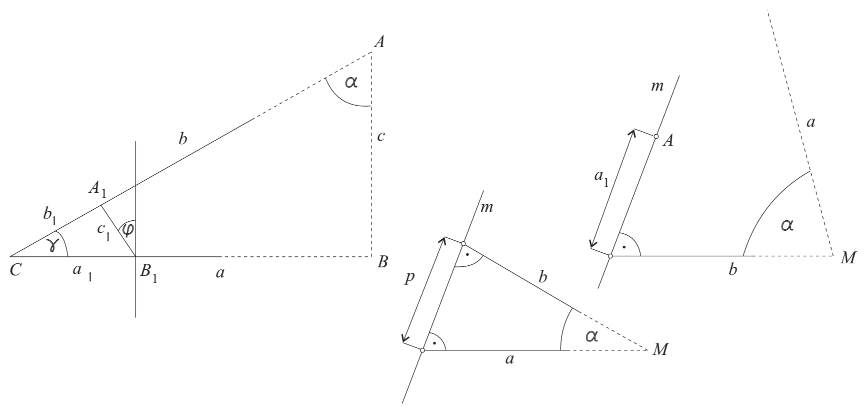

Figure 1. The cases of the ideal segment and angles.

The last situation contains only one case: A, B and AB are ideal elements, respectively. As we showed in [9]. **The length of an ideal segment on an ideal line is the angle of their polars multiplied by the imaginary unit i.**

<table>
<tr><td></td><td></td><td colspan="3">a</td></tr>
<tr><td></td><td></td><td>$\mathcal{R}$</td><td>$\mathcal{I}n$</td><td>$\mathcal{I}d$</td></tr>
<tr><td rowspan="3">b</td><td>$\mathcal{R}$</td>
<td><table><tr><td colspan="3">M</td></tr><tr><td>$\mathcal{R}$</td><td>$\mathcal{I}n$</td><td>$\mathcal{I}d$</td></tr><tr><td>φ
$\pi-\varphi$</td><td>0
π</td><td>$\frac{p}{\mathrm{i}}$
$\pi-\frac{p}{\mathrm{i}}$</td></tr></table></td>
<td><table><tr><td colspan="2">M</td></tr><tr><td>$\mathcal{I}n$</td><td>$\mathcal{I}d$</td></tr><tr><td>$\frac{\pi}{2}$
$\frac{\pi}{2}$</td><td>∞
$-\infty$</td></tr></table></td>
<td><table><tr><td>M</td></tr><tr><td>$\mathcal{I}d$</td></tr><tr><td>$\frac{\pi}{2}+\frac{a_1}{\mathrm{i}}$
$\frac{\pi}{2}-\frac{a_1}{\mathrm{i}}$</td></tr></table></td></tr>
<tr><td>$\mathcal{I}n$</td><td></td>
<td><table><tr><td>M</td></tr><tr><td>$\mathcal{I}d$</td></tr><tr><td>∞
$-\infty$</td></tr></table></td>
<td><table><tr><td>M</td></tr><tr><td>$\mathcal{I}d$</td></tr><tr><td>∞
$-\infty$</td></tr></table></td></tr>
<tr><td>$\mathcal{I}d$</td><td></td><td></td>
<td><table><tr><td>M</td></tr><tr><td>$\mathcal{I}d$</td></tr><tr><td>$\frac{p}{\mathrm{i}}$
$\pi-\frac{p}{\mathrm{i}}$</td></tr></table></td></tr>
</table>

Table 3. Angles of lines.

Similarly as in the previous paragraph we can deduce the angle between arbitrary kind of lines (see Table 3). In Table 3, a and b are the given lines, $M = a \cap b$ is their intersection point, m is the polar of M and A and B is the poles of a and b, respectively. The numbers p and a_1 represent real distances, can be seen on Fig 1, respectively. The general connection between the angles and distances is the following: **Every distance of a pair of points is the measure of the angle of their polars multiplied by i. The domain of the angle can be chosen on such a way, that we are going through the segment by a moving point and look at the domain which described by the moving polar of this point.**

1.3. Results on the three mean centers

There are many interesting statements on triangle centers. In this section we mention some of them concentrating only the centroid, circumcenters and incenters, respectively [9, 10].

The notation of this subsection follows the previous part of this paper: the vertices of the triangle are A, B, C, the corresponding angles are α, β, γ and the lengths of the sides opposite to the vertices are a, b, c, respectively. We also use the notion $2s = a+b+c$ for the perimeter of the triangle. Let denote R, r, r_A, r_B, r_C the radius of the circumscribed cycle, the radius of the inscribed cycle (shortly incycle), and the radiuses of the escribed cycles opposite to the vertices A, B, C, respectively. We do not assume that the points A, B, C are real and the distances are positive numbers. In most cases the formulas are valid for ideal elements and elements at infinity and when the distances are complex numbers, respectively. The only exception when the operation which needs to the examined formula is understandable. Before the examination of hyperbolic triangle centers we collect some further important formulas on hyperbolic triangles. We can consider them in our extracted manner.

1.3.1. Staudtian and angular Staudtian of a hyperbolic triangle. The **Staudtian of a hyperbolic triangle** something-like similar (but definitely distinct) to the concept of the Euclidean area. In spherical trigonometry the twice of this very important quantity called by Staudt the sine of the trihedral angle $O-ABC$ and later Neuberg suggested the names (first) "Staudtian" and the "Norm of the sides", respectively. We prefer in this paper the name "Staudtian" as a token of our respect for the great geometer Staudt. Let

$$n = n(ABC) := \sqrt{\sinh s \sinh(s-a) \sinh(s-b) \sinh(s-c)},$$

then we have

$$\sin\frac{\alpha}{2}\sin\frac{\beta}{2}\sin\frac{\gamma}{2} = \frac{n^2}{\sinh s\, \sinh a\, \sinh b\, \sinh c}.$$

This observation leads to the following formulas on the Staudtian:

$$\sin\alpha = \frac{2n}{\sinh b\, \sinh c}, \quad \sin\beta = \frac{2n}{\sinh a\, \sinh c}, \quad \sin\gamma = \frac{2n}{\sinh a\, \sinh b}. \tag{3}$$

From the first equality of (3) we get

$$n = \frac{1}{2}\sin\alpha\, \sinh b\, \sinh c = \frac{1}{2}\sinh h_C\, \sinh c, \tag{4}$$

where h_C is the height of the triangle corresponding to the vertex C. As a consequence of this concept we can give homogeneous coordinates for the points of the plane with respect to a basic triangle as follows:

Definition 1.1. *Let ABC be a non-degenerated reference triangle of the hyperbolic plane. If X is an arbitrary point we define its coordinates by the ratio of the Staudtian $X := (n_A(X) : n_B(X) : n_C(X))$ where $n_A(X)$, $n_B(X)$ and $n_C(X)$ means the Staudtian of the triangle XBC, XCA and XAB, respectively. This triple of coordinates is the* ***triangular coordinates*** *of the point X with respect to the triangle ABC.*

Consider finally the ratio of section (BX_AC) where X_A is the foot of the transversal AX on the line BC. If $n(BX_AA)$, $n(CX_AA)$ mean the Staudtian of the triangles BX_AA, CX_AA, respectively then using (4) we have

$$(BX_AC) = \frac{\sinh BX_A}{\sinh X_AC} = \frac{\frac{1}{2}\sinh h_C\, \sinh BX_A}{\frac{1}{2}\sinh h_C\, \sinh X_AC} = \frac{n(BX_AA)}{n(CX_AA)} =$$
$$= \frac{\frac{1}{2}\sinh c\, \sinh AX_A\, \sin(BAX_A)\measuredangle}{\frac{1}{2}\sinh b\, \sinh AX_A\, \sin(CAX_A)\measuredangle} = \frac{\sinh c\, \sinh AX\, \sin(BAX_A)\measuredangle}{\sinh b\, \sinh AX\, \sin(CAX_A)\measuredangle} = \frac{n_C(X)}{n_B(X)},$$

proving that

$$(BX_AC) = \frac{n_C(X)}{n_B(X)}, \qquad (CX_BA) = \frac{n_A(X)}{n_C(X)}, \qquad (AX_CB) = \frac{n_B(X)}{n_A(X)}. \tag{5}$$

The **angular Staudtian** of the triangle defined by the equality:

$$N = N(ABC) := \sqrt{\sin\delta\, \sin(\delta+\alpha)\, \sin(\delta+\beta)\, \sin(\delta+\gamma)},$$

is the "dual" of the concept of Staudtian and thus we have similar formulas on it. From the law of cosines on the angles we have

$$\cos\gamma = -\cos\alpha\,\cos\beta + \sin\alpha\,\sin\beta\,\cosh c$$

and adding to this the addition formula of the cosine function we get

$$\sin\alpha\,\sin\beta\,(\cosh c - 1) = \cos\gamma + \cos(\alpha+\beta) = 2\cos\tfrac{\alpha+\beta+\gamma}{2}\,\cos\tfrac{\alpha+\beta-\gamma}{2}.$$

From this we get

$$\sinh\tfrac{c}{2} = \sqrt{\tfrac{\sin\delta\,\sin(\delta+\gamma)}{\sin\alpha\,\sin\beta}}.$$

Analogously we get

$$\cosh\tfrac{c}{2} = \sqrt{\tfrac{\sin(\delta+\beta)\,\sin(\delta+\alpha)}{\sin\alpha\,\sin\beta}}.$$

From these equations

$$\cosh\tfrac{a}{2}\,\cosh\tfrac{b}{2}\,\cosh\tfrac{c}{2} = \tfrac{N^2}{\sin\alpha\,\sin\beta\,\sin\gamma\,\sin\delta}.$$

Finally we also have that

$$\sinh a = \tfrac{2N}{\sin\beta\,\sin\gamma}, \qquad \sinh b = \tfrac{2N}{\sin\alpha\,\sin\gamma}, \qquad \sinh c = \tfrac{2N}{\sin\alpha\,\sin\beta}, \tag{6}$$

and from the first equality of (6) we get

$$N = \tfrac{1}{2}\sinh a\,\sin\beta\,\sin\gamma = \tfrac{1}{2}\sinh h_C\,\sin\gamma.$$

The connection between the two Staudtians gives by the formula

$$2n^2 = N\sinh a\,\sinh b\,\sinh c. \tag{7}$$

In fact, from (3) and (6) we get

$$\sin\alpha\,\sinh a = \tfrac{4nN}{\sin\beta\,\sin\gamma\,\sinh b\,\sinh c}$$

implying that

$$\sin\alpha\,\sin\beta\,\sin\gamma\,\sinh a\,\sinh b\,\sinh c = 4nN.$$

On the other hand from (3) we get immediately that

$$\sin\alpha\,\sin\beta\,\sin\gamma = \tfrac{8n^3}{\sinh^2 a\,\sinh^2 b\,\sinh^2 c}$$

and thus

$$2n^2 = N\sinh a\,\sinh b\,\sinh c,$$

as we stated. The connection between the two types of the Staudtian can be understood if we dived to the first equality of (3) by the analogous one in (10) we get $\frac{\sin\alpha}{\sinh a} = \frac{n}{N}\frac{\sin\beta}{\sinh b}\frac{\sin\gamma}{\sinh c}$ implying the equality

$$\tfrac{N}{n} = \tfrac{\sin\alpha}{\sinh a}.$$

1.3.2. On the centroid (or median point) of a triangle. We denote the medians of the triangle by AM_A, BM_B and CM_C, respectively. The feet of the medians M_A, M_B and M_C. The existence of their common point M follows from the Menelaos theorem [17]. For instance if AB, BC and AC are real lines and the points A, B and C are ideal points then we have that $AM_C = M_CB = d = a/2$ implies that M_C is the middle point of the real segment lying on the line AB between the intersection points of the polars of A and B with AB, respectively (see Fig. 2).

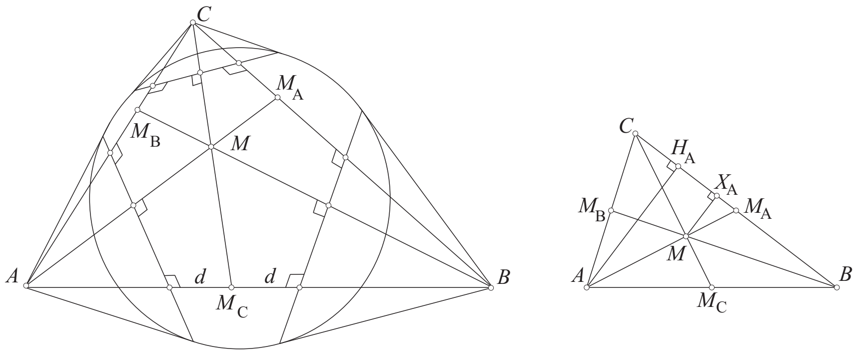

Figure 2. Centroid of a triangle with ideal vertices.

Theorem 1.2 ([10]). *We have the following formulas connected with the centroid:*

$$n_A(M) = n_B(M) = n_C(M), \tag{8}$$

$$\frac{\sinh AM}{\sinh MM_A} = 2\cosh\frac{a}{2}, \tag{9}$$

$$\frac{\sinh AM_A}{\sinh MM_A} = \frac{\sinh BM_B}{\sinh MM_B} = \frac{\sinh CM_C}{\sinh MM_C} = \frac{n}{n_A(M)} \tag{10}$$

$$\sinh d'_M = \frac{\sinh d'_A + \sinh d'_B + \sinh d'_C}{\sqrt{1+2(1+\cosh a+\cosh b+\cosh c)}}, \tag{11}$$

where d'_A, d'_B, d'_C, d'_M mean the signed distances of the points A, B, C, M to a line y, respectively. Finally we have

$$\cosh YM = \frac{\frac{\cosh YA+\cosh YB+\cosh YC}{n}}{\frac{n}{n_A(M)}}, \tag{12}$$

where Y a point of the plane. (11) *and* (12) *are called the "center of gravity" property of M and the "minimality" property of M, respectively.*

1.3.3. On the center of the circumscribed cycle. Denote by O the center of the circumscribed cycle of the triangle ABC. In the extracted plane O always exists and could be a real point, point at infinity or ideal point, respectively. Since we have two possibilities to choose the segments AB, BC and AC on their respective lines, we also have four possibilities to get a circumscribed cycle. One of them corresponds to the segments with real lengths and the others can be gotten if we choose one segment with real length and two segments with complex lengths, respectively. If A, B, C are real points the first cycle could be circle, paracycle or hypercycle, but the other three are always hypercycles, respectively. For example, let $a' = a = BC$ is a real length and $b' = -b+\pi\,\mathrm{i}$, $c' = -c+\pi\,\mathrm{i}$ are complex lengths, respectively. Then we denote by O_A the corresponding (ideal) center and by R_A the corresponding (complex) radius. We also note that the latter three hypercycle have geometric meaning. These are those hypercycles which fundamental lines contain a pair from the midpoints of the edge-segments and contain that vertex of the triangle which is the meeting point of the corresponding edges.

Theorem 1.3. *The following formulas are valid on the circumradii:*

$$\tanh R = \tfrac{\sin\delta}{N}, \qquad \tanh R_A = \tfrac{\sin(\delta+\alpha)}{N} \tag{13}$$
$$\tanh R = \frac{2\sinh\frac{a}{2}\,\sinh\frac{b}{2}\,\sinh\frac{c}{2}}{n}, \qquad \tanh R_A = \frac{2\sinh\frac{a}{2}\,\cosh\frac{b}{2}\,\cosh\frac{c}{2}}{n}$$
$$n_A(0) : n_B(O) = \cos(\delta+\alpha)\,\sinh a : \cos(\delta+\beta)\,\sinh b.$$

1.3.4. On the center of the inscribed and escribed cycles. We are aware that the bisectors of the interior angles of a hyperbolic triangle are concurrent at a point I, called the incenter, which is equidistant from the sides of the triangle. The radius of the **incircle** or **inscribed circle**, whose center is at the incenter and touches the sides, shall be designated by r. Similarly the bisector of any interior angle and those of the exterior angles at the other vertices, are concurrent at point outside the triangle; these three points are called **excenters**, and the corresponding tangent cycles **excycles** or **escribed cycles**. The excenter lying on AI is denoted ba I_A, and the radius of the escribed cycle with center at I_A is r_A. We denote by X_A, X_B, X_C the points where the interior bisectors meets BC, AC, AB, respectively. Similarly Y_A, Y_B and Y_C denote the intersection of the exterior bisector at A, B and C with BC, AC and AB, respectively.

We note that the excenters and the points of intersection of the sides with the bisectors of the corresponding exterior angle could be points at infinity or also could be ideal points. Let denote the touching points of the incircle Z_A, Z_B and Z_C on the lines BC, AC and AB, respectively and the touching points of the excycles with center I_A, I_B and I_C are the triples $\{V_{A,A}, V_{B,A}, V_{C,A}\}$, $\{V_{A,B}, V_{B,B}, V_{C,B}\}$ and $\{V_{A,C}, V_{B,C}, V_{C,C}\}$, respectively (see in Fig. 3).

Theorem 1.4 ([10])**.** *On the radiuses r, r_A, r_B or r_C we have the following formulas:*

$$\tanh r = \tfrac{n}{\sinh s}, \quad \tanh r_A = \tfrac{n}{\sinh(s-a)}, \tag{14}$$
$$\tanh r = \frac{N}{2\cos\frac{\alpha}{2}\,\cos\frac{\beta}{2}\,\cos\frac{\gamma}{2}},$$
$$\coth r = \frac{\sin(\delta+\alpha)+\sin(\delta+\beta)+\sin(\delta+\gamma)+\sin\delta}{2N}, \tag{15}$$
$$\coth r_A = \frac{-\sin(\delta+\alpha)+\sin(\delta+\beta)+\sin(\delta+\gamma)-\sin\delta}{2N}, \tag{16}$$
$$\tanh R + \tanh R_A = \coth r_B + \coth r_C,$$
$$\tanh R_B + \tanh R_C = \coth r + \coth r_A,$$

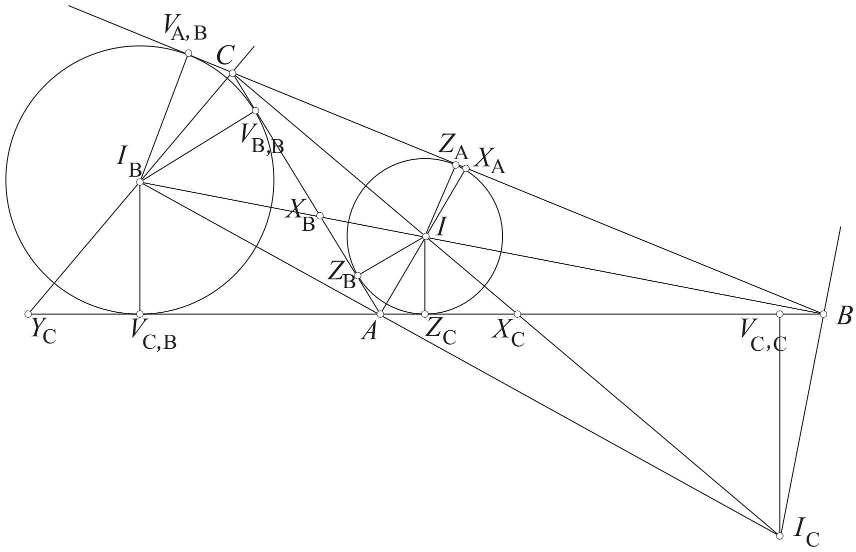

Figure 3. Incircles and excycles.

$$\begin{aligned} \tanh R + \coth r &= \tfrac{1}{2}\left(\tanh R + \tanh R_A + \tanh R_B + \tanh R_C\right), \\ n_A(I) : n_B(I) : n_C(I) &= \sinh a : \sinh b : \sinh c, \qquad (17) \\ n_A(I_A) : n_B(I_A) : n_C(I_A) &= -\sinh a : \sinh b : \sinh c. \end{aligned}$$

The following formulas connect the radiuses of the circles and the lengths of the edges of the triangle.

Theorem 1.5. *Let a, b, c, s, r_A, r_B, r_C, r, R be the values defined for a hyperbolic triangle above. Then we have the following formulas:*

$$-\coth r_A - \coth r_B - \coth r_C + \coth r = 2\tanh R, \tag{18}$$

$$\begin{aligned} &\coth r_A \, \coth r_B + \coth r_A \, \coth r_C + \coth r_B \, \coth r_C = \\ &\qquad = \tfrac{1}{\sinh s \, \sinh(s-a)} + \tfrac{1}{\sinh s \, \sinh(s-b)} + \tfrac{1}{\sinh s \, \sinh(s-c)}, \end{aligned} \tag{19}$$

$$\begin{aligned} &\tanh r_A \, \tanh r_B + \tanh r_A \, \tanh r_C + \tanh r_B \, \tanh r_C = \\ &= \tfrac{1}{2}\left(\cosh(a+b) + \cosh(a+c) + \cosh(b+c) - \cosh a - \cosh b - \cosh c\right), \end{aligned} \tag{20}$$

$$\begin{aligned} &\coth r_A + \coth r_B + \coth r_C = \\ &\qquad = \tfrac{1}{\tanh r}\left(\cosh a + \cosh b + \cosh c - \coth s\left(\sinh a + \sinh b + \sinh c\right)\right), \end{aligned} \tag{21}$$

$$\begin{aligned} &\tanh r_A + \tanh r_B + \tanh r_C = \\ &= \tfrac{1}{2\tanh r}\left(\cosh a + \cosh b + \cosh c - \cosh(b-a) - \cosh(c-a) - \cosh(c-b)\right), \end{aligned} \tag{22}$$

$$2(\sinh a\sinh b+\sinh a\sinh c+\sinh b\sinh c)=$$
$$=\tanh r\,(\tanh r_A+\tanh r_B+\tanh r_C)+\tanh r_A\,\tanh r_B+$$
$$+\tanh r_A\,\tanh r_C+\tanh r_B\,\tanh r_C.$$

Proof. From (15), (16) and (13) we get

$$-\coth r_A-\coth r_B-\coth r_C+\coth r=2\tfrac{\sin\delta}{N}=2\tanh R,$$

as we stated in (18).

To prove (19) consider the equalities in (14) from which

$$\coth r_A\,\coth r_B+\coth r_A\,\coth r_C+\coth r_B\,\coth r_C=$$
$$=\tfrac{\sinh(s-a)\,\sinh(s-b)+\sinh(s-a)\,\sinh(s-c)+\sinh(s-c)\,\sinh(s-b)}{n^2}=$$
$$=\tfrac{1}{\sinh s\,\sinh(s-a)}+\tfrac{1}{\sinh s\,\sinh(s-b)}+\tfrac{1}{\sinh s\,\sinh(s-c)}$$

Similarly we also get (20):

$$\tanh r_A\,\tanh r_B+\tanh r_A\,\tanh r_C+\tanh r_B\,\tanh r_C=$$
$$=\sinh s\,\sinh(s-a)+\sinh s\,\sinh(s-b)+\sinh s\,\sinh(s-c)=$$
$$=\tfrac{1}{2}\left(\cosh(a+b)+\cosh(a+c)+\cosh(b+c)-\cosh a-\cosh b-\cosh c\right).$$

Since we have

$$-2\tanh R+\coth r=\coth r_A+\coth r_B+\coth r_C=$$
$$=\tfrac{\sinh(s-a)+\sinh(s-b)+\sinh(s-c)}{n}=\tfrac{(\sinh(s-a)+\sinh(s-b)+\sinh(s-c))}{\sinh s\,\tanh r}=$$
$$=\tfrac{\cosh a+\cosh b+\cosh c-\coth s(\sinh a+\sinh b+\sinh c)}{\tanh r}$$

and so (20) is given. Furthermore we also have

$$\tanh r_A+\tanh r_B+\tanh r_C=$$
$$=\tfrac{n(\sinh(s-a)\sinh(s-b)+\sinh(s-a)\sinh(s-c)+\sinh(s-b)\sinh(s-c))}{\sinh(s-a)\sinh(s-b)\sinh(s-c)}=$$
$$=\tfrac{\sinh s}{n}\left(\sinh(s-a)\sinh(s-b)+\sinh(s-a)\sinh(s-c)+\sinh(s-b)\sinh(s-c)\right)=$$
$$=\tfrac{(\sinh(s-a)\sinh(s-b)+\sinh(s-a)\sinh(s-c)+\sinh(s-b)\sinh(s-c))}{\tanh r}=$$
$$=\tfrac{1}{2\tanh r}\left(\cosh a+\cosh b+\cosh c-\cosh(b-a)-\cosh(c-a)-\cosh(c-b)\right)$$

implying (21). From (19) and (21) we get

$$\tanh r\,(\tanh r_A+\tanh r_B+\tanh r_C)+\tanh r_A\,\tanh r_B+$$
$$+\tanh r_A\,\tanh r_C+\tanh r_B\,\tanh r_C=$$
$$=\cosh(a+b)+\cosh(a+c)+\cosh(b+c)-\cosh(b-a)-\cosh(c-a)-\cosh(c-b)=$$
$$=2(\sinh a\,\sinh b+\sinh a\,\sinh c+\sinh b\,\sinh c)$$

which implies (22). □

The following theorem gives a connection from among the distance of the incenter and circumcenter, the radiuses r,R and the side-lengths a, b, c.

Theorem 1.6 ([10]). *Let O and I the center of the circumsrcibed and inscribed circles, respectively. Then we have*

$$\cosh OI = 2\cosh\tfrac{a}{2}\, \cosh\tfrac{b}{2}\, \cosh\tfrac{c}{2}\, \cosh r\, \cosh R + \cosh\tfrac{a+b+c}{2}\, \cosh(R-r).$$

2. Further formulas on hyperbolic triangles

2.1. On the orthocenter of a triangle.

The most important formulas on the orthocenter are also valid in the hyperbolic plane. We give a collection in which the orthocenter is denoted by H, the feet of the altitudes are denoted by H_A, H_B and H_C, respectively. We also denote by h_a, h_b or h_c the heights of the triangle corresponding to the sides a, b or c, respectively.

Theorem 2.1. *With the notation above we have the formulas:*

$$\tanh HA \cdot \tanh HH_A = \tanh HB \cdot \tanh HH_B = \tanh HC \cdot \tanh HH_C =: h, \quad (23)$$

$$\sinh HA \cdot \sinh HH_A :\ \sinh HB \cdot \sinh HH_B :\ \sinh HC \cdot \sinh HH_C = \\ = \cosh h_A : \cosh h_B : \cosh h_C, \quad (24)$$

$$n_A(H) : n_B(H) : n_C(H) = \tan\alpha : \tan\beta : \tan\gamma. \quad (25)$$

Furthermore, if P is any point of the plane then we have

$$n_A(H)\cosh PA + n_B(H)\cosh PB + n_C(H)\cosh PC = n\cosh PH \quad (26)$$

and also

$$\cosh c\, \sinh H_AC + \cosh b\, \sinh BH_A = \cosh h_A\, \sinh a. \quad (27)$$

Finally we have also that

$$(h+1)\cosh OH = \left(\tfrac{\coth h_A}{\sinh HA} + \tfrac{\coth h_B}{\sinh HB} + \tfrac{\coth h_C}{\sinh HC}\right)\cosh R. \quad (28)$$

Before the proof we prove Stewart's Theorem on the hyperbolic plane.

Theorem 2.2 (Stewart's theorem). *Let ABC be a triangle and A' is a point on the side BC. Then we have*

$$\cosh AB\, \sinh A'C + \cosh AC\, \sinh BA' = \cosh AA'\, \sinh BC.$$

Proof. Using (2) to the triangles ABA' and ACA', respectively, we get

$$\cosh AA'\, \sinh BC = \cosh AA'\, \sinh(BA' + A'C) = \\ = \sinh BA'\, \cosh A'C\, \cosh AA' + \sinh A'C\, \cosh BA'\, \cosh AA' = \\ = \sinh BA'(\sinh A'C\, \sinh AA'\, \cos(AA'C_\measuredangle) + \cosh AC) + \\ + \sinh A'C(\sinh BA'\, \sinh AA'\, \cos(\pi - AA'C_\measuredangle) + \cosh AB) = \\ = \sinh BA'\, \cosh AC + \sinh A'C\, \cosh AB$$

as we stated. □

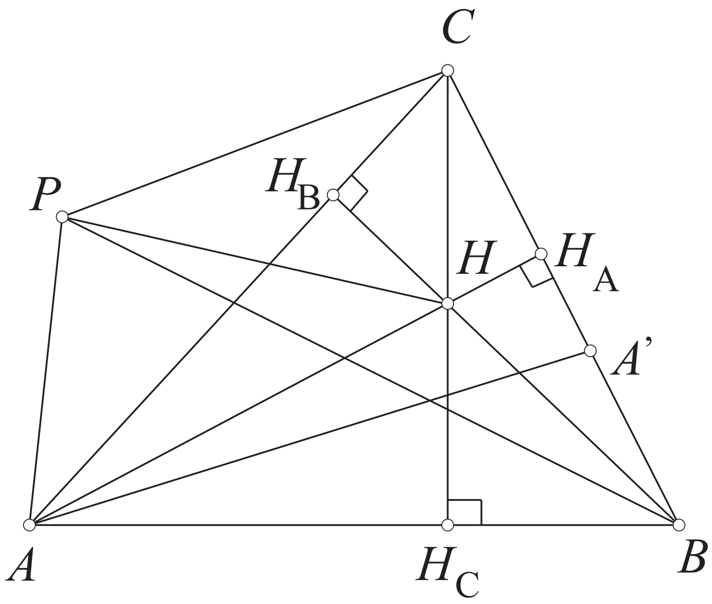

Figure 4. Stewart's theorem and the orthocenter.

Remark 2.3. Considering third-order approximation of the hyperbolic functions we get the equality:

$$\left(1+\frac{AA'^2}{2}\right)\left(BC+\frac{BC^3}{6}\right)=\left(1+\frac{b^2}{2}\right)\left(BA'+\frac{BA'^3}{6}\right)+\left(1+\frac{c^2}{2}\right)\left(A'C+\frac{A'C^3}{6}\right)$$

or equivalently the equation

$$a+\frac{AA'^2}{2}a+\frac{a^3}{6}=BA'+\frac{b^2}{2}BA'+\frac{BA'^3}{6}+A'C+\frac{c^2}{2}A'C+\frac{A'C^3}{6}.$$

Since $a=BA'+A'C$

$$\frac{AA'^2}{2}a+\left(\frac{BA'^3}{6}+\frac{BA'^2A'C}{2}+\frac{BA'A'C^2}{2}+\frac{A'C^3}{6}\right)=\frac{b^2}{2}BA'+\frac{BA'^3}{6}+\frac{c^2}{2}A'C+\frac{A'C^3}{6}$$

implying the well-known Euclidean Stewart's theorem:

$$\left(AA'^2+BA'\cdot A'C\right)a=b^2BA'+c^2A'C.$$

Proof. (Proof of Theorem 2.1) (27) is the Stewart's theorem for the point H_A. From the rectangular triangles HCH_A and HH_CA we get

$$\tanh HH_A:\tanh HC=\cos H_AHC\measuredangle=\tanh HH_C:\tanh HA.$$

Similarly we get also that

$$\tanh HH_B:\tanh HC=\cos H_BHC\measuredangle=\tanh HH_C:\tanh HB.$$

Thus we have (23):

$$\tanh HA\cdot\tanh HH_A=\tanh HB\cdot\tanh HH_B=\tanh HC\cdot\tanh HH_C.$$

From this we get

$$\frac{\sinh HA{\cdot}\sinh HH_A}{\cosh HA{\cdot}\cosh HH_A}=\frac{\sinh HB{\cdot}\sinh HH_B}{\cosh HB{\cdot}\cosh HH_B}.$$

Thus

$$\frac{\sinh HA{\cdot}\sinh HH_A}{\sinh HB{\cdot}\sinh HH_B}=\frac{\cosh HA{\cdot}\cosh HH_A}{\cosh HB{\cdot}\cosh HH_B}=\frac{\cosh AH_B}{\cosh BH_A}$$

implying (24). From (5) we get

$$n_A(H):n_B(H)=(AH_CB)=\sinh AH_C:\sinh H_CB=\tan\alpha:\tan\beta$$

implying (25). Use now the Stewart's Theorem for the triangle PAB and its secant PH_C (see in Fig. 4), where P is arbitrary point of the plane. Then we get

$$\cosh PA\,\sinh H_CB+\cosh PB\,\sinh AH_C=\cosh PH_C\,\sinh c.$$

Applying Stewart's theorem again to the triangle PCH_C and its secant PH, we get

$$\cosh PC\,\sinh HH_C+\cosh PH_C\,\sinh CH=\cosh PH\,\sinh CH_C.$$

Eliminating PH_C from these equations we get

$$\cosh PA\,\sinh H_CB+\cosh PB\,\sinh AH_C+\frac{\cosh PC\,\sinh HH_C\,\sinh c}{\sinh CH}=\\ =\frac{\cosh PH\,\sinh CH_C\,\sinh c}{\sinh CH}.$$

On the other hand we have

$$2n_C(H)=\sinh HH_C\,\sinh c.$$

We also have

$$2n_B(H)=2\sinh HH_B\,\sinh b=2\sinh CH_A\,\sinh AH=2\sinh AH_C\,\sinh CH,$$

and similarly

$$2n_A(H)=2\sinh H_CB\,\sinh CH$$

implying the equality

$$n_A(H)\cosh PA+n_B(H)\cosh PB+n_C(H)\cosh PC=\\ =\frac{\cosh PH\,\sinh CH_C\,\sinh c}{2}=n\cosh PH$$

as we stated in (26).

Use (26) in the case when $P=O$ is the circumcenter of the triangle. Then we have

$$n_A(H)\cosh R+n_B(H)\cosh R+n_C(H)\cosh R=n\cosh OH.$$

Thus we have

$$\cosh OH=\frac{n_A(H)+n_B(H)+n_C(H)}{n}\cosh R=\left(\frac{\sinh HH_A}{\sinh h_A}+\frac{\sinh HH_B}{\sinh h_B}+\frac{\sinh HH_C}{\sinh h_C}\right)\cosh R.$$

From (24) we get

$$\sinh HH_B=\sinh HH_A\frac{\sinh HA}{\sinh HB}\frac{\cosh h_B}{\cosh h_A}$$

and also

$$\sinh HH_C=\sinh HH_A\frac{\sinh HA}{\sinh HC}\frac{\cosh h_C}{\cosh h_A}$$

implying that

$$\cosh OH =$$
$$= \frac{\sinh HH_A \sinh HA}{\cosh h_A} \times \left(\frac{\cosh h_A}{\sinh HA \sinh h_A} + \frac{\cosh h_B}{\sinh HB \sinh h_B} + \frac{\cosh h_C}{\sinh HC \sinh h_C} \right) \cosh R =$$
$$= \left(\frac{\cosh h_A}{\sinh HA \sinh h_A} + \frac{\cosh h_B}{\sinh HB \sinh h_B} + \frac{\cosh h_C}{\sinh HC \sinh h_C} \right) \times \frac{\cosh R}{\tanh HH_A \tanh HA + 1}.$$

Now we have

$$(h+1) \cosh OH = \left(\frac{1}{\tanh h_A \sinh HA} + \frac{1}{\tanh h_B \sinh HB} + \frac{1}{\tanh h_C \sinh HC} \right) \cosh R,$$

showing (28). □

2.2. Isogonal conjugate of a point

Let define the **isogonal conjugate** of a point X of the plane in the following way: Reflect the lines through the point X and any of the vertices of the triangle with respect to the bisector of that vertex. Then the getting lines are concurrent at a point X' which we call the isogonal conjugate of X. To prove the concurrence of these lines we have to observe that if the lines AX and AX' intersect the line of the side BC in the points Y and Y' then the ratio of these points with respect to B and C has an inverse connection. In fact, by (1) we have that

$$\frac{\sinh c}{\sinh BY} = \frac{\sin AYB\measuredangle}{\sin BAY\measuredangle} \quad \text{and} \quad \frac{\sinh b}{\sinh YC} = \frac{\sin(\pi - AYB\measuredangle)}{\sin CAY\measuredangle}.$$

This implies that

$$(BYC) = \frac{\sinh BY}{\sinh YC} = \frac{\sinh c}{\sinh b}\frac{\sin BAY\measuredangle}{\sin CAY\measuredangle}.$$

For the point Y' we get similarly that

$$(BY'C) = \frac{\sinh c}{\sinh b}\frac{\sin BAY'\measuredangle}{\sin CAY'\measuredangle} = \frac{\sinh c}{\sinh b}\frac{\sin CAY\measuredangle}{\sin BAY\measuredangle}$$

implying the equation

$$(BYC)(BY'C) = \frac{\sinh^2 c}{\sinh^2 b}. \tag{29}$$

If Z, Z' or V, V' are the intersection points of the examined lines with the corresponding sides CA or AB, respectively, then we get the equation

$$(BYC)(BY'C)(CZA)(CZ'A)(AVB)(AV'B) = 1$$

showing that the first three lines are concurrent if and only if the second three lines are. Hence we can prove the following:

Lemma 2.4. *If X and X' are isogonal conjugate points with respect to the triangle ABC then their triangular coordinates have the following connection:*

$$n_A(X') : n_B(X') : n_C(X') = \frac{\sinh^2 a}{n_A(X)} : \frac{\sinh^2 b}{n_B(X)} : \frac{\sinh^2 c}{n_C(X)}. \tag{30}$$

Proof. Using (29) we have

$$(n_C(X) : n_B(X))\,(n_C(X') : n_B(X')) = (BN_AC)(BN'_AC) = \frac{\sinh^2 c}{\sinh^2 b}$$

implying that

$$n_B(X') : n_C(X') = \frac{\sinh^2 b}{n_B(X)} : \frac{\sinh^2 c}{n_C(X)}$$

as we stated in (30). □

Corollary 2.5. *As a first consequence we can see immediately* (17) *again on the triangular coordinates of the incenter. By* (30) *the triangular coordinates of the isogonal conjugate H' of the orthocenter is*

$$n_A(H') : n_B(H') : n_C(H') = \frac{\sinh^2 a}{\tan\alpha} : \frac{\sinh^2 b}{\tan\beta} : \frac{\sinh^2 c}{\tan\gamma}.$$

Thus

$$n_A(H') : n_B(H') = \frac{\sinh^2 a}{\tan\alpha}\frac{\tan\beta}{\sinh^2 b} = \frac{\sin\alpha\cos\alpha}{\sin\beta\cos\beta} = \frac{\sin 2\alpha}{\sin 2\beta}$$

implying that

$$n_A(H') : n_B(H') : n_C(H') = \sin 2\alpha : \sin 2\beta : \sin 2\gamma.$$

Comparing the coordinates of H' with the triangular coordinates of the circumcenter we can see that the isogonal conjugate of the orthocenter is the circumcenter if and only if the defect of the triangle is zero implying that the geometry of the plane is Euclidean.

A minimality property of the incenter follows from a generalization of the equality (26). Similarly as in the proof of (26) (see Theorem 2.1) we can prove that for any triangle ABC with any fixed point Q and any various point P of the plane the following equality holds:

$$n_A(Q)\cosh PA + n_B(Q)\cosh PB + n_C(Q)\cosh PC = n(ABC)\cosh PQ. \quad (31)$$

Theorem 2.6. *The sum of the triangular coordinates of a point P of the plane is minimal if and only if P is the center of the inscribed circle of the triangle ABC.*

Proof. Assume that the vertices of the triangle ABC are real points and the edges of it are those real segments which are connecting these real vertices, respectively. Let A', B' and C' be the respective poles of the lines BC, AC and AB. These poles are ideal points and the corresponding lines $A'B'$, $A'C'$ and $B'C'$ are also ideal lines, respectively. If P is any point of the plane let $d(P, BC)$, ε_A and α' be the distance of P and the line BC the sign of this distance and the angle of the polar triangle at the vertex A', respectively. We choose the sign to positive if P and A are the same (real) half-plane determined by the line BC. Then the investigated quantity is

$$\begin{aligned}
&n_A(P) + n_B(P) + n_C(P) = \\
&= \tfrac{1}{2}\big(\varepsilon_A \sinh d(P,BC)\sinh a + \varepsilon_B \sinh d(P,AC)\sinh b + \varepsilon_C \sinh d(P,AB)\sinh c\big) = \\
&= \tfrac{1}{2\,\mathrm{i}}\Big(\cosh\big(d(P,BC) + \varepsilon_A \tfrac{\pi}{2}\,\mathrm{i}\big)\sinh a + \cosh\big(d(P,AC) + \varepsilon_B \tfrac{\pi}{2}\,\mathrm{i}\big)\sinh b + \\
&\qquad\qquad + \cosh\big(d(P,AB) + \varepsilon_C \tfrac{\pi}{2}\,\mathrm{i}\big)\sinh c\Big) = \\
&= \tfrac{1}{2\,\mathrm{i}}\big(\cosh PA' \sinh a + \cosh PB' \sinh b + \cosh PC' \sinh c\big).
\end{aligned}$$

Hence using (31) we have that

$$\tfrac{1}{2\,\mathrm{i}}\big(\cosh PA' \sinh a + \cosh PB' \sinh b + \cosh PC' \sinh c\big) = \tfrac{1}{2\,\mathrm{i}} n(A'B'C')\cosh PQ,$$

where the triangular coordinates of the point Q with respect to the polar triangle are

$$n_{A'}(Q) = \sinh a, \quad n_{B'}(Q) = \sinh b, \quad \text{and} \quad n_{C'}(Q) = \sinh c.$$

It follows from (4) that the Staudtian of the triangle $A'B'C'$ is

$$n(A'B'C') = \tfrac{1}{2}\sin\alpha' \sinh b' \sinh c' = \tfrac{1}{2}\sin\tfrac{a}{\mathrm{i}} \sinh \mathrm{i}\,\beta \sinh \mathrm{i}\,\gamma = \tfrac{\mathrm{i}}{2}\sinh a \sin\beta \sin\gamma$$

implying that.

$$n_A(P) + n_B(P) + n_C(P) = \tfrac{1}{4}\sinh a \sin\beta \sin\gamma \cosh PQ = \tfrac{N}{2}\cosh PQ,$$

where the triangular coordinates of Q are $\sinh a$, $\sinh b$ and $\sinh c$, respectively. Thus we get $Q = I$ and the sum in the question is minimal if and only if P is equal to $Q = I$. This proves the statement. □

2.2.1. Symmedian point. We recall that the isogonal conjugate of the centroid is the so-called **symmedian point** of the triangle. The triangular coordinates of the symmedian point are

$$n_A(M') : n_B(M') : n_C(M') = \sinh^2 a : \sinh^2 b : \sinh^2 c.$$

From (4) immediately follows that the hyperbolic sine of the distances of the symmedian point to the sides are proportional to the hyperbolic sines of the corresponding sides:

$$\sinh d(M', BC) : \sinh d(M', AC) : \sinh d(M', AB) = \sinh a : \sinh b : \sinh c$$

showing the validity of the analogous Euclidean theorem in the hyperbolic geometry, too.

We note that the symmedian point of a hyperbolic triangle does not coincides with the **Lemoine point** L of the triangle. This center can be defined on the following way: If tangents be drawn at A, B, C to the circumcircle of the triangle ABC, forming a triangle $A'B'C'$, the lines AA', BB' and CC', are concurrent. The point of concurrence, is the Lemoine point of the triangle. The concurrency follows from Menelaos-theorem applying it to the triangle $A'B'C'$. We note that L is also (by definition) the so-called **Gergonne point** of the triangle $A'B'C'$. To prove that the symmedian point does not coincides with the Lemoine point we determine the triangular coordinates of the latter, too. Let L_A, L_B or L_C be the intersection point of $AA' \cap BC$, $BB' \cap AC$ or $CC' \cap AB$ (see in Fig. 5), respectively. Then we have

$$n_B(L) : n_A(L) = (AL_C B) = \frac{\sinh AL_C}{\sinh L_C B} = \frac{\sinh C'B}{\sinh C'A}\frac{\sin AC'L_C\measuredangle}{\sin BC'L_C\measuredangle} = \frac{\sin AC'L_C\measuredangle}{\sin BC'L_C\measuredangle}.$$

On the other hand we have by (1)

$$\frac{\sin AC'L_C\measuredangle}{\sin CAC'\measuredangle} = \frac{\sinh CA}{\sinh CC'} \quad \text{and} \quad \frac{\sin BC'L_C\measuredangle}{\sin CBC'\measuredangle} = \frac{\sinh CB}{\sinh CC'}$$

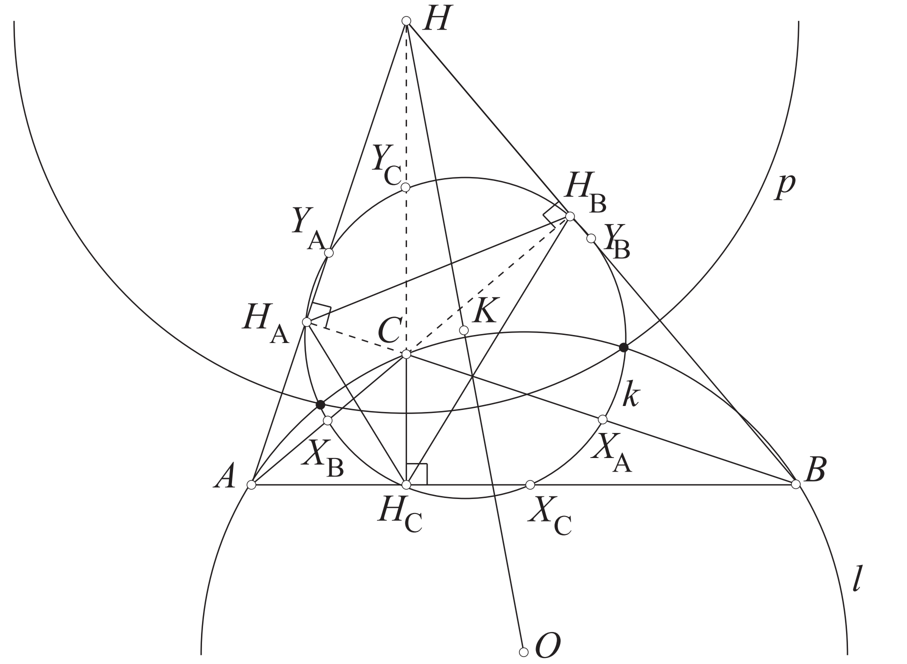

Figure 5. The Lemoine point of the triangle.

implying that

$$\frac{\sin AC'L_C\measuredangle}{\sin BC'L_C\measuredangle}=\frac{\sinh CA\ \sin CAC'\measuredangle}{\sinh CB\ \sin CBC'\measuredangle}=\frac{\sinh CA\ \cos CAO\measuredangle}{\sinh CB\ \sin CBO\measuredangle}=\frac{2\sinh\frac{CA}{2}\ \cosh\frac{CA}{2}\ \cos CAO\measuredangle}{2\sinh\frac{CB}{2}\ \cosh\frac{CB}{2}\ \sin CBO\measuredangle}=$$

$$=\frac{\sinh\frac{CA}{2}\ \cosh\frac{CA}{2}\ \frac{\tanh\frac{CA}{2}}{\tanh R}}{\sinh\frac{CB}{2}\ \cosh\frac{CB}{2}\ \frac{\tanh\frac{CB}{2}}{\tanh R}}=\frac{\sinh^2\frac{b}{2}}{\sinh^2\frac{a}{2}}=(\cosh b-1):(\cosh a-1)\,.$$

Thus the triangular coordinates of the Lemoine point are:

$$n_A(L):n_B(L):n_C(L)=(\cosh a-1):(\cosh b-1):(\cosh a-1)\,.$$

Now the symmedian point and the Lemoine point coincides for a triangle if and only if the equation array

$$\begin{aligned}(\cosh a-1)\sinh^2 b&=(\cosh b-1)\sinh^2 a,\\ (\cosh a-1)\sinh^2 c&=(\cosh c-1)\sinh^2 a\end{aligned}$$

gives an identity. Since

$$(\cosh a-1)(\cosh^2 b-1)=(\cosh a-1)(\cosh b-1)(\cosh b+1)=$$
$$=(\cosh b-1)(\cosh a-1)(\cosh a+1)=(\cosh b-1)\sinh^2 a$$

implies $a=b$, the only solution is when $a=b=c$ and the triangle is an equilateral (regular) one.

2.3. On the "Euler line".

An interesting question in elementary hyperbolic geometry is the existence of the Euler line. Known fact (see e.g. in [17]) that the circumcenter, the centroid and the orthocenter of a triangle having in a common line if and only if the triangle is isoscale. In this sense Euler line does not exist for each triangle. A nice result from the recent investigations on the triangle centers is the paper of A. V. Akopyan [1] in which the author defined the concepts of "pseudomedians" and "pseudoaltitudes" giving two new centers of the hyperbolic triangle holding a deterministic Euclidean property of Euclidean centroid and orthocenter, respectively. He proved that the circumcenter, the intersection points of the pseudomedians (pseudo-centroid), the intersection points of the pseudoaltitudes (pseudo-orthocenter) and the circumcenter of the circle through the footpoints of the bisectors (the center of the Feuerbach circle) are on a hyperbolic line. A line through a vertex is called by **pseudomedian** if divides the area of the triangle in half. (We note that in spherical geometry Steiner proved the statement that the great circles through angular points of a spherical triangle, and which bisect its area, are concurrent (see [5]). Of course the pseudomedians are not medians and their point of concurrency is not the centroid of the triangle. We call it **pseudo-centroid**. He called **pseudoaltitude** a cevian (AZ_A) with the property that with its foot Z_A on BC holds the equality

$$AZ_AB\measuredangle - Z_ABA\measuredangle - BAZ_A\measuredangle = CZ_AA\measuredangle - Z_AAC\measuredangle - ACZ_a\measuredangle,$$

where the angles above are directed, respectively. Throughout on his paper Akopyan assume that *"any two lines intersects and that three points determine a circle"*. He note in the introduction also that *"Consideration of all possible cases would not only complicate the proof, but would contain no fundamentally new ideas. To complete our arguments, we could always say that other cases follow from a theorem by analytic continuation, since the cases considered by us are sufficiently general (they include an interior point in the configuration space). Nevertheless, in the course of our argument we shall try to avoid major errors and show that the statements can be demonstrated without resorting to more powerful tools"*. We note that in our paper the reader can find this required extraction of the real elements by the ideal elements and the elements at infinity. We also defined all concepts using by Akopyan with respect to general points and lines, furthermore his lemmas and theorem can be extracted from circles onto cycles with our method. This prove the truth of Akopyan's note, post factum.

To see the equivalence of the two theory on real elements we recall that between the projective (Cayley-Klein-Beltrami) and Poincare models of the unit disk there is a natural correspondence, when we map to a line of the projective model to the line of the Poincare model with the same ends (points at infinity). On Fig. 6 we can see the corresponding mapping. A point P can be realized in the first model as the point P' and in the second one as the point P''. It is easy to see that if the hyperbolic distance of the points P and O is a then the Euclidean distances $P'O$ or $P''O$ are equals to $\tanh a$ or $\tanh(a/2)$, respectively. Thus our analytic definitions

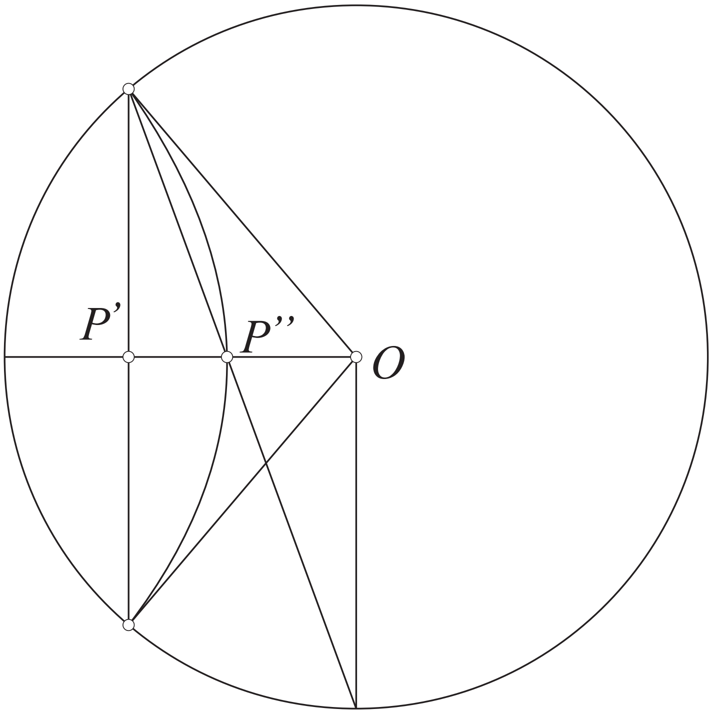

Figure 6. The connection between the projective and conformal models.

on similarity or inversion are model independent (end extracted) variations of the definitions of Akopyan, respectively. Thus we have

Theorem 2.7 ([1]). *The center O of the cycle around the triangle, the center of the cycle F around the feet of the pseudomedians, the pseudo-centroid S and the pseudo-orthocenter Z are on the same line.*

By Akopyan's opinion this is the **Euler line** of the triangle and thus he avoided the problem is to determination of the connection among the three important classical centers of the triangle. Our aim to give some analytic determination for the pseudo-centers introduced by Akopyan.

Theorem 2.8. *Let S_A, S_B, S_C be the feet of the pseudo-medians. Then we have the following formulas:*

$$\begin{array}{c} \sinh \frac{AN_C}{2} : \sinh \frac{N_CB}{2} = \cosh \frac{b}{2} : \cosh \frac{a}{2}, \\ \sinh \frac{BN_A}{2} : \sinh \frac{N_AC}{2} = \cosh \frac{c}{2} : \cosh \frac{b}{2}, \\ \sinh \frac{CN_B}{2} : \sinh \frac{N_BA}{2} = \cosh \frac{a}{2} : \cosh \frac{c}{2} \end{array} \tag{32}$$

implying that they are concurrent in a point S. We call S the ***pseudo-centroid*** *of the triangle. The triangular coordinates of the pseudo-centroid hold:*

$$n_A(R):n_B(R):n_C(R)=\frac{1}{\left(\cosh^2\frac{b}{2}\cosh^2\frac{c}{2}+\cosh\frac{a}{2}\cosh\frac{b}{2}\cosh\frac{c}{2}\right)}:$$
$$:\frac{1}{\left(\cosh^2\frac{a}{2}\cosh^2\frac{c}{2}+\cosh\frac{a}{2}\cosh\frac{b}{2}\cosh\frac{c}{2}\right)}:\frac{1}{\left(\cosh^2\frac{b}{2}\cosh^2\frac{a}{2}+\cosh\frac{a}{2}\cosh\frac{b}{2}\cosh\frac{c}{2}\right)}. \tag{33}$$

Proof. We know that

$$\cosh\frac{a}{2}\cosh\frac{b}{2}\cosh\frac{c}{2}=\frac{N^2}{\sin\alpha\sin\beta\sin\gamma\sin\delta}.$$

equation (7) says that

$$2n^2=N\sinh a\,\sinh b\,\sinh c,$$

and we also have

$$\sin\alpha\,\sin\beta\,\sin\gamma\,\sinh a\,\sinh b\,\sinh c=4nN.$$

From these equalities we get the analogous of the spherical Cagnoli's theorem:

$$\sin\delta=\frac{N^2}{\sin\alpha\sin\beta\sin\gamma\cosh\frac{a}{2}\cosh\frac{b}{2}\cosh\frac{c}{2}}=\frac{N^2\sinh a\sinh b\sinh c}{4nN\cosh\frac{a}{2}\cosh\frac{b}{2}\cosh\frac{c}{2}}=\frac{n}{2\cosh\frac{a}{2}\cosh\frac{b}{2}\cosh\frac{c}{2}}.$$

But

$$\cosh\frac{a}{2}\sinh\frac{b}{2}\sinh\frac{c}{2}=$$
$$=\sqrt{\frac{\sin(\delta+\beta)\sin(\delta+\gamma)}{\sin\gamma\,\sin\beta}}\sqrt{\frac{\sin\delta\sin(\delta+\beta)}{\sin\gamma\,\sin\alpha}}\sqrt{\frac{\sin\delta\sin(\delta+\gamma)}{\sin\alpha\,\sin\beta}}=\frac{N^2}{\sin(\delta+\alpha)\sin\alpha\sin\beta\sin\gamma},$$

implying (with the above manner) the equality

$$\sin(\delta+\alpha)=\frac{n}{2\cosh\frac{a}{2}\sinh\frac{b}{2}\sinh\frac{c}{2}}.$$

From these equalities we get

$$\frac{\sin(\delta+\alpha)}{\sin\delta}=\cos\alpha+\cot\delta\,\sin\alpha=\coth\frac{b}{2}\coth\frac{c}{2}.$$

Thus if the area of a triangle and one of its angles be given, the product of the semi hyperbolic tangents of the containing sides is given. Since the area of the examined triangles are equals to each other we get

$$\frac{n}{2\cosh\frac{a}{2}\cosh\frac{BN_C}{2}\cosh\frac{CN_C}{2}}=\frac{\sinh a\,\sinh BN_C\,\sin\beta}{4\cosh\frac{a}{2}\cosh\frac{BN_C}{2}\cosh\frac{CN_C}{2}}=\frac{\sinh\frac{a}{2}\sinh\frac{BN_C}{2}\sin\beta}{\cosh\frac{CN_C}{2}}$$

and similarly

$$\frac{n}{2\cosh\frac{b}{2}\cosh\frac{N_CA}{2}\cosh\frac{CN_C}{2}}=\frac{\sinh\frac{b}{2}\sinh\frac{N_CA}{2}\sin\alpha}{\cosh\frac{CN_C}{2}}$$

implying that

$$\sinh\frac{a}{2}\sinh\frac{BN_C}{2}\sin\beta=\sinh\frac{b}{2}\sinh\frac{N_CA}{2}\sin\alpha.$$

From this we get

$$\frac{\sinh\frac{AN_C}{2}}{\sinh\frac{N_CB}{2}}=\frac{\sinh\frac{a}{2}\sin\beta}{\sinh\frac{b}{2}\sin\alpha}=\frac{\cosh\frac{b}{2}}{\cosh\frac{a}{2}}$$

as we stated in (32). The product of the equalities in (32) gives the equality

$$\sinh\frac{AN_C}{2}\sinh\frac{BN_A}{2}\sinh\frac{CN_B}{2}=\sinh\frac{N_CB}{2}\sinh\frac{N_AC}{2}\sinh\frac{N_BA}{2}.$$

On the other hand the triangles CAN_C, N_BAB having equal areas and also have a common angle, in virtue of (32) we get

$$\tanh\frac{b}{2}\tanh\frac{AN_C}{2}=\tanh\frac{c}{2}\tanh\frac{N_BC}{2},$$

implying that

$$\tanh\frac{AN_C}{2}\tanh\frac{BN_A}{2}\tanh\frac{CN_B}{2}=\tanh\frac{N_BC}{2}\tanh\frac{N_CB}{2}\tanh\frac{N_AC}{2}.$$

So we also have

$$\cosh\frac{AN_C}{2}\cosh\frac{BN_A}{2}\cosh\frac{CN_B}{2}=\cosh\frac{N_BC}{2}\cosh\frac{N_CB}{2}\cosh\frac{N_AC}{2},$$

and as a consequence the equality

$$\sinh AN_C\sinh BN_A\sinh CN_B=\sinh N_CB\sinh N_AC\sinh N_BA.$$

Menelaos theorem now gives the existence of the pseudo-centroid.

From (32) we get

$$\frac{\cosh\frac{a}{2}}{\cosh\frac{b}{2}}=\frac{\sinh\left(\frac{c}{2}-\frac{AN_C}{2}\right)}{\sinh\frac{AN_C}{2}}=\sinh\frac{c}{2}\coth\frac{AN_C}{2}-\cosh\frac{c}{2},$$

hence

$$\coth\frac{AN_C}{2}=\frac{\cosh\frac{b}{2}\cosh\frac{c}{2}+\cosh\frac{a}{2}}{\sinh\frac{c}{2}\cosh\frac{b}{2}}$$

or equivalently

$$\cosh\frac{AN_C}{2}=\frac{\cosh\frac{b}{2}\cosh\frac{c}{2}+\cosh\frac{a}{2}}{\sinh\frac{c}{2}\cosh\frac{b}{2}}\sinh\frac{AN_C}{2}.$$

From this we get

$$1=\sinh^2\frac{AN_C}{2}\left(-1+\left(\frac{\cosh\frac{b}{2}\cosh\frac{c}{2}+\cosh\frac{a}{2}}{\sinh\frac{c}{2}\cosh\frac{b}{2}}\right)^2\right)=$$
$$=\frac{-\sinh^2\frac{c}{2}\cosh^2\frac{b}{2}+\left(\cosh\frac{b}{2}\cosh\frac{c}{2}+\cosh\frac{a}{2}\right)^2}{\sinh^2\frac{c}{2}\cosh^2\frac{b}{2}}\sinh^2\frac{AN_C}{2}=$$
$$=\frac{\cosh^2\frac{b}{2}+2\cosh\frac{a}{2}\cosh\frac{b}{2}\cosh\frac{c}{2}+\cosh^2\frac{a}{2}}{\sinh^2\frac{c}{2}\cosh^2\frac{b}{2}}\sinh^2\frac{AN_C}{2}.$$

Thus

$$\sinh AN_C=2\sinh\frac{AN_C}{2}\cosh\frac{AN_C}{2}=$$
$$=2\sinh^2\frac{AN_C}{2}\frac{\cosh\frac{b}{2}\cosh\frac{c}{2}+\cosh\frac{a}{2}}{\sinh\frac{c}{2}\cosh\frac{b}{2}}=2\frac{\sinh\frac{c}{2}\cosh\frac{b}{2}\left(\cosh\frac{b}{2}\cosh\frac{c}{2}+\cosh\frac{a}{2}\right)}{\cosh^2\frac{b}{2}+2\cosh\frac{a}{2}\cosh\frac{b}{2}\cosh\frac{c}{2}+\cosh^2\frac{a}{2}}.$$

Hence we also have

$$\sinh N_CB=2\frac{\sinh\frac{c}{2}\cosh\frac{a}{2}\left(\cosh\frac{a}{2}\cosh\frac{c}{2}+\cosh\frac{b}{2}\right)}{\cosh^2\frac{a}{2}+2\cosh\frac{a}{2}\cosh\frac{b}{2}\cosh\frac{c}{2}+\cosh^2\frac{b}{2}}$$

implying that

$$n_B(N):n_A(N)=(AN_CB)=$$
$$=\left(\cosh^2\frac{b}{2}\cosh\frac{c}{2}+\cosh\frac{b}{2}\cosh\frac{a}{2}\right):\left(\cosh^2\frac{a}{2}\cosh\frac{c}{2}+\cosh\frac{a}{2}\cosh\frac{b}{2}\right)=$$
$$=\left(\cosh^2\frac{b}{2}\cosh^2\frac{c}{2}+\cosh\frac{a}{2}\cosh\frac{b}{2}\cosh\frac{c}{2}\right):\left(\cosh^2\frac{a}{2}\cosh^2\frac{c}{2}+\cosh\frac{a}{2}\cosh\frac{b}{2}\cosh\frac{c}{2}\right).$$

From this we get

$$n_A(N):n_B(N)=$$
$$=\frac{1}{\left(\cosh^2\frac{b}{2}\cosh^2\frac{c}{2}+\cosh\frac{a}{2}\cosh\frac{b}{2}\cosh\frac{c}{2}\right)}:\frac{1}{\left(\cosh^2\frac{a}{2}\cosh^2\frac{c}{2}+\cosh\frac{a}{2}\cosh\frac{b}{2}\cosh\frac{c}{2}\right)}.$$

Similarly we get

$$n_B(N):n_C(N)=$$
$$=\frac{1}{\left(\cosh^2\frac{c}{2}\cosh^2\frac{a}{2}+\cosh\frac{c}{2}\cosh\frac{b}{2}\cosh\frac{a}{2}\right)}:\frac{1}{\left(\cosh^2\frac{b}{2}\cosh^2\frac{a}{2}+\cosh\frac{a}{2}\cosh\frac{b}{2}\cosh\frac{c}{2}\right)}$$

as we stated in (33). □

Remark 2.9. We note that there are many Euclidean theorems that can be investigated on the hyperbolic plane by our more–less trigonometric way. We note that on the hyperbolic plane the usual isoptic property of the circle lost (see [6]) and thus all the Euclidean statements using this property can be investigated only in the way mentioned in [1]. To that we can use trigonometry in this method we can concentrate on the introduced concept of angle sums which in a trigonometric calculation can be handed well. Thus the isoptic property of a cycle (or which is the same the cyclical property of a set of points) can lead for new hyperbolic theorems suggested by known Euclidean analogy.

Acknowledgement. Thank you Vojtech Bálint for helpful comment to this article.

References

[1] Akopyan A. V., *On some classical constructions extended to hyperbolic geometry*, 2011, http://arxiv.org/abs/1105.2153.

[2] Bell A., *Hansen's Right Triangle Theorem, Its Converse and a Generalization*, Forum Geometricorum **6**, (2006), 335–342.

[3] Cayley A., *Analytical Researches Connected with Steiner's Extension of Malfatti's Problem*, Phil. Trans. of the Roy. Soc. of London, **142**, (1852), 253–278.

[4] Casey J., *A sequel to the First Six Books of the Elements of Euclid, Containing an Easy Introduction to Modern Geometry with Numerous Examples*, 5th. ed., Hodges, Figgis and Co., Dublin, 1888.

[5] Casey J., *A treatise on spherical trigonometry, and its application to Geodesy and Astronomy, with numerous examples*, Hodges, Figgis and CO., Grafton-ST. London: Longmans, Green, and CO., 1889.

[6] Csima G., Szirmai J., *Isoptic curves of conic sections in constant curvature geometries*, http://arxiv.org/pdf/1301.6991v2.pdf.

[7] Dörrie H., *Triumph der Mathematik*, Physica-Verlag, Würzburg, 1958.

[8] Horváth G. Á., *Malfatti's problem on the hyperbolic plane*, Studia Sci. Math., (2014), DOI: 10.1556/SScMath.2014.1276.

[9] Horváth G. Á., *Hyperbolic plane-geometry revisited*, (submitted), 2014.

[10] Horváth G. Á., *Addendum to the paper "Hyperbolic plane-geometry revisited"*, http://www.math.bme.hu/~ghorvath/hyperbolicproofs.pdf.

[11] Hart A. S., *Geometric investigations of Steiner's construction for Malfatti's problem*, Quart. J. Pure Appl. Math. **1**, (1857), 219–221.

[12] Johnson R. A., *Advanced Euclidean Geometry, An elementary treatise on the geometry of the triangle and the circle*, Dover Publications, Inc. New York, (The first edition published by Houghton Mifflin Company in 1929), 1960.
[13] Malfatti G., *Memoria sopra un problema sterotomico*, Memorie di Matematica e di Fisica della Società Italiana delle Scienze, **10**, (1803), 235–244.
[14] Molnár E., *Inversion auf der Idealebene der Bachmannschen metrischen Ebene*, Acta Math. Acad. Sci. Hungar. **37/4**, (1981), 451–470.
[15] Steiner J., *Steiners gesammelte Werke*, (herausgegeben von K. Weierstrass), Berlin, 1881.
[16] Steiner J., *Einige geometrische Betrachtungen*, Journal für die reine und angewandte Mathematik **1/2**, (1826), 161–184, **1/3**, (1826), 252–288.
[17] Szász P., *Introduction to Bolyai-Lobacsevski's geometry* (Hungarian), 1973.
[18] Vörös C., *Analytic Bolyai's geometry* (Hungarian), Budapest, 1909.

Ákos G. Horváth, Department of Geometry, Budapest University of Technology, Egry József u. 1., H-1111 Budapest, Hungary,

E-mail address: `ghorvath@math.bme.hu`

Studies of the University of Žilina
Mathematical Series
Vol. 27/2015, 35–62

THE EUCLIDEAN VISUALIZATION AND PROJECTIVE MODELLING THE 8 THURSTON GEOMETRIES

E. MOLNÁR, I. PROK AND J. SZIRMAI

Abstract. The so-called *Thurston geometries are well known.* Here $\mathbf{E}^3$, $\mathbf{S}^3$ and $\mathbf{H}^3$ are the classical spaces of constant zero, positive and negative curvature, respectively; $\mathbf{S}^2\times\mathbf{R}$, $\mathbf{H}^2\times\mathbf{R}$ are direct product geometries with $\mathbf{S}^2$ spherical and $\mathbf{H}^2$ hyperbolic base plane, respectively, and a distinguished $\mathbf{R}$-line with usual $\mathbf{R}$-metric; $\widetilde{\mathbf{SL_2R}}$ and **Nil** with a twisted product of $\mathbf{R}$ with $\mathbf{H}^2$ and $\mathbf{E}^2$, respectively; furthermore **Sol** as a twisted product of the Minkowski plane $\mathbf{M}^2$ with $\mathbf{R}$. So that we have in each an infinitesimal (positive definite) Riemann metric, invariant under certain translations, guaranteing homogeneity in every point.

These translations are commuting only in $\mathbf{E}^3$, in general, but a discrete (discontinuous) translation group – as a lattice – can be defined with compact fundamental domain in Euclidean analogy, but with some different properties. The additional symmetries can define crystallographic groups with compact fundamental domain, again in Euclidean analogy, moreover nice tilings, packings, material possibilities, etc.

We emphasize some surprising facts. In **Nil** and in $\widetilde{\mathbf{SL_2R}}$ there are orientation preserving isometries, only. In **Nil** we have a lattice-like ball packing (with kissing number 14) denser than the Euclidean densest one [12, 19]. Moreover, in [23] we have formulated a conjectute in $\mathbf{S}^2\times\mathbf{R}$ for the densest geodesic ball packing with equal balls for all Thurston geometries. In **Sol** geometry there are 17 Bravais types of lattices, but depending on an infinite natural parameter $N>2$ [13]. Except $\mathbf{E}^3$, $\mathbf{S}^3$, $\mathbf{S}^2\times\mathbf{R}$, $\mathbf{H}^2\times\mathbf{R}$ there is no exact classification result for possible crystallographic groups.

Our projective spherical model, initiated in [10], is based on linear algebra over the real vector space $\mathbf{V}^4$ (for points) and its dual $\boldsymbol{V}_4$ (for planes), upto positive real factor, so that the proper dimension is 3, indeed. We illustrate and visualize the topic in the Euclidean screen of computer with some new pictures mainly in $\mathbf{H}^3$, $\widetilde{\mathbf{SL_2R}}$, **Sol** and **Nil** on the base of our publications [5, 6, 13, 16, 20, 21, 23].

After a more popular introduction to the classical projective space, we shall illustrate our topic more sketchily by figures and hints to our former works. As a new initiative, we give a fresh interpretation of **Nil** geometry on the base of [2] and [11].

Received December 22, 2014.

2000 *Mathematics Subject Classification.* Primary 15A75, 51N15, 65D18, 68U10, 52C17, 52C22, 52B15.

Key words and phrases. Thurston geometries, Euclidean-projective visualization, discrete geometrical problems in Thurston geometries.

This work was supported by the Visegrad Found, small grant 11420082.

1. On the classical projective geometry in $\mathbf{E}^3$

Analyzing the viewing process of a painter, Leonardo da Vinci and Albrecht Dürer ($\sim$ 1520) made the model of *practical perspective* in Fig. 1, 2. Here the (one) eye S of a painter looks at a (say) horizontal base plane Σ (e.g. the triangle ABC). and describes it on a vertical (say first) *picture plane* Π imitating the light rays into his eye S trough Π which meet it in the image points A', B', C', respectively.

We introduce the so-called *box model* with two additional planes through S with intersection line s: the *eye plane*, parallel to Σ meeting Π in the line l', *horizontal line*, and the *support plane*, parallel to Π meeting Σ in the line t, *pedal line*. The intersection line $x = \Sigma \cap \Pi$ is called axis, each of its points is fixed at this projection.

As a parallel line e to BC on Σ (in Fig. 1 (a) shows, its image e' in Π intersects $B'C'$ in I' on the horizontal line l', so that $SI' \parallel BC \parallel e$. This insists us to introduce a new point of Σ, the *ideal point* I, common with lines BC, e and SI', so that I' is just the image of this ideal point I on l' at the projection from S. Thinking of other parallel lines (as in a pencil) of Σ, we can introduce their new ideal point and its analogous image on l' at this projection.

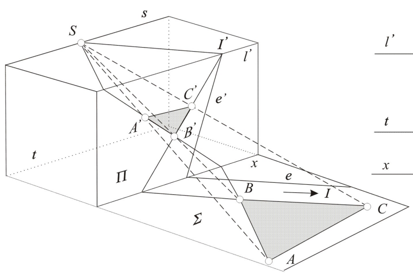

(a)

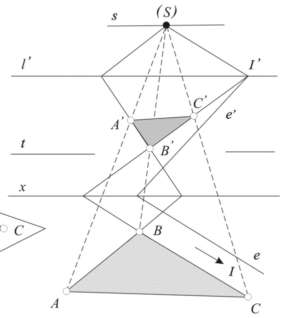

(b)

Figure 1. Box model and the "pushing" procedure.

The next step in the abstraction, that we consider the collection of ideal points in Σ as belonging to a new ideal line l of Σ, so that the horizontal line l' is just the image of this line l at the projection from S. Parallel planes will have common ideal line, so as Σ and the eye plane through S have the common ideal line l. Analyzing further the above situation, we see that the above pedal line t of Σ and of the support plane can be considered as *preimage* of the ideal line t' of the picture plane Π at the projection from S. This latter mapping then becomes a bijective one $\pi:\ \Sigma \cup l \to \Pi \cup t'$ between the extended planes, called then *projective planes*, with the same simpler notation.

Furthermore, any ideal line belongs to a parallel plane pencil. Then we unite all ideal lines to a unique *ideal plane* so that the Euclidean space $\mathbf{E}^3$ extends to a *projective space* $\mathcal{P}^3$.

The box model in Fig. 1 (a) is, and will be, the base of our further considerations. E.g. "pushing" together the side planes around the lines x, l', s, t onto the picture plane Π in Fig. 1 (b), we get an important construction mapping of the united $\Sigma = \Pi$ onto itself, from the above one with the same notations

$$A \to A',\ B \to B',\ C \to C',\ I \to I',\ e \to e',\ l \to l',\ t \to t',\ \text{etc.}$$

The derived mapping will be a *central axial collineation* with x as *axis*, where any line and its image line intersect; and with a *centre* (S), where the rays AA', BB', CC', $\ldots$, XX' meet, for any point X and its image X'. It turns out, from the above pushing procedure, that the centre (S) will be just the rotated image of the eye S about the horizontal line l' (compare Fig. 1 (a), (b).

Fig. 2 (a) shows, how to construct the picture of a cube by the above procedure, the height h of the cube is equal to the side of the rotated base square. The line x_h is the new axis for the upper face of the cube ($x \parallel x_h$ in distance h).

Fig. 2 (b) shows a principal procedure, used by the renaissance painters: For a given convex quadrangle $A'B'C'D'$, not a parallelogramme, construct the eye point S, so that $A'B'C'D'$ be a projection of a square $ABCD$ from S. First the "horizontal" line l' can be constructed by the intersection points $A'B' \cap D'C'$ and $A'D' \cap B'C'$. Then (S) will be the intersection of two Thales half-circles. Comparing with Fig. 1, we obtain S by a spacial construction, up to similarity.

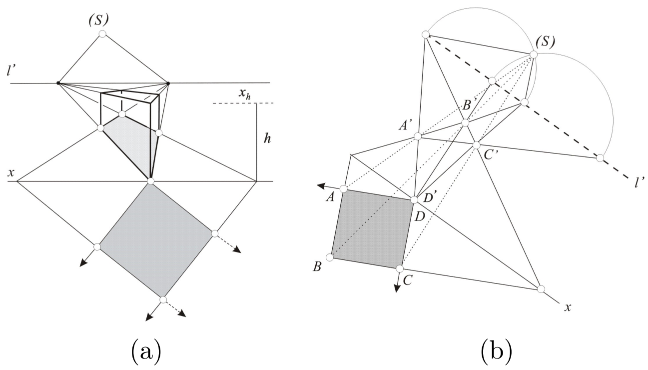

Figure 2. (a) How to picture a cube. (b) A quadrangle $A'B'C'D'$ can be the image of a square $ABCD$.

The practical perspective above is called also of *two direction points*. The integer coordinate pairs of an *infinite chess board* of Σ will be preserved in the quadrangle net at the projection in Fig. 2 (b). Imagine the origin at D (and D'), DA is the coordinate axis (new) x, DC is the y axis, so as $D'A' \to x'$ $D'C' \to y'$, respectively. The repeated quadrangles accumulate near the horizontal line l'. The "other side" of l' and "near the ideal line t'" the situation is not clear yet. This is why we shall prefer the so called homogeneous coordinate simplex later on (from Sect. 2).

At the cube picture in Fig. 2 (a) we can imagine also a spacial coordinate system, where the third z-axis is parallel to the picture plane Π. The so called *central* *or projective axonometry*, or also called *perspective of three direction points* will generalize the previous method. These ideas were also known for the renaissance painters.

We look at Fig. 3 (a) the picture plane Π, the eye S in distance d with orthogonal projection S_0, the distance circle centred in S_0 with radius $d = SS_0$. Space will be described by a Cartesian coordinate system . Its origin E_0 shall be in Π for simplicity; E_1^∞, E_2^∞, E_3^∞ are the ideal points of the coordinate axes x, y, z, respectively. E_{10}, E_{20}, E_{30}, are the corresponding unit points. Our task is to describe the projections from S into Π, so that the spacial situation has to be reconstructed from the picture, as Fig. 4 indicates it.

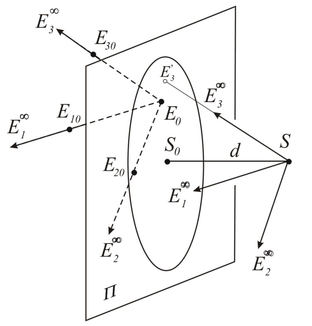

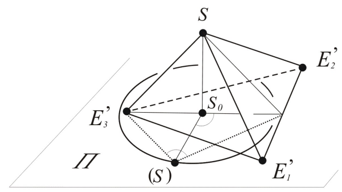

Figure 3. (a) General projection of a coordinate system E_0 E_1^∞ E_2^∞ E_3^∞. (b) Construction scheme for Fig. 4.

To this we translate the coordinate system to the eye S, so that $E_0 \to S$ and we determine the images $E_1' = U_x'$, $E_2' = U_y'$, $E_3' = U_z'$ of the ideal (infinite = unendliche in German) points of the axes, first in Fig. 3 (b), then in Fig. 4. Comparing these two figures, we see that a prescribed acute angle triangle $E_1'E_2'E_3'$ will define the situation above. Namely, the orthocentre (height point) of this latter triangle will be just S_0, and the distance $d = SS_0$ can be reproduced by the Thales half-circle over any height segment as diagonal (see Fig. 3 (b); the construction is not indicated over $E_3'T_3$ in Fig. 4: e.g. $d^2 = E_3'S_0 \cdot S_0T_3$).

The box model, now with not orthogonal base plane and picture plane can be applied also now for constructing the image unit points E_{10}', E_{20}', E_{30}'. By rotation of the coordinate plane, first $E_0E_1^\infty E_3^\infty$ with the eye plane $SE_1'E_3'$ about its horizontal line $E_1'E_3'$ and about axis through $E_0 = E_0'$ (a parallel to $E_1'E_3'$, not indicated in Figure 4), we get the rotated $(S)_2$ and $E_0(E_{10})_2 \parallel (S)_2E_1'$ and $E_0(E_{30})_2 \parallel (S)_2E_3'$. Then we get E_{10}' on the line $(S)_2(E_{10})_2$ and we get E_{30}' on the line $(S)_2(E_{30})_2$. Similar construction provides E_{20}' (and again E_{30}') from the rotation of the coordinate plane $E_0E_2^\infty E_3^\infty$ together with the eye plane $SE_2'E_3'$ about $E_2'E_3'$ and about its parallel through $E_0 = E_0'$ (first we get $(S)_1$ then $E_0(E_{20})_1 \parallel (S)_1E_2'$, then E_{20}' on $(S)_1(E_{20})_1$).

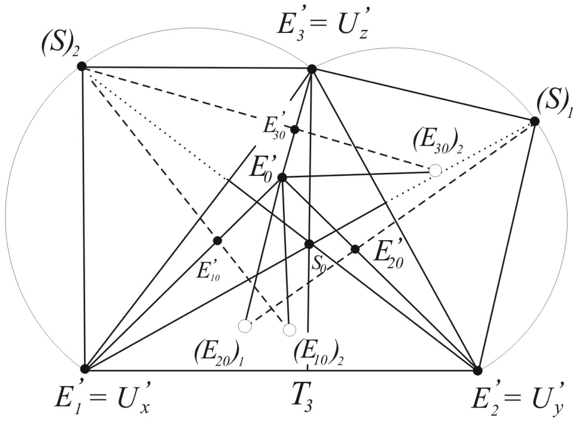

Figure 4. The basic constructions of central axonometry.

These classical drawing methods belong to mastership of an "old" architect. See e.g. the paper [25] of our architect colleague, *Mihály Szoboszlai.* Fig. 5 illustrates this construction by the computer program `AUTOCAD`. As an extra home work our MSC student, *Bettina Szukics* (2011) made a phantasy picture on the Paris' Triumphal Arch. Nowadays computer algorithms, on the base of homogeneous coordinates by linear algebra, are much more effective. This modern machinery will be applied in the following, by shorter introduction for the more experienced reader.

2. The projective sphere and plane modelled in Euclidean 3-space

All the Thurston 3-geometries will be uniformly modelled in the *projective spherical space* $\mathcal{PS}^3$ that can be embedded into the affine so into the *Euclidean 4-space.* Our main tool will be a 4-dimensional vector space $\mathbf{V}^4$ over the real numbers $\mathbf{R}$ with basis $\{\mathbf{e}_0, \mathbf{e}_1, \mathbf{e}_2, \mathbf{e}_3\}$, which is not assumed to be orthonormal.

Our goal will be to introduce *convenient additional structures* on $\mathbf{V}^4$ and on its dual $\boldsymbol{V}_4$.

The method will be illustrated and visualized first in dimensions 2 (Fig. 6) where $\mathbf{V}^3$ is the embedding real vector space with its affine picture $\mathcal{A}(O, \mathbf{V}^3, \boldsymbol{V}_3)$, so in $\mathbf{E}^3$. Let $\{O;\ \mathbf{e}_0, \mathbf{e}_1, \mathbf{e}_2\}$, be a *coordinate system* in the affine 3-space $\mathcal{A}^3 = \mathbf{E}^3$ with origin O and a (not necessarily orthonormal) vector basis $\{\mathbf{e}_0, \mathbf{e}_1, \mathbf{e}_2\}$, for $\mathbf{V}^3$, where our affine model plane $\mathcal{A}^2 = \mathbf{E}^2 \subset \mathcal{P}^2 = \mathcal{A}^2 \cup (\boldsymbol{i})$ is placed to the point $E_0(\mathbf{e}_0)$ with equation $x^0 = 1$. Here any non-zero vector $\mathbf{x} = x^0\mathbf{e}_0 + x^1\mathbf{e}_1 + x^2\mathbf{e}_2 =: x^i\mathbf{e}_i$ (the index convention of Einstein-Schouten will be used) represents a point $X(\mathbf{x})$ of $\mathcal{A}^2$, but also a point of the *projective sphere* $\mathcal{PS}^2$ after having introduced the following *positive equivalence.* For non-zero vectors $\mathbf{x} \sim c\mathbf{x}$ with $0 < c \in \mathbf{R}$ represent the same point

$$X = (\mathbf{x} \sim c\mathbf{x}) \text{ of } \mathcal{PS}^2; \quad \mathbf{z} \sim 0\,\mathbf{e}_0 + z^1\mathbf{e}_1 + z^2\mathbf{e}_2$$

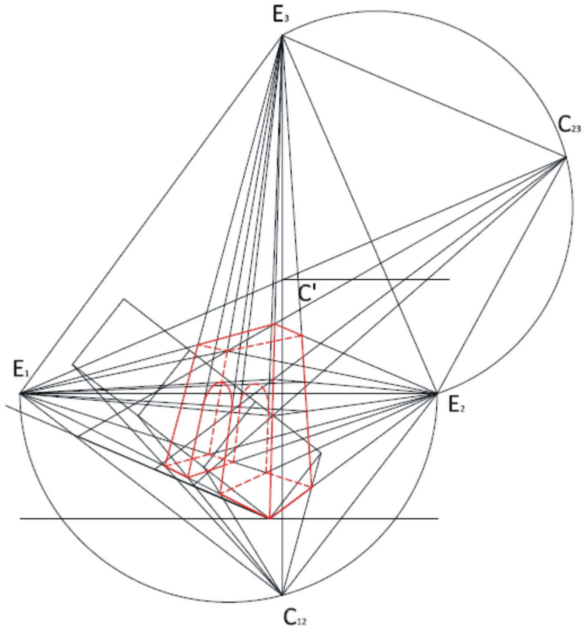

Figure 5. "The Triumphal Arch" in central axonometry.

will be an ideal point $(\mathbf{z})$ of $\mathcal{PS}^2$ to $\mathcal{A}^2$.

We write: $(\mathbf{z}) \in (\boldsymbol{i})$, where $(\boldsymbol{i})$ is the ideal line (circle) to $\mathcal{A}^2$, extending the affine plane $\mathcal{A}^2$ into the projective sphere $\mathcal{PS}^2$. Here $(\mathbf{z})$ and $(-\mathbf{z})$, and in general $(\mathbf{x})$ and $(-\mathbf{x})$, are opposite points of $\mathcal{PS}^2$. Then *identification* of the opposite point pairs of $\mathcal{PS}^2$ leads to the projective plane $\mathcal{P}^2$. Thus the embedding $\mathcal{A}^2 = \mathbf{E}^2 \subset \mathcal{P}^2 \subset \mathcal{PS}^2$ can be formulated in the vector space $\mathbf{V}^3$ in a unified way. We can present $\mathcal{PS}^2$ in Fig. 6 also as a usual sphere (of arbitrary radius) and think of the *celestial sphere* as the map of stars of the *Universe*. The equator $(x^0 = 0)$ represents the ideal points to $\mathcal{A}^2$, as ideal line (circle). The *upper half-sphere* describes $\mathcal{A}^2 = \mathbf{E}^2$ with $x^0 = 1$. We also see how the *double affine plane* describes $\mathcal{PS}^2$, as the opposite direction in the abstraction (see also the lower plane $x^0 = -1$ in Fig. 6).

Remark 2.1. *The above* 3*-dimensional embedding of the Euclidean, or the more general affine plane, to characterize the ideal (infinite) points as well, comes from the previous practical perspective. But there are some surprising facts in the history of projective geometry which show that a* 2*-dimensional plane cannot always embed into a 3-dimensional space. This topic, on the role of Desargues theorem (axiom) in the* 2*-dimensional affine-projective geometry, illustrate also the barrier of visuality in geometry and in mathematics, in general. We do not mention more details in this paper.*

The dual (form) space $\boldsymbol{V}_3$ to $\mathbf{V}^3$ is defined as the set of *real valued linear functionals* or forms on $\mathbf{V}^3$. That means that we pose the following requirements for any form $\boldsymbol{u} \in \boldsymbol{V}_3$

$$\boldsymbol{u} : \mathbf{V}^3 \ni \mathbf{x} \mapsto \mathbf{x}\boldsymbol{u} \in \mathbf{R}$$

with linearity

$$(a\mathbf{x} + b\mathbf{y})\boldsymbol{u} = a(\mathbf{x}\boldsymbol{u}) + b(\mathbf{y}\boldsymbol{u})$$

for any $\mathbf{x}, \mathbf{y} \in \mathbf{V}^3$ and for any $a, b \in \mathbf{R}$.

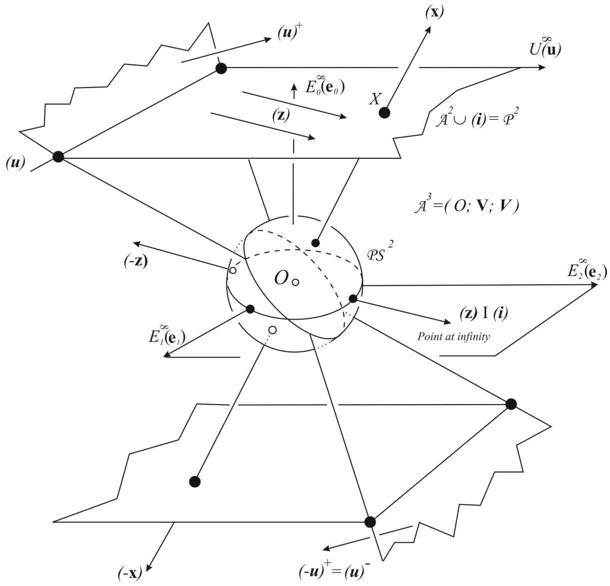

Figure 6. Our scene for dimensions 2 with projective sphere $\mathcal{PS}^2$ embedded into the real vector space $\mathbf{V}^3$ and its dual $\boldsymbol{V}_3$.

We emphasize our convention. *The vector coefficients are written from the left, then linear forms act on vectors on the right (as an easy associativity law, analogous conventions will be applied also later on).*

This “built in” linear structure allows us to define the addition $\boldsymbol{u} + \boldsymbol{v}$ of two linear forms $\boldsymbol{u}$, $\boldsymbol{v}$, and the multiplication $\boldsymbol{u}c$ of a linear form $\boldsymbol{u}$ by a real factor c, both resulting in linear forms of $\boldsymbol{V}_3$. Moreover,we can define for any basis $\{\mathbf{e}_i\}$ in $\mathbf{V}^3$ the *dual basis* $\{\boldsymbol{e}^j\}$ in $\boldsymbol{V}_3$ by the Kronecker symbol δ_i^j:

$$\mathbf{e}_i\boldsymbol{e}^j = \delta_i^j = \begin{cases} 1, & \text{if } i = j, \\ 0, & \text{if } i \neq j, \end{cases} \qquad i, j = 0, 1, 2.$$

Furthermore, we see that the general linear form $\boldsymbol{u} := \boldsymbol{e}^0 u_0 + \boldsymbol{e}^1 u_1 + \boldsymbol{e}^2 u_2 := \boldsymbol{e}^j u_j$ takes on the vector $\mathbf{x} := x^0\mathbf{e}_0 + x^1\mathbf{e}_2 + x^2\mathbf{e}_2 := x^i\mathbf{e}_i$ the real value

$$(x^i\mathbf{e}_i)(\boldsymbol{e}^j u_j) = x^i(\mathbf{e}_i\boldsymbol{e}^j)u_j = x^i\delta_i^j u_j = x^i u_j := x^0u_0 + x^1u_1 + x^2u_2.$$

Thus, a linear form $\boldsymbol{u} \in \boldsymbol{V}_3$ describes a *2-dimensional subspace* u, i.e. a vector plane of $\mathbf{V}^3$ through the origin. Moreover, forms

$$\boldsymbol{u} \sim \boldsymbol{u}k \text{ with } 0 < k \in \mathbf{R}$$

describe the same oriented plane of $\mathbf{V}^3$.

As in Fig. 6 a positive equivalence class of forms $(\boldsymbol{u})$ gives an open *half-space* $(\boldsymbol{u})^+$ of $\mathbf{V}^3$, i.e. the vector classes $(\mathbf{x})$ for which

$$(\boldsymbol{u})^+ : \{(\mathbf{x}) : \mathbf{x}\boldsymbol{u} > 0\}.$$

This gives also a corresponding half-sphere of $\mathcal{PS}^2$, and a corresponding half-plane of $\mathcal{A}^2$.

In order to concentrate on our main goal, we introduce a *bijective linear mapping* $\mathbf{T}$ of $\mathbf{V}^3$ onto itself, i.e.

$$\mathbf{T} : \mathbf{V}^3 \ni \mathbf{x} \mapsto \mathbf{x}\mathbf{T} =: \mathbf{y} \in \mathbf{V}^3$$

with requirements

$$x^i\mathbf{e}_i \mapsto (x^i\mathbf{e}_i)\mathbf{T} = x^i(\mathbf{e}_i\mathbf{T}) = x^i t_i^j \mathbf{e}_j =: y_j\mathbf{e}_j, \quad \det(t_i^j) \neq 0.$$

Assume that $\mathbf{T}$ has the above matrix (t_i^j) with respect to basis $\{\mathbf{e}_i\}$ of $\mathbf{V}^3$ $(i, j = 0, 1, 2)$. Then $\mathbf{T}$ defines a *projective point transformation* $\tau(\mathbf{T})$ of $\mathcal{PS}^2$ onto itself, which *preserves all the incidences of subspaces* of $\mathbf{V}^3$ and so *incidences of points and lines of* $\mathcal{PS}^2$, respectively. The matrix (t_i^j) and its positive multiples $(ct_i^j) = (t_i^j c)$ with $0 < c \in \mathbf{R}$ (and only these mappings) define the same point transformation $\tau(\mathbf{T} \sim \mathbf{T}c)$ of $\mathcal{PS}^2$ by the above requirements. As usual, we define the composition, or product, of transforms $\mathbf{T}$ and $\mathbf{W}$ of vector space $\mathbf{V}^3$ in the order (right action on $\mathbf{V}^3$) by

$$\mathbf{TW} : \mathbf{V}^3 \ni \mathbf{x} \to (\mathbf{xT})\mathbf{W} = \mathbf{yW} = \mathbf{z} =: \mathbf{x}(\mathbf{TW})$$

with matrices (t_i^j) and (w_j^k) to basis $\{\mathbf{e}_i\}$ $(i, j, k = 0, 1, 2)$ as follows by our index conventions:

$$\mathbf{e}_i(\mathbf{TW}) = (\mathbf{e}_i\mathbf{T})\mathbf{W} = (t_i^j\mathbf{e}_j)\mathbf{W} = (t_i^j)(w_j^k\mathbf{e}_k) = (t_i^j w_j^k)\mathbf{e}_k,$$

etc. with summation (from 0 to 2) for the occurring equal upper and lower indices. Moreover, we get the group of linear transforms of $\mathbf{V}^3$ in the usual way, and so the group of projective transforms of $\mathcal{PS}^2$ and $\mathcal{P}^2$, accordingly.

We also mention that the *inverse matrix class* of above (t_i^j), now denoted by $(T_j^k) \sim \frac{1}{c}T_j^k$, with $t_i^j T_j^k = \delta_i^k$ *induces the corresponding linear transform* $\boldsymbol{T}$ *of the dual* $\boldsymbol{V}_3$ *(i.e. for lines) onto itself, and its inverse* $\boldsymbol{T}^{-1}$, i.e. in

$$\boldsymbol{T} : \mathbf{V}^3 \ni \boldsymbol{v} \mapsto \boldsymbol{T}\boldsymbol{v} =: \boldsymbol{u} \in \boldsymbol{V}_3 \quad \text{so that } \mathbf{y}\boldsymbol{v} = (\mathbf{xT})\boldsymbol{v} = \mathbf{x}(\boldsymbol{T}\boldsymbol{v}) = \mathbf{x}\boldsymbol{u},$$

especially $0 = \mathbf{x}\boldsymbol{u} = (\mathbf{xT})(\boldsymbol{T}^{-1}\boldsymbol{u}) = \boldsymbol{y}\boldsymbol{v}$, so

$$0 = \mathbf{y}\boldsymbol{v} = (\mathbf{y}\mathbf{T}^{-1})(\boldsymbol{T}\boldsymbol{v}) = \mathbf{x}\boldsymbol{u}, \quad X\mathrm{I}u \leftrightarrow Y := X\tau\mathrm{I}v := \tau u \tag{1}$$

hold for the τ-images of points and lines, respectively. We can see that the induced action on the dual $\boldsymbol{V}_3$ is a *left action* and so is the induced action on the lines of $\mathcal{PS}^2$. This is according to our conventions, may be strange a little bit at the first glance, but we will utilize some benefits in the next sections.

3. Line → point polarity describing orthogonality of lines for $\mathbf{S}^2$, $\mathbf{E}^2$, $\mathbf{M}^2$, $\mathbf{G}^2$ and $\mathbf{H}^2$ geometries

Till now we have not considered *metric (distance, angle) problems* of our model plane in $\mathcal{PS}^2$. As we shall see, this will be related to the additional structure of the vector space $\mathbf{V}^3$ and that of its dual $\boldsymbol{V}_3$ (see e.g. in [1, 12]).

In our suggested interpretation the concept of polarity $\Pi(_*)$ has some advantages, considered as a linear symmetric mapping of the dual (form) space $\boldsymbol{V}_3$ into the starting vector space $\mathbf{V}^3$. Thus we associate with any (polar) line $u(\boldsymbol{u})$ its (pole) point $U(\mathbf{u})$ of $\mathcal{PS}^2$ as follows

$$\Pi(_*) : \boldsymbol{V}_3 \ni \boldsymbol{u} \mapsto \boldsymbol{u}_* =: \mathbf{u} \in \mathbf{V}^3$$

by the matrix π^{ij} to the dual basis pair $\{\boldsymbol{e}^i\}$, $\{\mathbf{e}_j\}$; $\mathbf{e}_j\boldsymbol{e}^i = \delta^i_j$ $(i,j = 0,1,2,)$, according to $\boldsymbol{e}^i \mapsto \boldsymbol{e}^i_* =: \mathbf{e}^i = \pi^{ij}\mathbf{e}_j$ with symmetry requirement $\pi^{ij} = \pi^{ji}$, thus

$$\boldsymbol{u} = \boldsymbol{e}^i u_i \to (\boldsymbol{e}^i u_i)_* = u_i \boldsymbol{e}^i_* = u_i \pi^{ij}\mathbf{e}_j =: u^j \mathbf{e}_j.$$

At the same time, we can introduce a symmetric bilinear scalar product by this polarity (and vice versa, equivalently):

$$\langle\ ,\ \rangle : \boldsymbol{V}_3 \times \boldsymbol{V}_3 \to \mathbf{R},\ \langle \boldsymbol{u}, \boldsymbol{v}\rangle = (\boldsymbol{u}_*)\boldsymbol{v} = \mathbf{u}\boldsymbol{v} \in \mathbf{R},$$
$$\langle \boldsymbol{u}, \boldsymbol{v}\rangle = \langle \boldsymbol{e}^i u_i, \boldsymbol{e}^j v_j\rangle = (u_i \boldsymbol{e}^i_*)(\boldsymbol{e}^j v_j) = u_i \pi^{ir}\delta^i_r v_j = u_i \pi^{ij} v_j.$$

This shows the usual computations and the symmetry $\langle \boldsymbol{u}, \boldsymbol{v}\rangle = \langle \boldsymbol{v}, \boldsymbol{u}\rangle$ as well.

Now we say that the line $u(\boldsymbol{u})$ is perpendicular or orthogonal to line $v(\boldsymbol{v})$, if the pole $(\boldsymbol{u}_*) = (\mathbf{u}) = U$ is incident to line $v(\boldsymbol{v})$. Then $0 = \boldsymbol{u}_*\boldsymbol{v} = \langle \boldsymbol{u}, \boldsymbol{v}\rangle = \langle \boldsymbol{v}, \boldsymbol{u}\rangle = \boldsymbol{v}_*\boldsymbol{u}$, so the pole $V(\mathbf{v})$ of $v(\boldsymbol{v})$ is also incident to $u(\boldsymbol{u})$, showing the symmetry of orthogonality as well.

Now we can define the classical plane geometries $\mathbf{S}^2$, $\mathbf{E}^2$, $\mathbf{H}^2$ in our "model plane" $\mathcal{PS}^2$ according to Fig. 6 and Fig. 7.

First, we geometrize the dual basis pair $\{\mathbf{e}_i\}$, $\{\boldsymbol{e}^j\}$ with $\mathbf{e}_i\boldsymbol{e}^j = \delta^j_i$ by introducing a coordinate triangle (simplex, in more general) with vertices $E_0(\mathbf{e}_0)$, $E_1(\mathbf{e}_1)$, $E_2(\mathbf{e}_2)$, and sides

$$e^0(\boldsymbol{e}^0) = E_1E_2, \quad e^1(\boldsymbol{e}^1) = E_2E_0, \quad e^2(\boldsymbol{e}^2) = E_0E_1.$$

Because of the positive equivalence, we also introduce the so-called *unit point* $E(\mathbf{e} \sim \mathbf{e}_0 + \mathbf{e}^1 + \mathbf{e}^2)$ and unit line $e(\boldsymbol{e} \sim \boldsymbol{e}_0 + \boldsymbol{e}^1 + \boldsymbol{e}^2)$ to fix the representative basis vectors $\{\mathbf{e}_i\}$ and basis forms $\{\boldsymbol{e}^j\}$ up to a common positive constant factor, say c to $\{\mathbf{e}_i\}$ and $\frac{1}{c}$ to $\{\boldsymbol{e}^j\}$; $(i,j = 0,1,2)$. This *projective freedom* provides benefits for later simplifications.

Now by symmetry of the polarity matrix π^{ij} above, it is well known (*Inertia law of Sylvester*), that π^{ij} has a so called diagonal form $\pi^{i'j'}$ to an appropriate dual basis pair $\{\mathbf{e}_{i'}\}$, $\{\boldsymbol{e}^{j'}\}$, $(i', j' = 0', 1', 2')$ Here primes refer to a linear basis change

(Schouten's primed index conventions). That means $\mathbf{e}_{j'}\boldsymbol{e}^{i'} = \delta^{i'}_{j'}$ (Kronecker) and

$$\boldsymbol{e}^{i'}_{*} \mapsto \mathbf{e}^{i'} = \pi^{i'j'}\mathbf{e}_{j'} \text{ so that } \pi^{i'j'} = 0 \text{ if } i' \neq j' \text{ and } \pi^{i'i'} = 1 \text{ or } 0, -1.$$

Moreover, although the basis change is not uniquely determined, the so-called signature, i.e. the range (sign) of diagonal elements is unique, up to permutation. Namely,

$$\mathbf{S}^2(1,1,1),\ \mathbf{E}^2(0,1,1),\ \mathbf{H}^2(-1,1,1),\ \mathbf{M}^2(0,-1,1),\ \mathbf{G}^2(0,0,1)$$

hold for $\mathbf{S}^2$ (spherical plane), $\mathbf{E}^2$ (Euclidean plane), $\mathbf{H}^2$ (hyperbolic or Bolyai-Lobachevsky plane), $\mathbf{M}^2$ (Minkowski or pseudo-Euclidean plane), $\mathbf{G}^2$ (Galilei or isotropic plane), respectively. Multiplication by (-1) provides equivalences

$$\mathbf{S}^2(-1,-1,-1),\ \mathbf{E}^2(0,-1,-1),\ \mathbf{H}^2(1,-1,-1),\ \mathbf{M}^2(0,1,-1),\ \mathbf{G}^2(0,0,-1).$$

Our Fig. 6 also illustrates the possible $\mathbf{S}^2$–structure if $\mathcal{PS}^2(\mathbf{V}^3, \boldsymbol{V}_3)$ is specified by polarity $\boldsymbol{e}^i \underset{*}{\longrightarrow} \mathbf{e}^i = \mathbf{e}_i$, $(i = 0,1,2)$ also by conventional matrix form

$$(\boldsymbol{e}^0, \boldsymbol{e}^1, \boldsymbol{e}^2) \underset{*}{\longrightarrow} \begin{pmatrix} \mathbf{e}^0 \\ \mathbf{e}^1 \\ \mathbf{e}^2 \end{pmatrix} = \begin{pmatrix} 1 & 0 & 0 \\ 0 & 1 & 0 \\ 0 & 0 & 1 \end{pmatrix} \begin{pmatrix} \mathbf{e}_0 \\ \mathbf{e}_1 \\ \mathbf{e}_2 \end{pmatrix}$$

(by usual row-column multiplication). That means that the basis $\{\boldsymbol{e}^i\}$ is orthonormal and our model plane $\mathcal{PS}^2$ becomes indeed to a metric sphere $\mathbf{S}^2$. The polarity orders to any line (equator circle) its usual pole.

The angle of lines (angular domain) of $u(\boldsymbol{u})$ and $v(\boldsymbol{v})$ is usually defined by

$$\cos\tfrac{1}{r}(u,v) = \tfrac{-\langle \boldsymbol{u},\boldsymbol{v}\rangle}{\sqrt{\langle \boldsymbol{u},\boldsymbol{u}\rangle\langle \boldsymbol{v},\boldsymbol{v}\rangle}}.$$

While $\cos\frac{1}{r}(U,V) = \langle \mathbf{u},\mathbf{v}\rangle / \sqrt{\langle \mathbf{u},\mathbf{u}\rangle\langle \mathbf{v},\mathbf{v}\rangle}$ leads to the (angular) distance or length of segment (U,V) between their poles $U(\mathbf{u})$ and $V(\mathbf{v})$, r denotes the radius of the sphere. This is natural, since the above polarity $\Pi(_*)$ with matrix π^{ij} is invertible. In our Fig. 6 there is indicated also the plane $\mathbf{E}^2$, i.e. the Euclidean structure of $\mathcal{PS}^2$ if our polarity is degenerate by

$$(\boldsymbol{e}^0, \boldsymbol{e}^1, \boldsymbol{e}^2) \underset{*}{\longrightarrow} \begin{pmatrix} \mathbf{0} \\ \mathbf{e}^1 \\ \mathbf{e}^2 \end{pmatrix} = \begin{pmatrix} 0 & 0 & 0 \\ 0 & 1 & 0 \\ 0 & 0 & 1 \end{pmatrix} \begin{pmatrix} \mathbf{e}_0 \\ \mathbf{e}_1 \\ \mathbf{e}_2 \end{pmatrix}.$$

That means that our ideal line $(\boldsymbol{i}) = (\boldsymbol{e}^0) = E_1^\infty(\mathbf{e}_1)E_2^\infty(\mathbf{e}_2)$ is considered to be orthogonal to any line (to itself as well). Parallel lines to line $u(\boldsymbol{u})$ have common orthogonal lines through the pole $U^\infty(\mathbf{u})$ at infinity, etc. Angles and distances can be defined according to usual conventions (see [1, 7, 10]).

We only remark that degenerate polarities by

$$(\boldsymbol{e}^0, \boldsymbol{e}^1, \boldsymbol{e}^2) \underset{*}{\longrightarrow} \begin{pmatrix} 0 & 0 & 0 \\ 0 & -1 & 0 \\ 0 & 0 & 1 \end{pmatrix} \begin{pmatrix} \mathbf{e}_0 \\ \mathbf{e}_1 \\ \mathbf{e}_2 \end{pmatrix} \text{ and } (\boldsymbol{e}^0, \boldsymbol{e}^1, \boldsymbol{e}^2) \underset{*}{\longrightarrow} \begin{pmatrix} 0 & 0 & 0 \\ 0 & 0 & 0 \\ 0 & 0 & 1 \end{pmatrix} \begin{pmatrix} \mathbf{e}_0 \\ \mathbf{e}_1 \\ \mathbf{e}_2 \end{pmatrix}$$

in Fig. 6 define Minkowski plane $\mathbf{M}^2$ (of special relativity) and Galilei plane $\mathbf{G}^2$ (for Newton mechanics), respectively [1].

The Bolyai-Lobachevsky hyperbolic plane $\mathbf{H}^2$ deserves special interest (Fig. 7). Here the polarity is defined by

$$(\boldsymbol{e}^0, \boldsymbol{e}^1, \boldsymbol{e}^2) \underset{*}{\longrightarrow} \begin{pmatrix} -1 & 0 & 0 \\ 0 & 1 & 0 \\ 0 & 0 & 1 \end{pmatrix} \begin{pmatrix} \mathbf{e}_0 \\ \mathbf{e}_1 \\ \mathbf{e}_2 \end{pmatrix}. \tag{2}$$

Now Fig. 7 has to be considered as extension of Fig. 6, i.e. $\mathcal{PS}^2$ with polarity given by (2), where the absolute cone (and conic section) is indicated (Beltrami-Cayley-Klein model). This is first the set of 2-subspaces of $\mathbf{V}^3$, described by the forms $(\boldsymbol{a})$ in $\boldsymbol{V}_3$, i.e. by lines $a(\boldsymbol{a})$ of $\mathcal{PS}^2$ which are incident to their poles $A(\mathbf{a})$. Thus for

$$\boldsymbol{a} = \boldsymbol{e}^0 a_0 + \boldsymbol{e}^1 a_1 + \boldsymbol{e}^2 a_2,$$
$$\boldsymbol{a}_* = a_0(-1)\mathbf{e}_0 + a_1(1)\mathbf{e}_1 + a_2(1)\mathbf{e}_2 = \mathbf{a} = a^0\mathbf{e}_0 + a^1\mathbf{e}_1 + a^2\mathbf{e}_2,$$

i.e. $a^0 = (-1)a_0$, $a^1 = a_1$, $a^2 = a_2$ follow, and hold

$$0 = -a_0a_0 + a_1a_1 + a_2a_2 = -a^0a^0 + a^1a^1 + a^2a^2$$

the quadratic equations of conics as line set and point set, respectively. That means, our polarity can be derived by conics, as it is pointed by

$$u \underset{*}{\longrightarrow} U \quad \text{and} \quad p \underset{*}{\longrightarrow} P$$

in Fig. 7. We refer to [1, 7] for other details.

After having introduced a polarity or scalar product in $\mathcal{PS}^2$ to get the above *metric geometries*, we can define their groups of transforms, first uniformly *as similarities*. These are special projective transforms, induced by linear transforms $(\mathbf{T}, \boldsymbol{T}^{-1})$ of $(\mathbf{V}^3, \boldsymbol{V}_3)$ by (1) up to certain equivalence, preserving the given polarity, as the following diagram obviously sketches

$$\begin{array}{ccccccc} & & x(\boldsymbol{x}) & \underset{*}{\longrightarrow} & X(\mathbf{x}) & & \\ \boldsymbol{V}_3 & \boldsymbol{T}^{-1} & \downarrow & & \downarrow & \mathbf{T} & \mathbf{V}^3 \\ & & y(\boldsymbol{y}) & \underset{*}{\longrightarrow} & Y(\mathbf{y}) & & \end{array} \quad \text{i.e. } \pi^{ij} \sim t^i_r \pi^{rs} t^j_s. \tag{3}$$

We only mention our – seemingly new – initiative to diagram (3): To some linear transforms ${}_g\tau({}_g\mathbf{T}, {}_g\boldsymbol{T}^{-1})$ $(g = 1, 2, 3, \dots)$ (left bottom index) "small number" of generators, for a group $\mathbf{G}$ with certain relations with free parameters), we can look for all possible polarities $({}_*)$ with (π^{ij}) which can be invariant under ${}_g\tau$, so under the group $\mathbf{G}$. Thus e.g., to $\mathbf{G}$ we look for possible geometries where $\mathbf{G}$ will be (may be) a discrete group of isometries (see e.g. [9, 10] for crystallographic applications and a possibility to attack *Thurston's geometrization conjecture*, in general, first for dimensions three, [9, 12, 15, 17, 26]).

We remark that in planes $\mathbf{S}^2$, $\mathbf{H}^2$, where the polarity is invertible, such transforms constitute the isometry group of $\mathbf{S}^2$ and $\mathbf{H}^2$, respectively, since in these cases distance between points will also be preserved. For the other geometries such a statement does not hold. Then the preserved (invariant) properties need some further characterizations. E.g. the concept of line reflection seems to be very natural to define isometries of the corresponding geometries. Line reflection is an involutive (involutory) transform, i.e. equal to its inverse, in an axis line $u(\boldsymbol{u})$ with its non incident pole $U(\mathbf{u})$ as centre. Namely, any isometry would be defined as composition or product of finitely many line reflections, as it is usual in Euclidean geometry $\mathbf{E}^2$ as well as also in $\mathbf{M}^2$ and $\mathbf{G}^2$ (as so-called affine metric geometries).

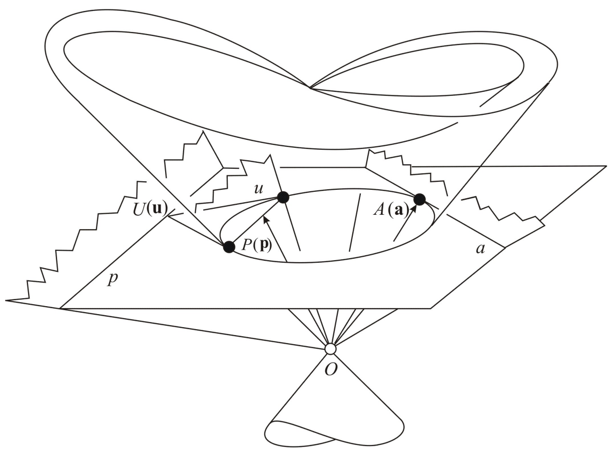

Figure 7. The hyperbolic plane $\mathbf{H}^2$, embedded into $\mathcal{P}^2 \subset \mathcal{PS}^2$ by a conic polarity $u(\boldsymbol{u}) \to U(\mathbf{u})$, $p \to P$, $a \to A$.

However, we shall see in dimensions three, such a plane reflection does not exist in some 3-geometries (e.g. in **Nil** and $\widetilde{\mathbf{SL_2R}}$).

We do not discuss here the differential geometry of the above 2-geometries. We know that $\mathbf{S}^2$, $\mathbf{E}^2$, $\mathbf{H}^2$ are Riemann spaces with infinitesimal arc-length, vectors as differential operators, of constant curvature and other invariants, etc. The standard method will be illustrated in the next sections for **Sol** and **Nil** geometry in some details, as examples.

4. Dimensions three, $\widetilde{\mathbf{SL_2R}}$ geometry modelled on the projective 3-sphere $\mathcal{PS}^3(\mathbf{V}^4, \boldsymbol{V}_4)$

The machinery introduced in the previous sections can be applied to model the classical 3-spaces $\mathbf{S}^3$, $\mathbf{E}^3$, $\mathbf{H}^3$ on the projective 3-sphere $\mathcal{PS}^3(\mathbf{V}^4, \boldsymbol{V}_4)$ (and for $\mathbf{E}^3$, $\mathbf{H}^3$ in $\mathcal{P}^3 \subset \mathcal{PS}^3$) in the same way with less visuality, but analogies and matrix (index) conventions can help. Let us introduce again the positive equivalence in $\mathbf{V}^4$ for non-zero vectors $\mathbf{x} \sim c\mathbf{x}$ with $0 < c \in \mathbf{R}$ defines the same point $X(\mathbf{x})$ of $\mathcal{PS}^3$, whose coordinates in $\mathbf{x} = x^i\mathbf{e}_i$, with respect to basis $\{\mathbf{e}_i\}$ $(i = 0, 1, 2, 3)$, can be written in matrix form

$$\mathbf{x} = (x^0, x^1, x^2, x^3) \begin{pmatrix} \mathbf{e}_0 \\ \mathbf{e}^1 \\ \mathbf{e}^2 \\ \mathbf{e}_3 \end{pmatrix}.$$

A form

$$Bu = \begin{pmatrix} \boldsymbol{e}^0 & \boldsymbol{e}^1 & \boldsymbol{e}^2 & \boldsymbol{e}^3 \end{pmatrix} \begin{pmatrix} u_0 \\ u_1 \\ u_2 \\ u_3 \end{pmatrix}$$

in the dual space $\boldsymbol{V}_4$, again up to positive equivalence, describes an oriented plane (2-sphere) of $\mathcal{PS}^3$ with the dual basis $\{\boldsymbol{e}^j\}$, $\mathbf{e}_i \boldsymbol{e}^j = \delta_i^j$ (the Kronecker symbol) $(i, j = 0, 1, 2, 3)$. Equalities

$$(x^i \mathbf{e}_i)(\boldsymbol{e}^j u_j) = x^i (\mathbf{e}_i \boldsymbol{e}^j) u_j = x^i \delta_i^j u_j = x^i u_j = 0 \tag{4}$$

express the incidence X I u. Formula (4) describes the set of varying points $X(\mathbf{x})$ on the fixed plane $u(\boldsymbol{u})$, and at the same time, the set of planes $u(\boldsymbol{u})$ incident to the fixed point $X(\mathbf{x})$. The projective transform $\tau(\mathbf{T}, \boldsymbol{T}^{-1})$ with inverse matrix pair (t_i^j) to $\mathbf{T}$ of $\mathbf{V}^4$ and $(t_i^j)^{-1} \sim (T_j^k)$ to $\boldsymbol{T}^{-1}$ of $\boldsymbol{V}_4$ – with respect to the dual basis pair $\{\mathbf{e}_i\}$, $\{\boldsymbol{e}^j\}$, as in formulas (1) – can be described in matrix form. First for points it is:

$$(x^0, x^1, x^2, x^3) \begin{pmatrix} t_0^0 & t_0^1 & t_0^2 & t_0^3 \\ t_1^0 & t_1^1 & t_1^2 & t_1^3 \\ t_2^0 & t_2^1 & t_2^2 & t_2^3 \\ t_3^0 & t_3^1 & t_3^2 & t_3^3 \end{pmatrix} \begin{pmatrix} \mathbf{e}_0 \\ \mathbf{e}_1 \\ \mathbf{e}_2 \\ \mathbf{e}_3 \end{pmatrix} \sim (y^0, y^1, y^2, y^3) \begin{pmatrix} \mathbf{e}_0 \\ \mathbf{e}_1 \\ \mathbf{e}_2 \\ \mathbf{e}_3 \end{pmatrix}$$

and for planes briefly $\boldsymbol{e}^i T_i^k u_k \sim \boldsymbol{e}^i v_i$. This $\tau(\mathbf{T}, \boldsymbol{T}^{-1})$ preserves the incidence by $0 = (\mathbf{x}\boldsymbol{u}) = (\mathbf{y}\boldsymbol{v})$. These are, again up to positive equivalence, related to a coordinate simplex $E_0E_1E_2E_3$ with the unit point $E(\mathbf{e} = \mathbf{e}_0 + \mathbf{e}_1 + \mathbf{e}_2 + \mathbf{e}_3$ and to $e^0e^1e^2e^3$ with the unit plane $e(\boldsymbol{e} = \boldsymbol{e}^0 + \boldsymbol{e}^1 + \boldsymbol{e}^2 + \boldsymbol{e}^3$, where $e^i = (E_jE_kE_l)$ with $\{0, 1, 2, 3\} = \{i, j, k, l\}$, etc.

Spherical space geometry $\mathbf{S}^3$ will be defined with the additional polarity $\Pi(_*)$ or scalar product $\langle\ ,\ \rangle$ in $\boldsymbol{V}_4$, with positive diagonal (π^{ij}) matrix, and we have $\boldsymbol{e}_*^i = \mathbf{e}^i = \pi^{ij}\mathbf{e}_j$,

$$(\boldsymbol{e}^0, \boldsymbol{e}^1, \boldsymbol{e}^2, \boldsymbol{e}^3) \underset{*}{\longrightarrow} \begin{pmatrix} \mathbf{e}^0 \\ \mathbf{e}^1 \\ \mathbf{e}^2 \\ \mathbf{e}^3 \end{pmatrix} = \begin{pmatrix} 1 & 0 & 0 & 0 \\ 0 & 1 & 0 & 0 \\ 0 & 0 & 1 & 0 \\ 0 & 0 & 0 & 1 \end{pmatrix} \begin{pmatrix} \mathbf{e}_0 \\ \mathbf{e}_1 \\ \mathbf{e}_2 \\ \mathbf{e}_3 \end{pmatrix}.$$

For Euclidean $\mathbf{E}^3$ geometry and hyperbolic $\mathbf{H}^3$ (Bolyai-Lobachevsky) geometry we indicate only the corresponding π^{ij} matrices $(i, j \in \{0, 1, 2, 3\})$, respectively:

$$\mathbf{E}^3: \begin{pmatrix} 0 & 0 & 0 & 0 \\ 0 & 1 & 0 & 0 \\ 0 & 0 & 1 & 0 \\ 0 & 0 & 0 & 1 \end{pmatrix}, \quad \mathbf{H}^3: \begin{pmatrix} -1 & 0 & 0 & 0 \\ 0 & 1 & 0 & 0 \\ 0 & 0 & 1 & 0 \\ 0 & 0 & 0 & 1 \end{pmatrix}.$$

To other Thurston geometries we attach here Table 1 by [10], where additional and modified information for transform groups are also indicated.

Now we concentrate on $\widetilde{\mathbf{SL_2R}}$ geometry. The real 2×2 matrices, say in the form

$$\begin{pmatrix} d & b \\ c & a \end{pmatrix} \quad \text{with unit determinant } ad - bc = 1. \tag{5}$$

have many applications. They define the special linear group acting on the real 2-dimensional plane, preserving orientation and area (equiaffine transforms).

These matrices constitute a Lie transformation group by the usual product operation, taken to act on row matrices as on point coordinates on the right as follows

$$(z^0, z^1) \begin{pmatrix} d & b \\ c & a \end{pmatrix} = (z^0 d + z^1 c,\ z^0 b + z^1 a) = (w^0, w^1).$$

We get another important application, if $z^1/z^0 =: z$ represents a point of the complex projective line $\mathbf{C} \cup \infty =: \mathbf{C}_\infty$ (or the usual complex number plane). Then the projective mapping $z \to w := w^1/w^0$ is given by the above matrix and related with the Poincaré upper half-plane model of hyperbolic plane $\mathbf{H}^2$ (see later on and [7, 10]).

At the same time, this group is a 3-dimensional manifold, because of its 3 independent real coordinates (and its usual neighbourhood topology).

In order to have a more geometrical interpretation on the projective 3-sphere $\mathcal{PS}^3$, we introduce new coordinates x^0, x^1, x^2, x^3) (for (5), say by

$$a := x^0 + x^3, \quad b := x^1 + x^2, \quad c := -x^1 + x^2, \quad d := x^0 - x^3,$$

with positive equivalence as a projective freedom. Then it follows that

$$0 > bc - ad = -x^0 x^0 - x^1 x^1 + x^2 x^2 + x^3 x^3 \tag{6}$$

describes the same 3-dimensional set, namely the interior of the above unparted (one-sheet) hyperboloid (Fig. 8). Indeed, for $x^0 \neq 0$,

$$x^1/x^0 =: x, \quad x^2/x^0 =: y, \quad x^3/x^0 =: z, \qquad \text{lead to} \quad 0 > -1 - xx + yy + zz \tag{7}$$

and to the usual 4-dimensional embedding (in analogy to Fig. 6–7). We look at the coordinate simplex $E_0 E_1^\infty E_2^\infty E_3^\infty$ where $E_0(\mathbf{e}_0 \sim (1, 0, 0, 0))$ is the origin and $E_1^\infty(\mathbf{e}_1 \sim (0, 1, 0, 0))$ is the ideal (infinite) point of the axis x, and both lie in the interior of the hyperboloid solid $\mathcal{H}$. The boundary points of $\mathcal{H}$ lie on straight lines of the surface. Horizontal intersection e.g. with $E_0 E_2^\infty E_3^\infty$ provides the Beltrami-Cayley-Klein model of the hyperbolic plane $\mathbf{H}^2$ if we take $x = 0$ $(= x^1)$ as base plane. From points of this $\mathbf{H}^2$ the pairwise skew straight line fibres "grow out". The "gum-fibre model" of H. Havlicek and R. Riesinger shows this in Fig. 8. Imagine first two circle disks connected with a rotation axis (a piece of $E_0 E_1^\infty = x$). Some points (along concentric circles, say) of lower disk are clipped out, the same is done with their translated points on the upper disk. Gum-fibres connect the translated clipped points. This first situation naturally models $\mathbf{H}^2 \times \mathbf{R}$ (see Tab. 1), the direct product of $\mathbf{H}^2$ (Beltrami-Cayley-Klein model) and $\mathbf{R}$ (real gum-lines).

An alternative model of $\mathbf{H}^2 \times \mathbf{R}$ can be seen also in Fig. 7. Here "translation" by $r \in \mathbf{R}$ can be imagined as a multiplication by e^r – a similarity from the origin cone apex. Parallel conic sections are the different $\mathbf{H}^2$ levels. The logarithm function provides the natural connection between the two models. Note that $\mathbf{S}^2\times\mathbf{R}$ can be modelled in analogous way by Fig. 6 [10, 21, 23].

Secondly, twist the gum fibre model (Fig. 8), by rotating the upper disk about the axis, through a fixed angle. Then the gum-fibres become pairwise skew lines, so that we obtain the above hyperboloid solid $\mathcal{H}$ by (6), as a twisted product of $\mathbf{H}^2$ and $\mathbf{R}$ (gum-fibres).

Table 1. Thurston geometries each modelled on $\mathcal{PS}^3$ by specified polarity or scalar product and isometry group.

Space $\mathbf{X}$	Signature of polarity $\Pi(\star)$ or scalar product $\langle\ ,\ \rangle$ in $\boldsymbol{V}_4$	Domain of proper points of $\mathbf{X}$ in $\mathcal{PS}^3$ $(\mathbf{V}^4(\mathbf{R}), \boldsymbol{V}_4)$	The group $G = \mathrm{Isom}\,\mathbf{X}$ as a special collineation group of $\mathcal{PS}^3$
$\mathbf{S}^3$	$(+ + ++)$	$\mathcal{PS}^3$	Coll $\mathcal{PS}^3$ preserving $\Pi(\star)$
$\mathbf{H}^3$	$(- + ++)$	$\{(\mathbf{x}) \in \mathcal{P}^3 : \langle\mathbf{x},\mathbf{x}\rangle < 0\}$	Coll $\mathcal{P}^3$ preserving $\Pi(\star)$
$\widetilde{\mathbf{SL_2R}}$	$(- - ++)$ with skew line fibering	Universal covering of $\mathcal{H} := \{[\mathbf{x}] \in \mathcal{PS}^3 : \langle\mathbf{x},\mathbf{x}\rangle < 0\}$ by fibering transformations	Coll $\mathcal{PS}^3$ preserving $\Pi(\star)$ and fibres with 4 parameters
$\mathbf{E}^3$	$(0 + ++)$	$\mathcal{A}^3 = \mathcal{P}^3 \setminus \{\omega^\infty\}$ where $\omega^\infty := (\boldsymbol{b}^0)$, $\boldsymbol{b}^0_\star = \mathbf{0}$	Coll $\mathcal{P}^3$ preserving $\Pi(\star)$, generated by plane reflections
$\mathbf{S}^2\times\mathbf{R}$	$(0 + ++)$ with O-line bundle fibering	$\mathcal{A}^3 \setminus \{O\}$, O is a fixed origin	G is generated by plane reflections and sphere inversions, leaving invariant the O-concentric 2-spheres of $\Pi(\star)$
$\mathbf{H}^2\times\mathbf{R}$	$(0 - ++)$ with O-line bundle fibering	$\mathcal{C}^+ = \{X \in \mathcal{A}^3 : \langle\overrightarrow{OX},\overrightarrow{OX}\rangle < 0$, half cone$\}$ by fibering	G is generated by plane reflections and hyperboloid inversions, leaving invariant the O-concentric half-hyperboloids in the half-cone $\mathcal{C}^+$ by $\Pi(\star)$
Sol	$(0 - ++)$ and parallel plane fibering with an ideal plane ϕ	$\mathcal{A}^3 = \mathcal{P}^3 \setminus \phi$	Coll. of $\mathcal{A}^3$ preserving $\Pi(*)$ and the fibering with 3 parameters
Nil	Null-polarity $\Pi(\star)$ with parallel line bundle fibering F with its polar ideal plane ϕ	$\mathcal{A}^3 = \mathcal{P}^3 \setminus \phi$	Coll. of $\mathcal{A}^3$ preserving $\Pi(\star)$ with 4 parameters

Let us express this more exactly. First we take the following screw transforms $\mathbf{S}(\phi) = \mathbf{S}$ by an (additive) parameter ϕ

$$\mathbf{x} = (x^0, x^1, x^2, x^3)\begin{pmatrix}\mathbf{e}^0\\ \mathbf{e}^1\\ \mathbf{e}^2\\ \mathbf{e}^3\end{pmatrix} \to \mathbf{x}\mathbf{S},$$

$$(x^0, x^1, x^2, x^3)\begin{pmatrix} \cos\phi & \sin\phi & 0 & 0 \\ -\sin\phi & \cos\phi & 0 & 0 \\ 0 & 0 & \cos\phi & -\sin\phi \\ 0 & 0 & \sin\phi & \cos\phi \end{pmatrix}\begin{pmatrix} \mathbf{e}_0 \\ \mathbf{e}_1 \\ \mathbf{e}_2 \\ \mathbf{e}_3 \end{pmatrix}. \tag{8}$$

This describes the fibre translation and the fibre orbit line for any point $\mathbf{x}$.

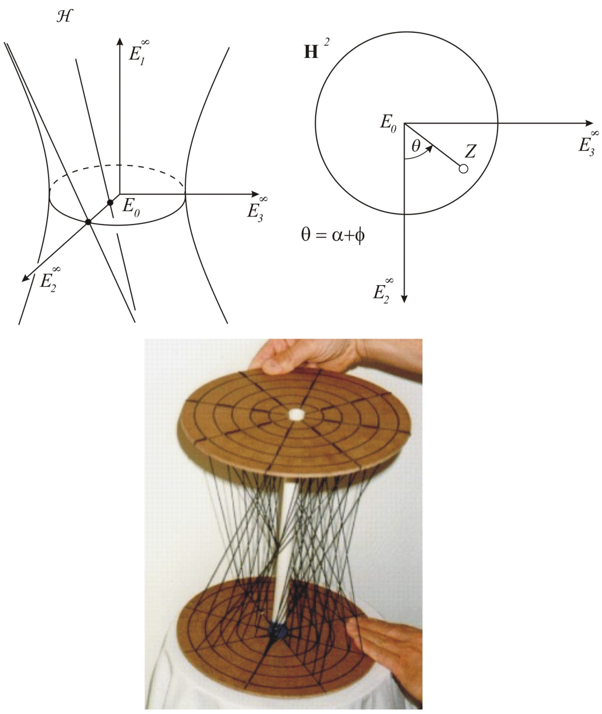

Figure 8. The unparted hyperboloid model of $\widetilde{\mathbf{SL_2R}} = \widetilde{\mathcal{H}}$ of skew line fibres growing in points of a hyperbolic base plane $\mathbf{H}^2$. Gum-fibre model of Hans Havlicek and Rolf Riesinger, used also by Hellmuth Stachel with other respects (Vienna UT).

We look at the following periodicities: either by π and $-\frac{\pi}{2} < \phi < \frac{\pi}{2}$ leads to $\mathcal{P}^3$–action (equivalence by $\mathbf{R}^0$-factor, without zero); or by 2π and $-\pi < \phi < \pi$ leads to $\mathcal{PS}^3$ action (by $\mathbf{R}^+$, i.e. positive equivalence). The case $\phi \in \mathbf{R}$ leads to complete $\mathbf{R}$ fibres, i.e. to a covering action leading to the model $\widetilde{\mathbf{SL_2R}} = \widetilde{\mathcal{H}}$ in a geometric way.

Namely, $\mathbf{S}(\phi)$ maps $\mathcal{H}$ by (6) and (7) onto itself, while horizontal plane intersection lifts the $x = 0$ plane by $\phi = 0$ to $x \to \infty$ by $\phi \to \frac{\pi}{2}$, the fibre lines are twisted in the negative direction (clock-wise, see first picture in Fig. 8), then $\frac{\pi}{2} < \phi < \pi$ lifts the $x = 0$ plane section to that by $-\infty < x < 0$, etc. we sweep the hyperboloid solid $\mathcal{H}$ (i.e. cover it) many times as ϕ varies in $\mathbf{R}$ by periods. Imagine this also in the 4-dimensional space, where $\phi = \pi$ leads to

$(x^0, x^1, x^2, x^3) \to (-x^0, -x^1, -x^2, -x^3)$ (opposite points in $\mathcal{PS}^3$, but the same point in $\mathcal{P}^3$.

A fibre through $X(\mathbf{x} \sim x^i \mathbf{e}_i$ intersects the $x = 0$ base plane in a trace point

$$Z(z^0 = x^0x^0 + x^1x^1,\;\; z^1 = 0,\;\; z^2 = x^0x^2 - x^1x^3,\;\; z^3 = x^0x^3 + x^1x^2) \tag{9}$$

uniquely, up to positive proportionality, as follows from (8) (Fig. 8 second picture).

We define the isometry group $\mathbf{G}$ of our space $\widetilde{\mathbf{SL}_2\mathbf{R}} = \widetilde{\mathcal{H}}$ by linear transforms of $\mathbf{V}^4$ leaving invariant our quadratic form and line fibres in (6), (8) both. This is discussed in [10, 14, 16] in more details. Here we simply give the specific subgroup $\mathbf{T}$, called the *translation group*, represented by matrices

$$\mathbf{T} : (t_i^j) = \begin{pmatrix} x^0 & x^1 & x^2 & x^3 \\ -x^1 & x^0 & x^3 & -x^2 \\ x^2 & x^3 & x^0 & x^1 \\ x^3 & -x^2 & -x^1 & x^0 \end{pmatrix}$$

with inverse (up to positive determinant factor)

$$(t_i^j)^{-1} = (T_j^k) \begin{pmatrix} x^0 & -x^1 & -x^2 & -x^3 \\ x^1 & x^0 & -x^3 & x^2 \\ -x^2 & -x^3 & x^0 & -x^1 \\ -x^3 & x^2 & x^1 & x^0 \end{pmatrix}. \tag{10}$$

This $\mathbf{T}$ above acts transitively on the space $\widetilde{\mathcal{H}}$ (by the former covering extension); (t_i^j) maps the origin $E_0(1,0,0,0)$ onto $X(x^0, x^1, x^2, x^3)$. We can check $\mathbf{ST} = \mathbf{TS}$, i.e. $\mathbf{T}^{-1}\mathbf{ST} = \mathbf{S}$, thus $\mathbf{T}$ preserves the fibering (8).

It turns out that the above isometry group $\mathbf{G}$ has compact stabilizer $\mathbf{G}_0$ at E_0. E.g. it maps the fibre parameter ϕ to $-\phi$ by a half-turn about the horizontal line $E_0E_2^\infty$. Finally, $\mathbf{G}_0$ consists of matrices of the form

$$\mathbf{G}_0 : \begin{pmatrix} 1 & 0 & 0 & 0 \\ 0 & \pm 1 & 0 & 0 \\ 0 & 0 & \cos\omega & \sin\omega \\ 0 & 0 & \mp\sin\omega & \pm\cos\omega \end{pmatrix}, \quad -\pi < \omega \le \pi \pmod{2\pi}.$$

We can introduce also a so-called hyperboloid parametrization by [10] as follows

$$X(x^0 = \cosh r \cos\phi,\;\; x^1 = \cosh r \sin\phi,$$
$$x^2 = \sinh r \cos(\theta - \phi),\;\; x^3 = \sinh r \cos(\theta - \phi)$$

with

$$\langle \mathbf{x}, \mathbf{x} \rangle = -x^0x^0 - x^1x^1 + x^2x^2 + x^3x^3 = -\cosh^2 r + \sinh^2 r = -1. \tag{11}$$

The fibre line through point X intersects the base plane $z^1 = 0$ in the trace point Z by (9) with inhomogeneous coordinates

$$Z\big(\tfrac{z^1}{z^0} = 0,\;\; \tfrac{z^2}{z^0} = \tanh r \cos\theta,\;\; \tfrac{z^3}{z^0} = \tanh r \sin\theta\big).$$

Here the meaning of r and θ becomes obvious, as the polar coordinates of Z in the hyperbolic base plane $\mathbf{H}^2$ (Fig. 8 second picture).

In the following we only mention the concept of *translation line* from a starting point with given unit velocity, then the *translation sphere* with given centre and radius. Furthermore, we recall the well-known concept of *geodesic line* from a given starting point with unit velocity, then the *geodesic sphere* with given centre and radius (see e.g. [4, 10, 14, 16] for more details).

Choose the origin $(x^0,\ x^1,\ x^2,\ x^3) = (1, 0, 0, 0)$, of $\widetilde{\mathbf{SL_2R}} = \widetilde{\mathcal{H}}$ in our hyperboloid model, and a starting unit velocity vector with coordinates $\boldsymbol{\omega} = (0,\, u = \sin\phi,\, v = \cos\phi\cos\theta,\ w = \cos\phi\sin\theta)$. The roles of ϕ and θ are consequent with the above notations in (8) and (11). In general, a curve $(x^0(s),\ x^1(s),\ x^2(s),\ x^3(s))$ with arc-length parameter $s = t$ is called a *translation curve*, iff by (10) it holds

$$(q, u, v, w)\begin{pmatrix} x^0(s) & x^1(s) & x^2(s) & x^3(s) \\ -x^1(s) & x^0(s) & x^3(s) & -x^2(s) \\ x^2(s) & x^3(s) & x^0(s) & x^1(s) \\ x^3(s) & -x^2(s) & -x^1(s) & x^0(s) \end{pmatrix} = (\dot{x}^0(s), \dot{x}^1(s), \dot{x}^2(s), \dot{x}^3(s))$$

(upper dot means derivative by s), as a first order ordinary differential equation system (see [14] for special straight line solutions in the hyperboloid model). That means, the translation to point of parameter s carries the initial tangent into the tangent at point of s.

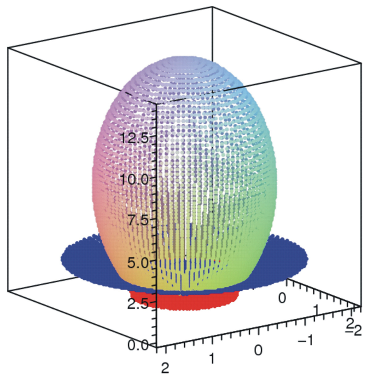

Figure 9. Translation half sphere with separating "light-cone" in $\widetilde{\mathbf{SL_2R}}$, $R = 1.5$.

Our Fig. 9 shows a translation half-sphere with 3 domains of a delicate discussion. The above parameters θ and ϕ in the formula of the above unit starting velocity vector $\boldsymbol{\omega}$ are just the longitude and altitude parameters of the translation sphere. The radius R is the final arc-length parameter $s = R$ to each translation curve, starting in the sphere centre in (θ, ϕ)-direction with unit velocity as well. A geodesic line is of locally minimal arc-length, thus it satisfies a second order nonlinear ordinary differential equation system. This can be derived as our colleagues explicitly solved it in [4].

Geodesics can start from the origin of the hyperboloid model by (11) and with some extensions $r(0) = 0,\ \phi(0) = 0,\ \theta(0) = \theta_0$ and starting unit velocities as well. Finally we substitute into (11) for visualization. Fig. 10 shows some geodesic half spheres as illustrations here, on the base of the explicit solution by [4].

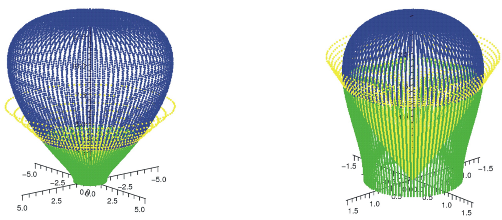

(a) (b)

Figure 10. Geodesic half-spheres in $\widetilde{\mathbf{SL_2R}}$ $R = 1.5$ and $R = 1.2$ with "light cone" in the interior.

5. On **Sol** and **Nil** geometries

5.1. Sol geometry

Sol is an affine metric geometry of projective metric signature $(0, -, +, +)$ (see Tab. 1), again with

$$(\boldsymbol{e}^0, \boldsymbol{e}^1, \boldsymbol{e}^2, \boldsymbol{e}^3) \underset{*}{\longrightarrow} \begin{pmatrix} \mathbf{e}^0 \\ \mathbf{e}^1 \\ \mathbf{e}^2 \\ \mathbf{e}^3 \end{pmatrix} = \begin{pmatrix} 0 & 0 & 0 & 0 \\ 0 & -1 & 0 & 0 \\ 0 & 0 & 1 & 0 \\ 0 & 0 & 0 & 1 \end{pmatrix} \begin{pmatrix} \mathbf{e}_0 \\ \mathbf{e}_1 \\ \mathbf{e}_2 \\ \mathbf{e}_3 \end{pmatrix}.$$

Sol is derived by an affine Lie transform group with right action on points (a, b, c) or in homogeneous coordinates

$$(1; a, b, c) \to (1; a, b, c) \begin{pmatrix} 1 & x & y & z \\ 0 & e^{-z} & 0 & 0 \\ 0 & 0 & e^{z} & 0 \\ 0 & 0 & 0 & 1 \end{pmatrix} = (1; x + ae^{-z}, y + be^{z}, z + c). \tag{12}$$

We refer to [13, 20] for more details. For example the invariant arc-length-square is derived by pull-back with inverse of (12) to the origin (1,0,0,0):

$$(\mathrm{d}s)^2 = (\mathrm{d}x)^2 e^{2z} + (\mathrm{d}y)^2 e^{-2z} + (\mathrm{d}z)^2. \tag{13}$$

Then the complete isometry group of 3 parameters in **Sol** can be defined by extending the above translations with a finite linear stabilizer subgroup $\mathbf{G}_0$ of the origin which leaves invariant the quadratic differential form (13). We have two generators for this $\mathbf{G}_0$. First, symbolically, then in (12)–type matrix form. These involutive (involutory) two isometries are the following:

$y \leftrightarrow -y$ reflection in the plane (x, z); and $x \leftrightarrow y$ $z \leftrightarrow -z$ half-turn about bisector line of axes x and y, or

$$\begin{pmatrix} 1 & 0 & 0 & 0 \\ 0 & 1 & 0 & 0 \\ 0 & 0 & -1 & 0 \\ 0 & 0 & 0 & 1 \end{pmatrix}; \qquad \begin{pmatrix} 1 & 0 & 0 & 0 \\ 0 & 0 & 1 & 0 \\ 0 & 1 & 0 & 0 \\ 0 & 0 & 0 & -1 \end{pmatrix}, \tag{14}$$

respectively. That means $\mathbf{G}_0 = \mathbf{D}_4$ is a discrete dihedral group of 8 elements. Its cyclic subgroup $\mathbf{C}_4$ of order 4 is generated by the product of the former two generators in (14), a so-called rotatory reflection

$$\mathbf{C}_4 : \begin{pmatrix} 1 & 0 & 0 & 0 \\ 0 & 0 & 1 & 0 \\ 0 & -1 & 0 & 0 \\ 0 & 0 & 0 & -1 \end{pmatrix}.$$

Then

$$\mathbf{C}_2 : \begin{pmatrix} 1 & 0 & 0 & 0 \\ 0 & -1 & 1 & 0 \\ 0 & 1 & -1 & 0 \\ 0 & 0 & 0 & 1 \end{pmatrix}, \tag{15}$$

by a usual half turn about the z-axis, defines also a typical stabilizer of second order. In analogy to Euclidean geometry $\mathbf{E}^3$, we can define a discrete lattice $\Gamma(\tau_1, \tau_2, \tau_3)$, generated by two commuting horizontal translations

$$\tau_1 := (t_1^1, t_1^2, 0) \begin{pmatrix} \mathbf{e}^1 \\ \mathbf{e}^2 \\ \mathbf{e}^3 \end{pmatrix}, \quad \tau_2 := (t_2^1, t_2^2, 0) \begin{pmatrix} \mathbf{e}^1 \\ \mathbf{e}^2 \\ \mathbf{e}^3 \end{pmatrix},$$

and by

$$\tau_3 := (t_3^1, t_3^2, t_3^3), \quad \text{or } \tau_3 : \begin{pmatrix} 1 & t_3^1 & t_3^2 & t_3^3 \\ 0 & e^{-t_3^3} & 0 & 0 \\ 0 & 0 & e^{t_3^3} & 0 \\ 0 & 0 & 0 & 1 \end{pmatrix}.$$

The third one is, in more exact (12)–type matrix form with non-zero vertical component

$$t_3^3 = \log\left(\frac{N+\sqrt{N^2-4}}{2}\right), \quad \text{where } N := p + s > 2, \tag{16}$$

by the next Theorem 5.1. This N is a natural parameter fixed for a lattice $\Gamma(\tau_1, \tau_2, \tau_3)$ above. All these are essentially connected with the commutator relations in the characterizing

Theorem 5.1 ([13, 17]). *Each lattice* $\Gamma(\tau_1, \tau_2, \tau_3)$ *of* **Sol** *has a group presentation*

$$\Gamma = \Gamma(\Phi) = \{\tau_1, \tau_2, \tau_3 : [\tau_1, \tau_2] = \tau_1^{-1}\tau_2^{-1}\tau_1\tau_2 = 1, \tau_3^{-1}\tau_1\tau_3 = \tau_1\Phi^T, \tau_3^{-1}\tau_2\tau_3 = \tau_2\Phi^T\},$$

where $\Phi = \begin{pmatrix} p & q \\ r & s \end{pmatrix} \in \mathbf{SL}_2\mathbf{Z}$ *with* $\mathrm{tr}(\Phi) =: p + s =: N > 2$, $ps - qr = 1$, *such that the above matrix* $\begin{pmatrix} t_1^1 & t_1^2 \\ t_2^1 & t_2^2 \end{pmatrix} =: T \in \mathbf{GL}_2\mathbf{R}$ *satisfies*

$$\Phi^T = T^{-1}\Phi T = \begin{pmatrix} e^{-t_3^3} & 0 \\ 0 & e^{t_3^3} \end{pmatrix} \tag{17}$$

that is just a hyperbolic mapping in the Minkowski base plane $\mathbf{M}^2$ *(Section 3), however now by* (13)*, fixed by the component* t_3^3 *by* (16) *in* τ_3 *above.*

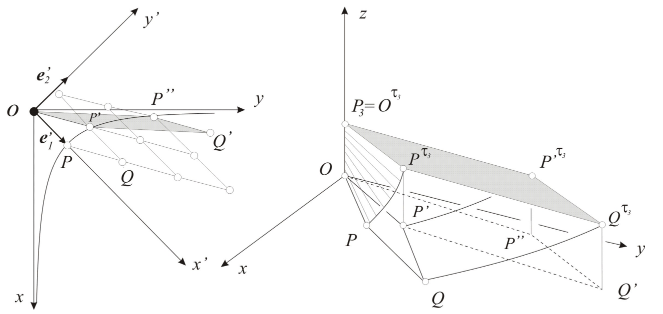

Figure 11. A fundamental lattice of **Sol** for $N = 3$ of fundamental "parallelepiped" with continuous translation from $(OPQP') \to (OPQP')^{\tau_3}$.

This is a very concise characterization that has some consequences.

(a) **Sol** has Minkowski base planes (of special relativity but by (13)), depending on a natural parameter N by (16) and Theorem 5.1.

(b) For the Minkowski base lattice (τ_1, τ_2) by T above we have some freedom in choosing $\tau_1(t_1^1, t_1^2)$ but then

$$\frac{t_2^1}{t_1^1} = \frac{N-2p-\sqrt{N^2-4}}{2q}, \quad \frac{t_2^2}{t_1^2} = \frac{N-2p+\sqrt{N^2-4}}{2q} \tag{18}$$

determine $\tau_2(t_2^1, t_2^2)$ by (N, p, q) in Theorem 5.1.

(c) The number theoretical form of N tells us the possibilities for stabilizer symmetry group $\mathbf{G}_0$ of $\Gamma(\tau_1, \tau_2, \tau_3)$ together with

$$\begin{aligned} &(t_3^1, t_3^2) = (0,0) \bmod \langle \tau_1, \tau_2 \rangle, && \text{as main case I, or} \\ &(t_3^1, t_3^2) \neq (0,0) \bmod \langle \tau_1, \tau_2 \rangle && \text{main case II.} \end{aligned}$$

(d) We can define affine equivalence of lattices $\Gamma(N, p, q)$, with finitely many affine types for given N, but we prefer a seemingly coarser algorithmic equivalence into so-called Bravais types [13] in

Theorem 5.2. *The lattices in the above main cases I and II, for fixed natural parameter* $2 < N \in \mathbf{Z}$*, form at most* 17 *(seventeen) Bravais types in* **Sol** *space.*

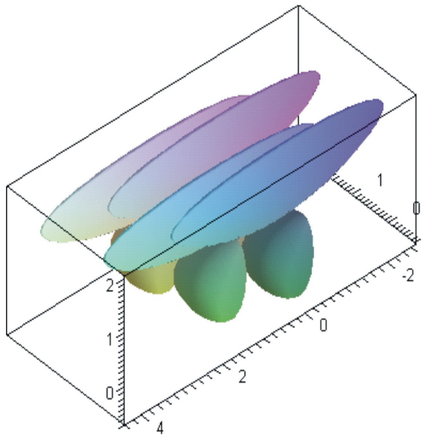

Figure 12. The densest translation ball packing by fundamental lattices of Bravais type $I/1$ in **Sol** space $N=4$ (see [20]).

This is in analogy to the 14 Bravais types of the Euclidean lattices in $\mathbf{E}^3$.

$N=6$ is the smallest natural number for that all Bravais types are realizable. For example, the so called fundamental lattices, with

$$\begin{pmatrix} p & q \\ r & s \end{pmatrix} = \begin{pmatrix} 0 & 1 \\ -1 & N \end{pmatrix}; \quad (t_3^1, t_3^2) = (0,0) \mod\langle \tau_1, \tau_2 \rangle \tag{19}$$

by (18), belong to type $I/1$ of primitive monoclinic lattice with point group $\mathbf{G}_0 = \mathbf{C}_2$ by (15), see also Fig. 11 for $N=3$. To these fundamental lattices we make some remarks.

Remark 5.3. *The orbit space* $\mathbf{Sol}/\Gamma$*, with lattice* Γ *above by* (19) *and Theorem 5.1. (just in analogy to compact Euclidean spaceform* $\mathbf{E}^3/\Gamma$*, where* $\Gamma = \mathbf{P}_1$ *is a usual Euclidean lattice), defines a* **Sol** *space form series* $\mathcal{M}_N$ *with fundamental group by* (17) *and presentation*

$$\Gamma_N = \left\{ \tau_1, \tau_2, \tau_3 : 1 = \tau_1^{-1}\tau_2^{-1}\tau_1\tau_2 = \tau_3^{-1}\tau_1\tau_3\tau_2^{-1} = \tau_3^{-1}\tau_2^{-1}\tau_3\tau_2^{N}\tau_1 \right\}.$$

Then, by expressing $\tau_2 = \tau_3^{-1}\tau_1\tau_3$ *and changing to notations* $\tau_1 =: x$ *and* $\tau_3 := y$ *we get a 2-generator fundamental group with presentation*

$$\Gamma_N = \left\{ x, y : xyx^{-1}y^{-1}x^{-1}yxy^{-1} = 1 = yxy^{-2}xyx^{-N} \right\}.$$

In the joint work [3] we gave some topological characterizations of these space forms $\mathcal{M}_N$ which can wear **Sol** metrics by (13) with "tetrahedron" fundamental domains, according to the two generators.

5.2. Nil geometry

Nil is also an affine metric geometry. It was derived originally from the Heisenberg matrix group from the left action as the matrix product

$$\begin{pmatrix}1 & x & z\\ 0 & 1 & y\\ 0 & 0 & 1\end{pmatrix}\begin{pmatrix}1 & a & c\\ 0 & 1 & b\\ 0 & 0 & 1\end{pmatrix}=\begin{pmatrix}1 & a+x & c+xb+z\\ 0 & 1 & b+y\\ 0 & 0 & 1\end{pmatrix}$$

$((a,b,c),(x,y,z)\in\mathbf{R}^3)$ show, how a translation (x,y,z) acts on a point (a,b,c) of the 3-space **Nil**. The fibre translations $(0,0,z)$ constitute the centre, commuting with all **Nil** transforms (see e.g. [2, 10, 11, 17, 26]).

Now we equivalently and more briefly introduce **Nil** (see [2, 11]) by the help of null-polarity $\Pi(_*)$ in $\mathcal{A}^3\subset\mathcal{P}^3$. Here a distinguished point F and its line bundle provide the fibre structure. The polar plane ϕ I F will be the ideal plane of $\mathcal{A}^3=\mathcal{P}^3\setminus\phi$. This structure will be the scene of **Nil** geometry. The isometry group **G** of **Nil** consist of collineations of $\mathcal{A}^3$ preserving the null polarity $\Pi(_*)$ given say, by

$$\boldsymbol{e}^i_*=\pi^{ij}\mathbf{e}_j \quad \text{with } \pi^{ji}=-\pi^{ij};$$
$$(_*):(\boldsymbol{e}^0,\boldsymbol{e}^1,\boldsymbol{e}^2,\boldsymbol{e}^3)\underset{*}{\longrightarrow}\begin{pmatrix}\boldsymbol{e}^0_*\\ \boldsymbol{e}^1_*\\ \boldsymbol{e}^2_*\\ \boldsymbol{e}^3_*\end{pmatrix}=\begin{pmatrix}0 & 0 & 0 & 1\\ 0 & 0 & -2 & 0\\ 0 & 2 & 0 & 0\\ -1 & 0 & 0 & 0\end{pmatrix}\begin{pmatrix}\mathbf{e}_0\\ \mathbf{e}_1\\ \mathbf{e}_2\\ \mathbf{e}_3\end{pmatrix}.$$

This antisymmetric matrix π^{ij} of $\Pi(_*)$ guarantees that any pole $\boldsymbol{u}_*=\mathbf{u}(u_3,2u_2,-2u_1,u_0)$ is incident with its polar plane $\boldsymbol{u}(u_0,u_1,u_2,u_3)^T$, as any circle plane coincides with the centre of a circle.

The translations, rotations about the z-axis, and horizontal line reflection in the x-axis

$$\begin{pmatrix}1 & x & y & z\\ 0 & 1 & 0 & -\frac{1}{2}y\\ 0 & 0 & 1 & \frac{1}{2}x\\ 0 & 0 & 0 & 1\end{pmatrix},\quad \begin{pmatrix}1 & 0 & 0 & 0\\ 0 & \cos\alpha & \sin\alpha & 0\\ 0 & -\sin\alpha & \cos\alpha & 0\\ 0 & 0 & 0 & 1\end{pmatrix},\quad \begin{pmatrix}1 & 0 & 0 & 0\\ 0 & 1 & 0 & 0\\ 0 & 0 & -1 & 0\\ 0 & 0 & 0 & -1\end{pmatrix},\tag{20}$$

respectively, are typical isometries of **Nil**. These preserve the null-polarity by the scheme (3). Thus, they generate the complete isometry group of 4 parameters in **Nil** as specific collineations of $\mathcal{P}^3\setminus\phi=\mathcal{A}^3$. Here $\phi=(1,0,0,0)^T$ is the invariant ideal plane, whose pole $F(0,0,0,1)$ just defines the fibre line bundle parallel to the z axis, as in the former classical interpretation.

As a benefit to the former interpretation, now it is more clear the role of the commutator translation of $\tau_1(x_1,y_1,z_1)$ and $\tau_2(x_2,y_2,z_2)$ as the following matrix product shows,

$$\tau_1^{-1}\tau_2^{-1}\tau_1\tau_2(0,0,x_1x_2-x_2x_1)$$

is a fibre translation, indeed.

The pull back of a the coordinate differentials $(0, \mathrm{d}x, \mathrm{d}y, \mathrm{d}z)$ at point $(1, x, y, z)$ into the origin $(1, 0, 0, 0)$

$$(0, \mathrm{d}x, \mathrm{d}y, \mathrm{d}z)\begin{pmatrix}1 & -x & -y & -z\\ 0 & 1 & 0 & \frac{1}{2}y\\ 0 & 0 & 1 & -\frac{1}{2}x\\ 0 & 0 & 0 & 1\end{pmatrix} = (0, \mathrm{d}x, \mathrm{d}y, \tfrac{1}{2}(\mathrm{d}x\cdot y - \mathrm{d}y\cdot x) + \mathrm{d}z)$$

provides the arc-length-square, as the standard Riemann metric, invariant under all transforms of (20):

$$\begin{aligned}(\mathrm{d}s)^2 = (\mathrm{d}x)^2 + (\mathrm{d}y)^2 + \left[\tfrac{1}{2}(\mathrm{d}x\cdot y - \mathrm{d}y\cdot x) + \mathrm{d}z\right]^2 &=\\ = (\mathrm{d}r)^2 + (\mathrm{d}\theta)^2 r^2 + \left[(\mathrm{d}z - r^2\mathrm{d}\theta)\right]^2 &=\\ = (\mathrm{d}r, \mathrm{d}\theta, \mathrm{d}z)\begin{pmatrix}1 & 0 & 0\\ 0 & r^2+r^4 & -r^2\\ 0 & -r^2 & 1\end{pmatrix}\begin{pmatrix}\mathrm{d}r\\ \mathrm{d}\theta\\ \mathrm{d}z\end{pmatrix}&, \quad (21)\end{aligned}$$

if we prefer cylinder coordinates (r, θ, z) by $x = r\cos\theta$, $y = r\sin\theta$, z.

These lead, with a standard method, to a second order differential equation system. Our new explicit but non-elementary solution will be left to another publication.

As a benefit of this new interpretation we discuss the so-called translation curves, which will be straight lines in this model of **Nil**, the curve $[x(t), y(t), z(t)]$ whose tangent $[\dot{x}(t), \dot{y}(t), \dot{z}(t)]$ will be translation of the starting tangent $\dot{x}(0) = u$, $\dot{y}(0) = v$, $\dot{z}(0) = w$ in the origin $x(0) = y(0) = z(0) = 0$. In the matrix form

$$(0, \dot{x}(t), \dot{y}(t), \dot{z}(t)) = (0, u, v, w)\begin{pmatrix}1 & x(t) & y(t) & z(t)\\ 0 & 1 & 0 & -\frac{1}{2}y(t)\\ 0 & 0 & 1 & \frac{1}{2}x(t)\\ 0 & 0 & 0 & 1\end{pmatrix},$$

i.e. $\dot{x}(t)=u$, $\dot{y}(t)=v$, $\dot{z}(t)=w$, yield $x(t)=ut$, $y(t)=vt$, $z(t)=wt$ as desired, where the unit velocity $u^2+v^2+w^2 = 1$, also by (21) leads to arc-length parameter $t=s$.

The publications, e.g. [2, 11, 19, 22] contain surprising results in **Nil** geometry, whose new visualization we are working on. In Fig. 13 we illustrate geodesic and translation balls in the old model by Heisenberg group.

In the new linear model of **Nil**, translation ball will be the same as the Euclidean one, but only at the origin. The metric will be deformed in other points, so a unit ball can be touched by 14 disjoint other unit balls (see [19] and [22]). In $\mathbf{E}^3$ this "kissing" number is 12, only.

6. On higher dimensional regular polytopes moving in the computer screen

The theoretical background of our topic is also the d-dimensional projective spherical space $\mathcal{PS}^d(\mathbf{V}^{d+1}; \boldsymbol{V}_{d+1}; \mathbf{R}; \sim)$ or projective space $\mathcal{P}^d$. These are modelled as subspace incidence structure of the real $d+1$-dimensional vector space $\mathbf{V}^{d+1}$ for

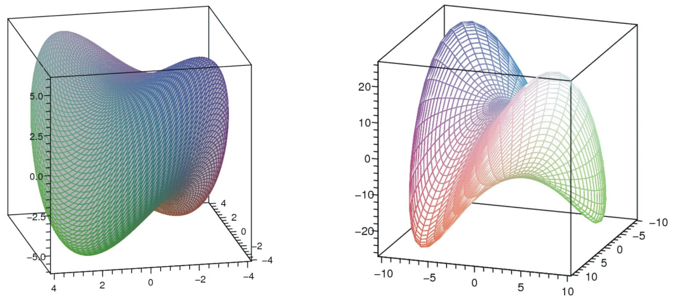

Figure 13. The geodesic ($R = 4$, left) and translation ($R = 10$, right) balls of **Nil** space in the old model by Heisenberg group.

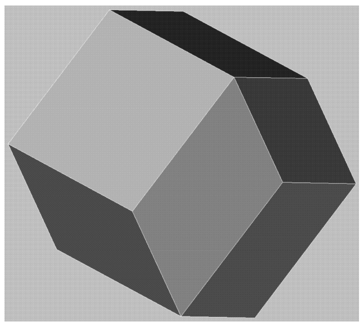

Figure 14. The 4-cube with Coxeter-Schläfli symbol $(4, 3, 3)$.

points or its dual $\boldsymbol{V}^{d+1}$ for hyperplanes, respectively (see Sect. 2–4). Here $\sim$ indicates the multiplicative equivalence by positive reals $\mathbf{R}^+$ in case $\mathcal{PS}^d$, or by non-zeros $\mathbf{R}_0 = \mathbf{R} \setminus \mathbf{0}$ for $\mathcal{P}^d$. E.g. non-zero $\mathbf{V}^{d+1}$ vectors $\mathbf{x} \sim c\mathbf{x}$ describe the same point $X(\mathbf{x})$ in $\mathcal{PS}^d$ iff $c \in \mathbf{R}^+$.

In this Sect. 6 we only indicate the basic algorithms in visualizing higher dimensional regular polytopes P of Euclidean d-space $\mathbf{E}^d$, in the computer p-screen, projected from a complementary $d - p - 1 = s$-dimensional centre figure C. The animation with visibility and shading are our new initiative. See our references [5, 6] for $d = 4$, $p = 2$, $s = 1$ and the homepage `http://www.math.bme.hu/~prok` of I. Prok for free download, hopefully in a more developed form in the future. Their analogues can exist in each dimension. Projection into $p = 3$-space seems to have interesting and important applications as well.

6.1. Concepts and algorithmic problems

1. Projective d-sphere and d-space ($d = 2, 3, 4$).
2. Metrics by hyperplane $\rightarrow$ point polarities, non-Euclidean geometries.
3. Polyhedron tiling by barycentric subdivision and D-symbol.

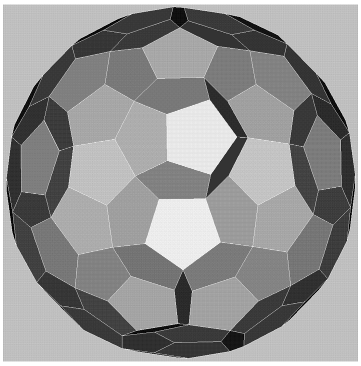

Figure 15. The 120-cell with Coxeter-Schläfli symbol $(5, 3, 3)$.

4. Regular polytope.
5. Symmetry by linear mapping, reflection and motion, affine and projective mapping.
6. Projection by $d \to p$ mapping.
7. Visibility and shading.
8. The algorithms will be combined with each other.

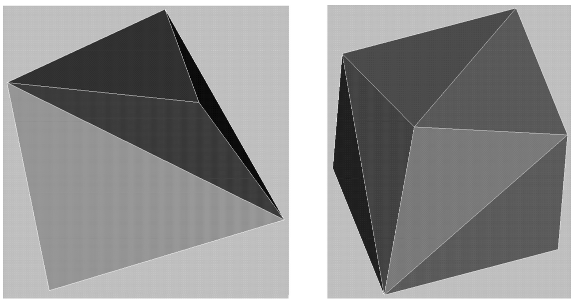

Figure 16. The 5 cell with Coxeter-Schläfli symbol $(3, 3, 3)$ and the 16 cell with Coxeter-Schläfli symbol $(3, 3, 4)$.

Only some aspects have been mentioned in this survey by pictures and titles. See also our papers [5, 6] furthermore [8, 9, 10, 15, 18, 24, 27] for the combinatorial and algebraic-geometric theory.

References

[1] Bölcskei A., Molnár E., *Classification and projective metric realizations of tile-transitive triangle tilings*, J. Geometry and Graphics **11/2**, (2007), 137–163.

[2] Brodaczewska K., *Elementargeometrie in* **Nil**, Dissertation (Dr. rer. nat.) Fakultät Mathematik und Naturwissenschaften der Technischen Universität Dresden, (2014).

[3] Cavichioli A., Molnár E., Spaggiari F., Szirmai J., *Some tetrahedron manifolds with* **Sol** *geometry*, J. Geometry, **105/3**, (2014), 601–614.

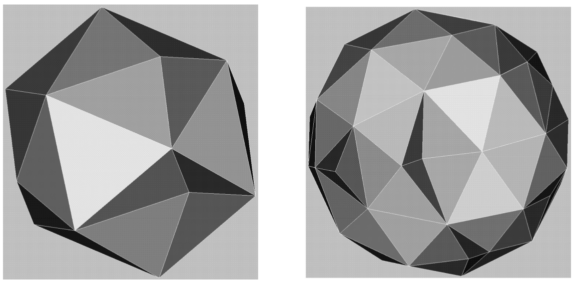

Figure 17. The 24 cell with Coxeter-Schläfli symbol $(3, 4, 3)$ and the 600 cell with Coxeter-Schläfli symbol $(3, 3, 5)$.

[4] Divjak B., Erjavec Z., Szabolcs B., Szilágyi B., *Geodesics and geodesic spheres in* $\widetilde{\mathbf{SL}(2, \mathbf{R})}$ *geometry*, Math. Commun., **14/2**, (2009), 413–424.

[5] Katona J., Molnár E., Prok I., Szirmai J., *Higher dimensional central projection into 2-plane with visibility and applications*, Kragujevac Journal of Mathematics, **35/2**, (2011), 249–263.

[6] Katona J., Molnár E., Prok I., Szirmai J., *Visualization with visibility of higher dimensional and non-Euclidean geometries*, Proceedings of the 16th International Conference on Geometry and Graphics, H. Schröcker, M. Husty (ed.); Innsbruck University Press, Innsbruck (2014), No. 60, ISBN: 978-3-902936-46-2.

[7] Molnár E., *Projective Metrics and hyperbolic volume*, Annales Univ. Sci. Budapest, Sect. Math., (1989), **32**, 127–157.

[8] Molnár E., *Polyhedron complexes with simply transitive group actions and their realizations*, Acta Math. Hung., (1991), **59/1-2**, 175–216.

[9] Molnár E., *Combinatorial construction of tilings by barycentric simplex orbits (D symbols) and their realizations in Euclidean and other homogeneous spaces*, Acta Cryst., (2005), **A61**, 541–552.

[10] Molnár E., *The projective interpretation of the eight 3-dimensional homogeneous geometries*, Beitr. Alg. Geom., (Contr. Alg. Geom.), (1997), **38/2**, 261–288.

[11] Molnár E., *On projective models of Thurston geometries, some relevant notes on* **Nil** *orbifolds and manifolds*, Siberian Electronic Mathematical Reports, `http://semr.math.nsc.ru`, (2010), **7**, 491–498.

[12] Molnár E., Szirmai J., *Symmetries in the 8 homogeneous 3-geometries*, Symmetry Cult. Sci., **21/1–3**, (2010), 87–117.

[13] Molnár E., Szirmai J., *Classification of* **Sol** *lattices*, Geom. Dedicata, **161/1**, (2012), 251–275, DOI: 10.1007/s10711-012-9705-5.

[14] Molnár E., Szilágyi B., *Translation curves and their spheres in homogeneous geometries*, Publ. Math. Debrecen., **78/2**, (2011), 327–346.

[15] Molnár E., Prok I., Szirmai J., *Classification of tile-transitive 3-simplex tilings and their realizations in homogeneous spaces*, A. Prékopa and E. Molnár, (eds.). Non-Euclidean Geometries, János Bolyai Memorial Volume, Mathematics and Its Applications, Springer (2006), Vol. **581**, 321–363.

[16] Molnár E., Szirmai J., Vesnin A., *Packings by translation balls in* $\widetilde{\mathbf{SL}_2\mathbf{R}}$, J. Geometry, **105/2**, (2014), 287–306, DOI: 10.1007/s00022-013-0207-x.

[17] Scott P., *The geometries of 3-manifolds*, Bull. London Math. Soc., **15**, (1983), 401–487.

[18] Szirmai J., *The optimal ball and horoball packings to the Coxeter honeycombs in the hyperbolic d-space*, Beitr. Alg. Geom., (Contr. Alg. Geom.), (2007), **48/1**, 35–47.

[19] Szirmai J., *The densest geodesic ball packing by a type of* **Nil** *lattices*, Beitr. Alg. Geom., (Contr. Alg. Geom.), (2007), **48/2**, 383–397.

[20] Szirmai J., *The densest translation ball packing by fundamental lattices in* **Sol** *space*, Beitr. Alg. Geom., (Contr. Alg. Geom.), (2010), **51/2**, 353–373.

[21] Szirmai J., *Geodesic ball packing in* $\mathbf{S}^2 \times \mathbf{R}$ *space for generalized Coxeter space groups*, Beitr. Alg. Geom., (Contr. Alg. Geom.), (2011), **52**, 413–430.

[22] Szirmai J., *Lattice-like translation ball packings in* **Nil** *space*, Publ. Math. Debrecen, (2012), **80/3-4**, 427–440, DOI: 10.5486/PMD.2012.5117.

[23] Szirmai J., *A candidate to the densest packing with equal balls in the Thurston geometries*, Beitr. Algebra Geom., (2014), **55/2**, 441–452, DOI 10.1007/s13366-013-0158-2.

[24] Szirmai J., *Horoball packings to the totally asymptotic regular simplex in the hyperbolic n-space*, Aequat. Math., (2013), **85**, 471–482, DOI: 10.1007/s00010-012-0158-6.

[25] Szoboszlai M., *Helicoids and their projection*, Katachi U Symmetry, Springer Verlag, Tokyo, (1996), 185–191.

[26] Thurston W. P., *Three-Dimensional Geometry and Topology*, Princeton University Press, Princeton, New Jersey, Vol.**1**, (1997).

[27] Weeks J. R., *Real-time animation in hyperbolic, spherical, and product geometries*, A. Prékopa and E. Molnár (eds.), Non-Euclidean Geometries, János Bolyai Memorial Volume, Mathematics and Its Applications, Springer (2006), Vol. **581**, 287–305.

E. Molnár, Budapest University of Technology and Economics, Institute of Mathematics, Department of Geometry, H-1521 Budapest, Hungary,
E-mail address: `emolnar@math.bme.hu`

I. Prok, Budapest University of Technology and Economics, Institute of Mathematics, Department of Geometry, H-1521 Budapest, Hungary,
E-mail address: `prok@math.bme.hu`

J. Szirmai, Budapest University of Technology and Economics, Institute of Mathematics, Department of Geometry, H-1521 Budapest, Hungary,
E-mail address: `szirmai@math.bme.hu`

Studies of the University of Žilina
Mathematical Series
Vol. 27/2015, 63–66

A GEOMETRICAL PROOF OF SUM OF $\cos n\varphi$

LÁSZLÓ NÉMETH

Abstract. In this article, we present a geometrical proof of sum of $\cos \ell\varphi$ where ℓ goes from 1 up to m. Although there exist some summation forms and the proofs are simple, they use complex numbers. Our proof comes from a geometrical construction. Moreover, from this geometrical construction we obtain an other summation form.

1. Introduction

The Lagrange's trigonometric identities are well-known formulas. The one for sum of $\cos \ell\varphi$ ($\varphi \in (0, 2\pi)$) is

$$\sum_{\ell=1}^{m} \cos \ell\varphi = \frac{1}{2}\left(\frac{\sin\,(m+\frac{1}{2})\varphi}{\sin\frac{1}{2}\varphi} - 1\right). \tag{1}$$

The proof of equation (1) is based on the theorem of the complex numbers in all the books, articles and lessons at the universities ([1], [2]). In the following we give a geometrical construction which implies the formula (1) and using certain geometrical properties we obtain an other summation formula without half angles ($\varphi \in (0, 2\pi)$, $\varphi \neq \pi$)

$$\sum_{\ell=1}^{m} \cos \ell\varphi = \frac{1}{2}\left(\frac{\sin(m+1)\varphi + \sin m\varphi}{\sin\varphi} - 1\right). \tag{2}$$

2. Geometrical construction

Let x and e be two lines with the intersection point A_0. Let the angle of them is α as x is rotated to e (Figure 1). Let the point A_1 be given on x such that the distance between the points A_0 and A_1 is 1. Let the point A_2 be on the line e such that the distance of A_1 and A_2 is also equal to 1 and $A_2 \neq A_0$ if $\alpha \neq \pi/2$ and $\alpha \neq 3\pi/2$. Then let the new point A_3 be on the line x again such that $A_2A_3 = 1$ and $A_3 \neq A_1$ if it is possible. Recursively, we can define the point A_ℓ ($\ell \geq 2$) on one of the lines x or e if ℓ is odd or even, respectively, where $A_{\ell-1}A_\ell = 1$ and $A_\ell \neq A_{\ell-2}$ if it is possible. Figure 1 shows the first six points and Figure 2 shows

Received December 22, 2014.
2000 *Mathematics Subject Classification.* Primary 11L03.
Key words and phrases. Lagrange's trigonometric identities, sum of $\cos n\varphi$.
This work was supported by the Visegrad Fund, small grant 11420082.

some general points. We can easily check that the rotation angels at vertices A_ℓ ($\ell \geq 1$) between the line e (or the axis x) and the segments $A_{\ell-1}A_\ell$ or $A_\ell A_{\ell+1}$ are $(\ell-1)\alpha$ or $(\ell+1)\alpha$, respectively, as the triangles $A_{\ell-1}A_\ell A_{\ell+1}$ are isosceles. (The angle $i\alpha$ can be larger the $\pi/2$, even larger than 2π. The vertices A_ℓ can be closer to A_0 then $A_{\ell-2}$ – see Figure 3.) If A_1 is on the line e we obtain a similar geometric construction. In that case those points A_ℓ are on line x which have even indexes.

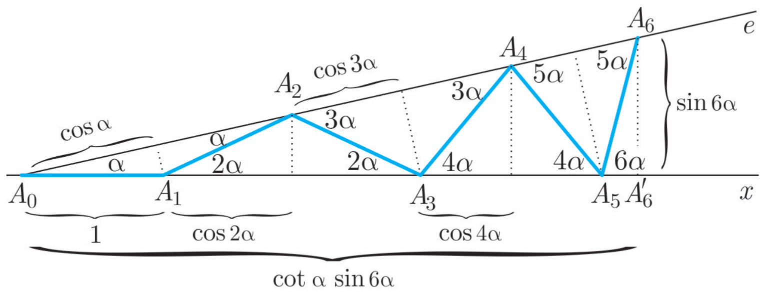

Figure 1. First seven points of the geometrical construction.

Let A_0 be the origin and the line x is the axis x. Then the equation of the line e is $\cos\alpha \cdot y = \sin\alpha \cdot x$. Let A_n' be the orthogonal projection of $A_n \in e$ $(n \geq 2)$ onto the axis x then from right angle triangle $A_0A_n'A_n$ the coordinates of the points A_n (see Figure 1) are

$$\begin{aligned} x_n(\alpha) &= \cot\alpha \sin n\alpha, \\ y_n(\alpha) &= \sin n\alpha. \end{aligned} \tag{3}$$

If $\alpha = \pi/2$ and $\alpha = 3\pi/2$ then all the points A_n coincide the points A_0 or A_1, so in the following we exclude this cases.

The parametric equation system of the orbits of the points $A_n \in e$ can be given by the help of the Chebyshev polynomial too (for more details and for some figures of orbits, see in [3]). The equation system is

$$\begin{aligned} x_n(\alpha) &= \cos\alpha\ U_{n-1}(\cos\alpha), \\ y_n(\alpha) &= \sin\alpha\ U_{n-1}(\cos\alpha), \end{aligned} \tag{4}$$

where α goes from 0 to 2π and $U_{n-1}(x)$ is a Chebyshev polynomial of the second kind [4].

Let $A_1 \in x$ and n be even so that $n = 2k+2$. We take the orthogonal projections of the segments $A_{\ell-1}A_\ell$ $(\ell = 1, 2, \dots, n)$ onto the line x (see Figure 1 and 2). Then we realize

$$x_n(\alpha) = 1 + 2\left(\cos 2\alpha + \cos 4\alpha + \cdots + \cos 2k\alpha\right) + \cos(2k+2)\alpha, \tag{5}$$

on the other hand, from (3) or from (4) we have

$$x_n(\alpha) = \cos\alpha\ \tfrac{\sin(2k+2)\alpha}{\sin\alpha}. \tag{6}$$

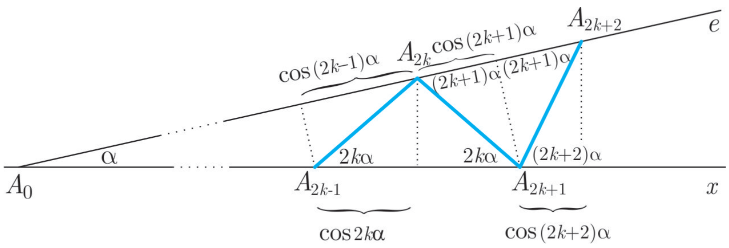

Figure 2. General points of the geometrical construction.

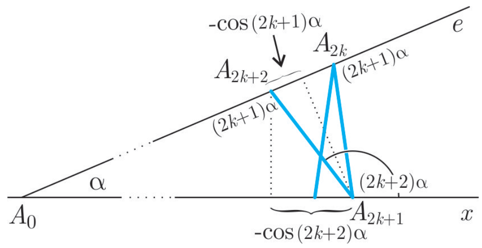

Figure 3. General points.

Comparing (5) and (6) we obtain

$$1+2\sum_{\ell=1}^{k}\cos 2\ell\alpha+\cos(2k+2)\alpha=\cos\alpha\,\frac{\sin(2k+2)\alpha}{\sin\alpha}. \tag{7}$$

Using the addition formula for cosine we receive from (7) that

$$\sum_{\ell=1}^{k}\cos 2\ell\alpha=\tfrac{1}{2}\left(\cos\alpha\,\frac{\sin(2k+2)\alpha}{\sin\alpha}-\cos(2k+2)\alpha-1\right)= \tag{8a}$$

$$=\tfrac{1}{2}\left(\frac{\cos\alpha\sin(2k+2)\alpha-\sin\alpha\cos(2k+2)\alpha}{\sin\alpha}-1\right)= \tag{8b}$$

$$=\tfrac{1}{2}\left(\frac{\sin((2k+2)-1)\alpha}{\sin\alpha}-1\right)= \tag{8c}$$

$$=\tfrac{1}{2}\left(\frac{\sin(2k+1)\alpha}{\sin\alpha}-1\right). \tag{8d}$$

If $\varphi=2\alpha$ then

$$\sum_{\ell=1}^{k}\cos\ell\varphi=\tfrac{1}{2}\left(\frac{\sin(k+\frac{1}{2})\varphi}{\sin\frac{1}{2}\varphi}-1\right). \tag{9}$$

3. Other summation form

In this section, we give an other summation form for the cosines without half angles by the help of the defined geometrical construction. Now let us take the orthogonal projection of the segments $A_{\ell-1}A_\ell$ ($\ell = 1, 2, \ldots, n$) onto the line e (see Figure 1 and 2) and summarize them for all ℓ from 1 to $2k+1$. (The sum is equal to $x(\alpha)$ if $n = 2k+1$ and $A_1 \in e$.) Now we gain a similar equation to (7), namely

$$2\left(\cos\alpha + \cos 3\alpha + \cdots + \cos(2k-1)\alpha\right) + \cos(2k+1)\alpha = \cos\alpha\, \tfrac{\sin(2k+1)\alpha}{\sin\alpha}. \tag{10}$$

With analogous calculation to (8) we obtain

$$\sum_{\ell=1}^{k} \cos(2\ell-1)\alpha = \tfrac{1}{2}\left(\cos\alpha\, \tfrac{\sin(2k+1)\alpha}{\sin\alpha} - \cos(2k+1)\alpha\right) = \tag{11a}$$

$$= \tfrac{1}{2}\left(\tfrac{\sin 2k\alpha}{\sin\alpha}\right). \tag{11b}$$

Summing equations (8d) and (11b), we have

$$\sum_{\ell=1}^{k} \cos 2\ell\alpha + \sum_{\ell=1}^{k} \cos(2\ell-1)\alpha = \tfrac{1}{2}\left(\tfrac{\sin(2k+1)\alpha}{\sin\alpha} + \tfrac{\sin 2k\alpha}{\sin\alpha} - 1\right), \tag{12}$$

and finally if $m = 2k$ and $\varphi = \alpha$ we obtain formula (2).

References

[1] Muñiz E. O., *A Method for Deriving Various Formulas in Electrostatics and Electromagnetism Using Lagrange's Trigonometric Identities*, American Journal of Physics 21 (2), p. 140 (February 1953).

[2] Jeffrey A., Dai H-h., *Handbook of Mathematical Formulas and Integrals (4th ed.)*, Academic Press, 2008, ISBN 978-0-12-374288-9.

[3] Németh L., *A new type of lemniscate*, NymE SEK Tudományos Közlemények XX, Természettudományok 15, Szombathely, (2014), pp. 9–16.

[4] Rivlin T. J., *Chebyshev polynomials*, New York Wiley, 1990.

László Németh, Bajcsy Zs. u.4, 8942 Sopron, Hungary,

E-mail address: `nemeth.laszlo@emk.nyme.hu`

Studies of the University of Žilina
Mathematical Series
Vol. 27/2015, 67–74

PENDENTIVE REDEFINED

LÁSZLÓ STROMMER

Abstract. This article tries to clarify and refine the geometrical content of the architectural term **pendentive** whose description is often not only incomplete and self-contradictory even in the professional practice, but it contradicts the conventional denominations of historical architectural forms also.

Understanding the Undefined

It may seem to be truism that every concept and object needs a definition – a definite explanation that describes its meaning – yet, we manage to learn the meaning of the words of our native language mostly without such precise definitions. We have learned it the hard way how difficult it is to teach a computer the difference between for example dogs and cats. Some recent object recognition algorithms try to achieve this goal by traditional means: "*instead of telling the computer what to look at to distinguish between two objects, they simply feed it a set of images and it learns on its own means of show*" [1].

However, this approach evidently does not eliminate the necessity of a proper definition – it only takes it one step further, since someone has to clearly identify (i.e. understand) the image first in order to be able to teach the computer properly. Another problem is that in order to reach the desired level of understanding, you have to present images that are selected with great care, so that they include not only the most relevant, but all possible forms (since the computer has to identify all breeds of dogs regardless their differences).

Perhaps surprisingly, the designation of architectural elements (shapes and structures alike) often raises similar questions. There are some obvious and strict definitions – but the reality (i.e. architecture itself) often presents forms that are difficult to classify.

Of course one may argue that all previous generations of architects managed to get by without such exact definitions – but they were part of a given architectural tradition, hence it was enough to have a "local" consent about the meaning of the words that were necessary to describe the building (both the object and

Received December 22, 2014.
2000 *Mathematics Subject Classification.* Primary 97M80.
Key words and phrases. pendentive, architecture.
This work was supported by the Visegrad Fund, small grant 11420082.

the process).[1] Obviously, it does not mean that there were no widely accepted basic concepts – but the actual details were often different, and these small but sometimes vital nuances often went unnoticed.

The penetration of 3D CAD modelling have undermined this comfortable "ignorance". Previously it was enough (or it was often thought to be enough) to know 2D plans and elevations of buildings – now it turns out that these does not contain sufficient information to "build" even a simplified 3D model, and those previously overlooked subtle differences can gain much higher importance.[2] To make things even worse, in most cases the definitions describe only the most basic and common shapes – which leaves plenty of room for ambiguity and uncertainty.

In this article we narrow our examination to the term **pendentive**, and we try to determine the limits of the domain where this term can be used.

The Traditional Definition

The pendentive is arguably one of the best known architectural terms, therefore one would think that it has a definite description – but unfortunately it is not the case.

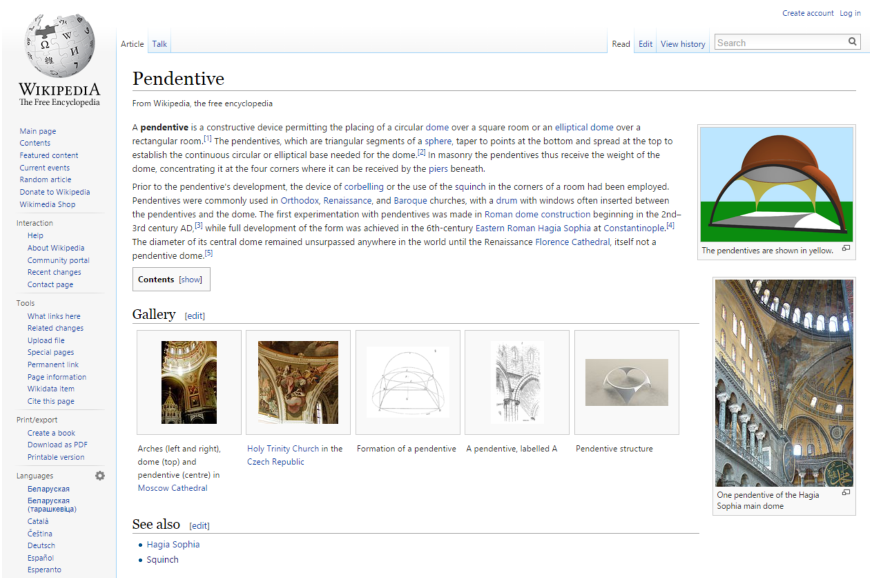

Pendentive

From Wikipedia, the free encyclopedia

A **pendentive** is a constructive device permitting the placing of a circular dome over a square room or an elliptical dome over a rectangular room.[1] The pendentives, which are triangular segments of a sphere, taper to points at the bottom and spread at the top to establish the continuous circular or elliptical base needed for the dome.[2] In masonry the pendentives thus receive the weight of the dome, concentrating it at the four corners where it can be received by the piers beneath.

Prior to the pendentive's development, the device of corbelling or the use of the squinch in the corners of a room had been employed. Pendentives were commonly used in Orthodox, Renaissance, and Baroque churches, with a drum with windows often inserted between the pendentives and the dome. The first experimentation with pendentives was made in Roman dome construction beginning in the 2nd–3rd century AD,[3] while full development of the form was achieved in the 6th-century Eastern Roman Hagia Sophia at Constantinople.[4] The diameter of its central dome remained unsurpassed anywhere in the world until the Renaissance Florence Cathedral, itself not a pendentive dome.[5]

Contents [show]

Gallery [edit]

Arches (left and right), dome (top) and pendentive (centre) in Moscow Cathedral

Holy Trinity Church in the Czech Republic

Formation of a pendentive

A pendentive, labelled A

Pendentive structure

The pendentives are shown in yellow.

One pendentive of the Hagia Sophia main dome

See also [edit]

- Hagia Sophia
- Squinch

Figure 1. The Definition of Pendentive in Wikipedia.

Let us start with the definition that can be found in the Wikipedia [2]: "*A pendentive is a constructive device permitting the placing of a circular dome over*

[1] One might say that vernacular architecture needs only vernacular language – but the real point is that even "academic" architecture tends to become "localized" based on local needs, materials, and traditions.

[2] If a picture is worth a thousand words – then a model is worth a thousand pictures.

a square room or an elliptical dome over a rectangular room. The pendentives, which are triangular segments of a sphere, taper to points at the bottom and spread at the top to establish the continuous circular or elliptical base needed for the dome."

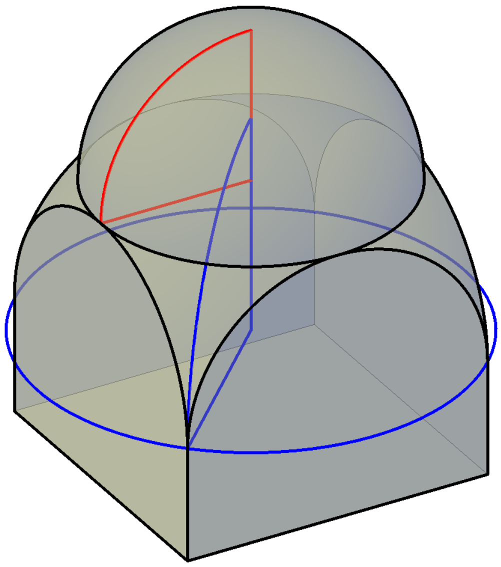

Figure 2. Pendentive – the Traditional Definition.

We may supplement that the upper dome can be placed either on a cylindrical wall called drum, or directly on the top of the pendentives (like in Figure 2). The dome itself obviously can have any shape, but when the joining curve of the pendentive and the dome is continuous, without a break it is called pendentive dome, or more commonly, sail vault [3].

The Base and the Boundary

The above definition duly deals with the possibility of a rectangular room (although it does not mention that the pendentives in that case should be segments of an ellipsoid, not a sphere). On the other hand, it is obviously a mistake to say that pendentives can only be used over four-sided (square or rectangular) base. Theoretically the base can be any polygon that can be inscribed in a circle (or ellipse), however, aesthetical considerations strongly favour rotational or axial symmetry, and practical reasons usually limit the number of sides (probably to about 8).

The most surprising aspect is that in most cases the definitions consistently and exclusively speak about the tapering surface of the pendentive as being triangular

– totally ignoring the fact that it is often untrue.[3] A real pendentive can deviate from the textbook form in two ways: firstly, instead of tapering to a single point at the bottom it can end in a horizontal arc or line, and have a trapezium-like appearance, and secondly, it can reach higher than the apexes of the side arches, forming a continuous secondary domical surface (a segment of the abovementioned sail vault shape) below the dome.

The pendentive in Figure 3 has been constructed over an octagonal base with uneven sides – and it illustrates a combination of all three previous deviations (different base, bottom, and top side).

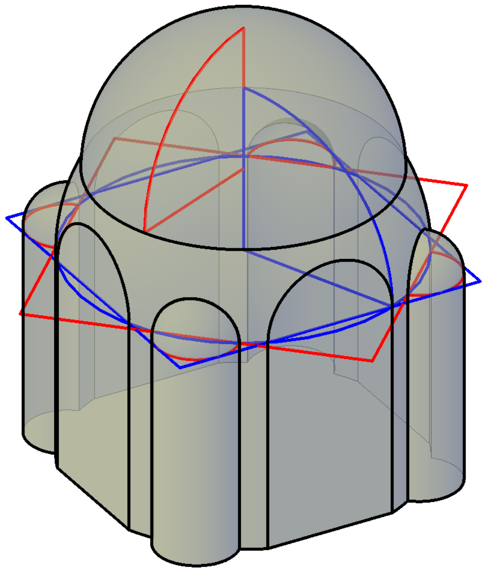

Figure 3. Pendentive – Generalization.

The Surface

Probably the most common deficiency of the definitions is that if they say anything at all about the pendentive surface, they describe it as "segment of a sphere" – they seem to rule out any other possibility. However, if one knows what to look for, it is quite easy to find visual evidences that disprove this restriction.

The intersection of a sphere and a plane (if it exists, and it is not a single point) is always a circle. The straight line which is perpendicular to the plane of this circle and passes through its centre is the axis of the circle – and this axis passes through the centre of the sphere also. Consequently, when a surface is bounded

[3]Actually, the English version of Wikipedia presents three photos as illustrations of the pendentive shape – and none of them has triangular form.

by arcs whose axis does not intersect each other in a single point, the surface is surly not a spherical segment.

The above consideration means that when we see a pendentive whose top edge is a full circle, but the side arches are pointed, the pendentive obviously cannot be a spherical segment. (e.g. Sultan Ahmed Mosque, Istanbul [A]).

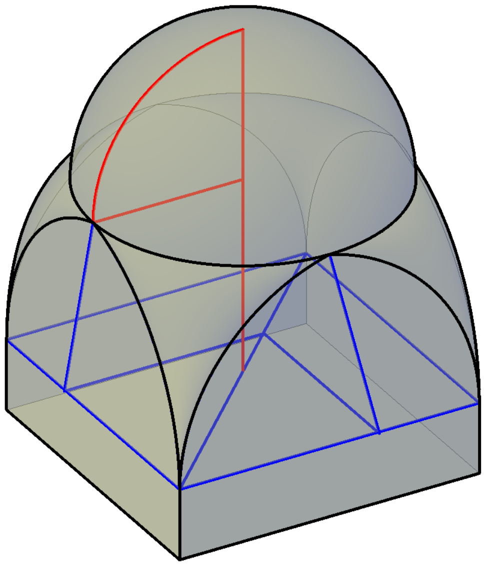

Figure 4. Pendentives with Pointed Arches.

As it can be seen in Figure 4, if the base of the vaulting bay is a rotationally symmetric polygon bounded by pointed arches of equal size, then the horizontal axes of two adjacent arc segments meet each other on the angle bisector of the base polygon[4]. However, this intersection obviously occurs beyond the centre of the base[5], hence these horizontal axes do not meet the vertical axis of the horizontal circular top edge of the pendentive – therefore the two vertical arcs cannot be sections of the same sphere as the horizontal circle.

Of course it is easy to find visually similar solutions even in these cases – using equal radii in every horizontal section for example – but it still means that these pendentives can never be segments of a sphere.

[4]More generally in the vertical plane of the angle bisector, if we take into consideration the possibility of drop arches whose centre points are located beneath the level of the imposts.

[5]A pointed arch can be seen as a semicircular arch whose middle section has been removed and the two remaining parts has been placed next to each other. This way the original centre point obviously gets doubled, and the centres of the arc segments will be located on the opposite side of the arch.

The same reasoning applies when the bottom edge of a pendentive is a quarter-circle (e.g. St. Stephen Basilica, Budapest [B]), since this arc evidently cannot lie on the same sphere as the circle of the top edge.

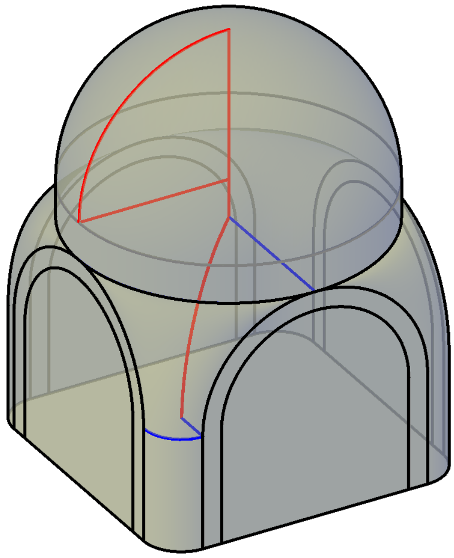

Figure 5. Pendentives with Rounded Corners.

As it can be seen in Figure 5, if every horizontal section of the pendentive is a quarter-circle, then obviously the bottommost horizontal edge will have the smallest radius – while the topmost edge will have the same radius as in the case of a spherical pendentive surface (see Figure 2).

Altogether it means that even if we consider the upper horizontal edge of the pendentive to be determined by the dome above, from that level down the curvature can either decrease or increase, or it even can stay the same – hence the shape of the pendentive can be significantly different. It is worth noting also that we cannot be sure whether the surface is truly spherical even if the edges of the pendentive would allow it – despite its different constructional logic, a surface which has a constant horizontal curvature shows only a relatively small deviation from the spherical surface [4].

Summary

The main goal of this article is to unravel some of the existing ambiguities in the terminology of architectural shapes. Based on what we have learned we can safely say that the academic and everyday use of the term **pendentive** is considerably different (much more permissive) than the "official" definitions.

This paper has tried to gather the principal aspects that we should consider when we try to distinguish this particular form from the “concurrent” types of vaulting (e.g. squinch).

As it can be seen in Figure 6, there are other shapes also, which can be seen as some kind of transitional forms (e.g. Imamaden Mosque, Shiraz [C]). Thus, it is certainly not the end, but the beginning of the process which might result in a self-consistent terminology [5].

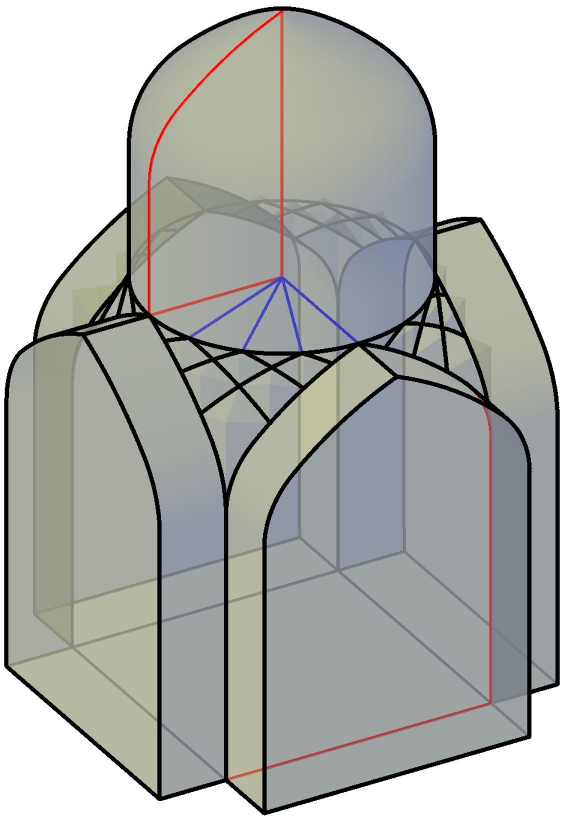

Figure 6. Schematic Model of Imamaden Mosque, Shiraz.

References

[1] Lillywhite K., Lee D. J., Tippetts B., Archibald J., *A feature construction method for general object recognition*, Pattern Recognition, **46**, (2013), 3300–3314, `http://www.sciencedirect.com/science/article/pii/S0031320313002549`.

[2] *Pendentive*, `http://en.wikipedia.org/wiki/Pendentive`.

[3] Dodge H., *Building materials and techniques in the Eastern Mediterranean from the Hellenistic period to the fourth century AD*, PhD Thesis, Newcastle University, (1984), 276, https://theses.ncl.ac.uk/dspace/handle/10443/868.

[4] Strommer L., *Történeti boltozati formák geometriai elemzése... (Geometrical Analysis and CAD Representation of Historical Vault Forms)*, PhD Thesis, BME, Csonka Pál Doktori Iskola, (2008), 7, http://www.omikk.bme.hu/collections/phd/Epiteszmernoki_Kar/2008/Strommer_Laszlo.

[5] Strommer L., *Boltozat-morfológia (Vault-morphology)*, Építés – Építészettudomány, (2006), vol. XXXIV (3–4), 347–359.

[A] http://http://commons.wikimedia.org/wiki/File:Blue_Mosque_Interior_Wikimedia_Commons.JPG.

[B] http://commons.wikimedia.org/wiki/File:Budapest_-_Saint_Stephen's_Basilica_-_Interior.jpg.

[C] http://commons.wikimedia.org/wiki/File:Imamaden_mosque_interiors,_Shiraz.jpg.

László Strommer, Budapest University of Technology and Economics, Műegyetem rkp. 3., Budapest, Hungary,

E-mail address: strommer@arch.bme.hu, http://www.epab.bme.hu/Strommer

Studies of the University of Žilina
Mathematical Series
Vol. 27/2015, 75–80

DEVELOPMENT OF COMPUTER-BASED VISUAL DEMONSTRATIONS IN ENGINEERING EDUCATION

MIHÁLY SZOBOSZLAI AND ÁDÁM TAMÁS KOVÁCS

Abstract. This paper deals with the question of methods of visualisation using traditional blackboard construction and using computer programs for descriptive geometry in engineering education.

Geometry and visualization

There are no doubts that geometry is one of the subjects in basic studies of engineering education, especially in architecture and civil engineering, where visualization is a key-feature of training. Most of the results of design processes are presented with drawings, both freehand sketches and constructed figures. Scaled drawings, like floor plans, sections, elevations, and axonometric or perspective drawings of buildings and built environment are based on projections with „geometrical accuracy". Basic projection rules and methods are used in the frame of descriptive geometry, which is a subset of constructive geometry.

Teaching descriptive geometry for engineering students in university courses one should lay down some theoretical principles, but for understanding gist of this practical subject is highly depends on constructions made with traditional tools: triangles and a pair of compasses in lecture halls. Readers were drawing on the blackboard, showing geometrical construction step-by-step, the constructed figure was developed together with the students. Drawing on the blackboard made lectures „slow enough" to be followed by students, since their pencil-made sketches or construction drawings are 10 or 20-times smaller, then drawings of lecturer. For many decades this traditional way of teaching was given at many courses, at least in our practice for students of architecture.

Long tradition and modern technologies

There was not a big advance in modernizing traditional drawing tools for a long period. If we want to be cynic we can summarize development in lecture-drawing

Received December 22, 2014.
2000 *Mathematics Subject Classification.* Primary 97G80.
Key words and phrases. visual communication, descriptive geometry, CAD, software integration.
This work was supported by the Visegrad Fund, small grant 11420082.

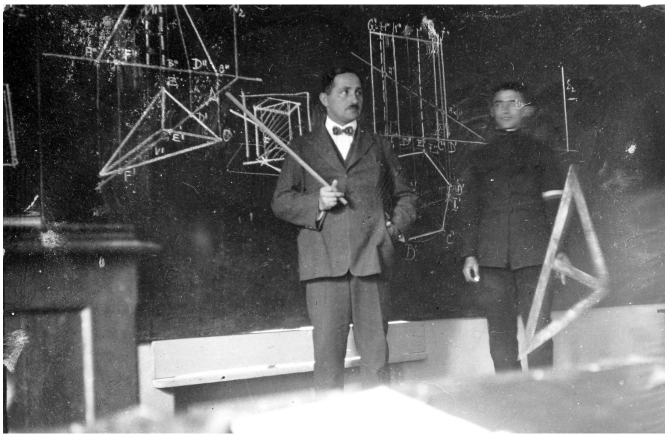

Figure 1. Blackboard lecture in descriptive geometry in the beginning of the 20th century.

in a multi-angle triangle, which made our constructions easier: without a second triangle one can draw perpendicular and 30–45–60 degree angles.

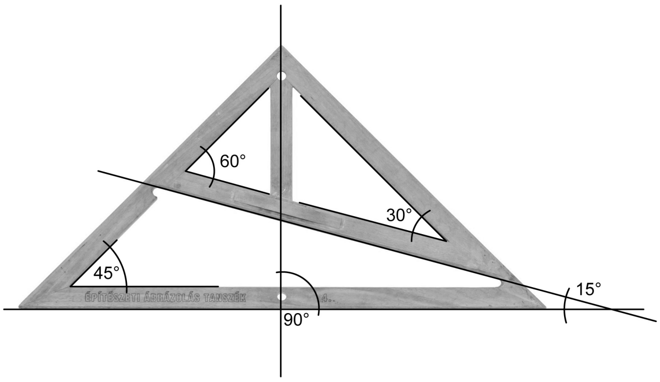

Figure 2. Multi-angled triangle for construction.

Beside showing theoretical proofs in a lecture there is an enormous demand from students for constructing figures on the blackboard with compasses and triangles. Advantage of live construction (while lecturer explains what is going on) is, that speed of explanation and time for understanding are automatically scaled with speed of construction. Live constructions have a kind of miracle and a satisfaction for the audience, when they get the same result in their notebooks as shown on the blackboard. This raises their confidences about a subject, which would be hard to follow on their own. This brings a stimulation to continue on self-paced problem solving.

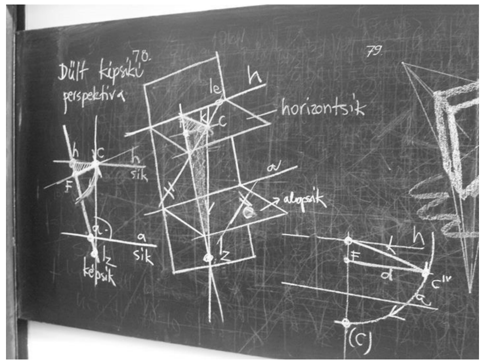

Figure 3. Constructions on a slate chalkboard.

Some 20 years ago slide-driven courses were promising in descriptive geometry as well. First those were done with overhead projectors, with pre-constructed geometrical figures, then computer-based solutions (slide-projections) were used in lectures and in classrooms for practical lessons. Showing the constructions with phase-figures helps to understand gist of a theory.

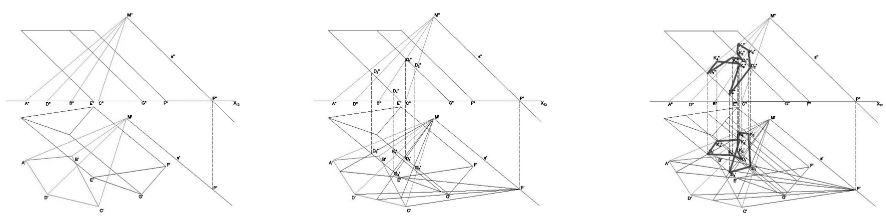

Figure 4. Multi-angled triangle for construction.

Even if computer-assisted lessons brought some revolution to slide-driven classroom experience, there were many debates on Power Point-based lectures [1]. However constructions with phase-figures can be shown more dynamically and evolution of problem-solving is more adequate for students, speed of lecture is less controllable, if we want students to be more active with drawing together, not only listening lecture.

Visualisation with CAD/CADD programs

There was a big revolutionary change in engineering and architecture by using computer based design and drafting in offices in the last 2–3 decades. These computer programs are specialized for different professions.

CAD program for architects (CAAD, Computer Aided Architectural Design) are fairly differing from CAD programs for mechanical engineers, or other engineering. CAD programs become more and more complex and sophisticated tools

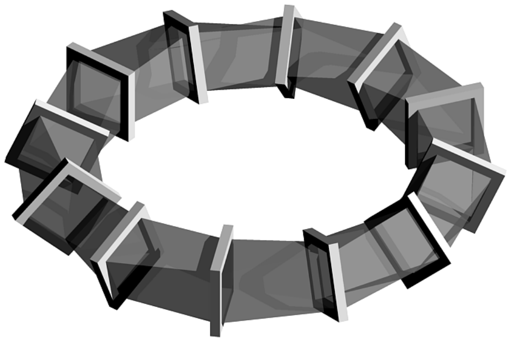

Figure 5. Repetitive construction using computer program.

in engineering practice year by year. Newly graduated engineers will raise the level of usage of those CAD programs which usually are company standards after a while and reached a satisfactory usage among older users. Usual CAD programs are not tailored for basic geometrical constructions. Those are developed for professional use of designing structures and buildings. It is an important question about systematic use of computers and visual demonstrations in lecture halls and classrooms is whether we can use those as live demonstration of constructing "pure" geometric figures.

Well positioned elements (points, lines) in a prepared starting stage will determine whether drawings will be nice-looking and comprehending. Use of state of the art computer aided drafting and design (CAD/CADD) application turned into one of the most crucial question in engineering education in the last two decades. Besides studying theoretical disciplines, students are expected to acquire practical, ready to use engineering skills in design by using CAD programs.

One of the most excited and useful moment in demonstrating 2-dimensional geometrical problems, when one turns 2-dimensional construction into 3-dimensional environment.

Unplugged geometry

We think that there is a disbelief that using CAD programs will substitute learning geometric principles and descriptive geometry. Some users state that no need for traditional human constructions in geometry, since computer programs replaces all those "old-fashioned" construction in descriptive geometry as well. We have realised in our teaching experience at university level, that those students, who were weak in geometry, could not use CAD programs effectively and ergonomically, some could not solve geometrical problems with computers at all. We believe that the main advantage of using computers is making engineering work more ergonomic and more precise. Creativity and solving spatial problems needs more

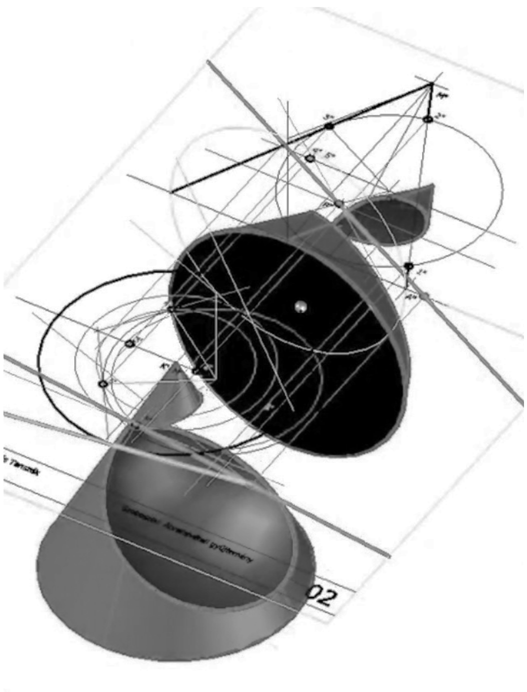

Figure 6. 2-dimensional construction in a 3-D environment.

pure ("unplugged") geometry to know. One should know basic behaviour of shapes and forms in order to get satisfactory compound spatial objects.

Embedded descriptive geometry

Engineering schools try to keep up with CAD technology and introduce the state of the art systems to students. Those CAD programs will be used in practice when students get their degrees. While trying to introduce the latest versions of CAD applications we are facing to a problem: what graphical applications should we use for helping teachers job in basic subjects like descriptive geometry. Is there any dedicated software which serve all pedagogical purposes of teaching descriptive geometry? We have researched and tested many dynamic geometry programs, most of them are 2-dimensional, but we did not find any which fully satisfy our needs from the view of descriptive geometry courses.

Our finding is that we should rather embed problems and geometry courses into CAD programs, than to wait for getting a dedicated system for just teaching purposes. If students use CAD systems for solving geometrical problems, they will became skilled users of the CAD system, while discover the power of solving problems in space.

References

[1] Young J. R., *When Computers Leave Classrooms, so Does Boredom, Chronicle of Higher Education*, Vol. 55, No. 42, (2009).

[2] Schmid-Kirsch A., *Starting with a Cube as the Perfect Guide to Sketch Geometry in Design and Architecture Journal for Geometry and Graphics*, Volume 14, No. 1, (2010), 117–123.

Mihály Szoboszlai, Budapest University of Technology and Economics, Műegyetem rkp. 3, Budapest, Hungary,
E-mail address: `szoboszlai@arch.bme.hu`, `http://www.epab.bme.hu`

Ádám Tamás Kovács, Budapest University of Technology and Economics, Műegyetem rkp. 3, Budapest, Hungary,
E-mail address: `kovacsadam@arch.bme.hu`, `http://www.epab.bme.hu`

Studies of the University of Žilina
Mathematical Series
Vol. 27/2015, 81–86

VORONOI'S CONJECTURE FOR CONTRACTIONS OF DIRICHLET-VORONOI CELLS OF LATTICES

ATTILA VÉGH

ABSTRACT. Let $\mathcal{P}$ and $\mathcal{P} \oplus S(\mathbf{z})$ be parallelotopes, where $S(\mathbf{z})$ is a segment and $\oplus$ denotes the Minkowski sum. A. MAGAZINOV proved that Voronoi's conjecture holds for the parallelotope $\mathcal{P} \oplus S(\mathbf{z})$, if it holds for the parallelotope $\mathcal{P}$. We prove that Voronoi's conjecture is true for the parallelotope $\mathcal{P}$ if it is valid for the parallelotope $\mathcal{P} \oplus S(\mathbf{z})$.

1. INTRODUCTION

DIRICHLET [2] and VORONOI [17] introduced the notion of the Dirichlet-Voronoi cell, which is called Voronoi polytope, too. We use shortly the name of DV cell.

Definition 1.1. *Consider a discrete point set L in the n-dimensional Euclidean space $\mathbb{E}^n$. The **DV cell** of a point P_i of the set L is the set of all points that are closer to the point P_i than to any other point P_j of the set L.*

The DV cells of the lattices are special parallelotopes where the **parallelotope** $\mathcal{P}$ is a convex polytope which translated copies tile the space in a face to face way. The centers of the parallelotopes form an n-dimensional lattice. The following important theorem was proved by B. A. VENKOV [15] and later P. MC-MULLEN [12].

Theorem 1.2. *A polytope $\mathcal{P}$ is a parallelotope if and only if*

(i) $\mathcal{P}$ is centrally symmetric,
(ii) each facet of $\mathcal{P}$ is centrally symmetric, and
(iii) the 2-dimensional orthogonal projection along any $(n-2)$-face of $\mathcal{P}$ is either a parallelogram or a centrally symmetric hexagon.

The edges of the parallelogram and the centrally symmetric hexagon of the above property (iii) are the projections of the facets of the parallelotope $\mathcal{P}$. These facets form a 4 and a 6-**belt**, respectively.

Consider the parallelotopes $\mathcal{P}$ and $\mathcal{Q}$ of dimension n. Denote by $S(\mathbf{z})$ the segment of the direction $\mathbf{z}$ and of the length z. If there exists a direction $\mathbf{z}$ for which $\mathcal{P} \oplus S(\mathbf{z}) = \mathcal{Q}$, where $\oplus$ denotes the Minkowski sum, then $\mathcal{P}$ is called the **contraction** of $\mathcal{Q}$ and $\mathcal{Q}$ is the **extension** of $\mathcal{P}$. V. GRISHUKHIN [7] called the vector $\mathbf{z}$

Received December 5, 2014.
2000 *Mathematics Subject Classification.* Primary 52B11, 52B12, 52B20, 52C07, 52C22.
Key words and phrases. Dirichlet-Voronoi cell, Voronoi polyhedron, parallelotope, parallelohedron, Voronoi's conjecture, Minkowski sum, shadow boundary.
This work was supported by the Visegrad Fund, small grant 11420082.

free if the Minkowski sum $\mathcal{P} \oplus S(\mathbf{z})$ is again a parallelotope. A parallelotope is called **free**, if it has free vectors. V. Grishukhin [6] gave a criterion that any vector is free and M. Dutour [4] completed the proof of this statement. A vector $\mathbf{z}$ is free, if $S(\mathbf{z})$ is parallel to at least one facet of each belt of a parallelotope $\mathcal{P}$. The width z of a parallelotope $\mathcal{P}$ along $\mathbf{z}$ is the minimal length of the intersections of the parallelotope $\mathcal{P}$ and the lines parallel to $\mathbf{z}$. If this minimal length is equal to zero then a parallelotope $\mathcal{P}$ is of **zero width** in the direction $\mathbf{z}$.

2. Voronoi's conjecture

G. F. Voronoi asked whether each parallelotope is the affine image of a DV cell. He proved [17], [18] the conjecture in that case if the parallelotope is primitive. A parallelotope is called **primitive**, if every vertex of the parallelotope belongs to exactly $n+1$ translates of the parallelotope. O. K. Zhitomirskii [19] extended the G. F. Voronoi's proof to $(n-2)$**-primitive** parallelotopes, i.e. for such parallelotopes that every $(n-2)$-dimensional face of the parallelotope contains exactly 3 tiles. In this case each belt of the parallelotope is a 6-belt. P. McMullen [11] proved the conjecture for zonotopes from the parallelotopes. R. M. Erdahl gave an other proof for this in [5].

The **zonotope** is a Minkowski sum of several segments. A. Ordine [14] proved the Voronoi's conjecture for 3-irreducible parallelotopes. This result generalizes the theorems of G. F. Voronoi and O. K. Zhitomirskii. A. Magazinov [13] proved that if $\mathcal{P}$ and $\mathcal{P} \oplus S(\mathbf{z})$ are parallelotopes and the parallelotope $\mathcal{P}$ is the affine image of a DV cell, then the extension of $\mathcal{P}$ is again the affine image of a DV cell. In this paper we prove the converse of this statement, if the parallelotope $\mathcal{P} \oplus S(\mathbf{z})$ is the affine image of a DV cell, then the parallelotope $\mathcal{P}$ is the affine image of a DV cell, too. From the two statements it follows that a parallelotope and one of its extraction are affine images of DV cells at the same time.

In this paper we give a new and direct proof for this statement using constructive geometric methods, though it can be proved using the Voronoi's condition [1], [17]: the parallelotope $\mathcal{P}$ is an affine image of a DV cell if and only if the set $\pm U$ of normal vectors to the facets of $\mathcal{P}$ can be chosen so that, if $n_i, n_j, n_k \in \pm U$ are normal vectors to alternate facets in a 6-belt, then $n_i + n_j + n_k = 0$.

3. Shadow boundary

Definition 3.1. *The **shadow boundary** of a parallelotope $\mathcal{P}$ in the direction $\mathbf{z}$ consists of all boundary points $\mathbf{x}$ of $\mathcal{P}$ for which the line $\{\mathbf{x}+\lambda\mathbf{z} | \lambda \in \mathbb{R}\}$ is a support line of $\mathcal{P}$. (There is no point of the line $\{\mathbf{x}+\lambda\mathbf{z} | \lambda \in \mathbb{R}\}$ belonging to the interior of $\mathcal{P}$). It is denoted by $sh_{\mathbf{z}}(\mathcal{P})$.*

It is well known that the shadow boundary of a convex polytope is the union of its some closed $(n-1)$ and $(n-2)$-dimensional faces [10]. If the parallelotope $\mathcal{P} \oplus S(\mathbf{z})$ is of non-zero width in a direction $\mathbf{z}$ then the shadow boundary contains only facets which are called facets parallel to $\mathbf{z}$ by B. A. Venkov [16].

We denote by F_i a facet of the parallelotope $\mathcal{P}$ and by $\mathbf{t}_i$ the lattice vector connecting the center of the parallelotope $\mathcal{P}$ with a parallelotope $\mathcal{P}_i$ where $\mathcal{P}$

and $\mathcal{P}_i$ are adjacent by the facet F_i. We call this lattice vector as the **relevant vector** of F_i.

Á. G. Horváth proved in [8] that if the intersection $\mathcal{P} \cap \mathcal{Q}$ of the parallelotopes $\mathcal{P}$ and $\mathcal{Q}$ is a k-dimensional face, where $0 \leq k \leq n-1$, then this face is centrally symmetric with the center $\frac{1}{2}PQ$, where the lattice points P and Q are centers of $\mathcal{P}$ and $\mathcal{Q}$. N. Dolbilin [3] introduced the term **standard face**. So if $\dim(\mathcal{P} \cap \mathcal{Q}) = n-2$, then the face $\mathcal{P} \cap \mathcal{Q}$ is centrally symmetric, exactly four parallelotopes contain this face and $\mathcal{P}$ and $\mathcal{Q}$ are centrally symmetric with respect to the center of $\mathcal{P} \cap \mathcal{Q}$. V. Grishukhin [6] defined the $\mathbf{z}$-cap of a parallelotope $\mathcal{P}$. A. Magazinov and Á. G. Horváth used this concept in [13], [9].

Definition 3.2. *Let $\mathcal{P}$ be an n-dimensional parallelotope and the vector $\mathbf{z}$ be a free vector. The $\mathbf{z}$-cap $\mathrm{Cap}_{\mathbf{z}}(\mathcal{P})$ of a parallelotope $\mathcal{P}$ consisting of all facets F of the parallelotope $\mathcal{P}$ satisfying the condition*

$$\mathbf{z} \cdot \mathbf{n}(F) < 0,$$

where $\mathbf{n}(F)$ is the normal vector of the facet F.

Each direction defines two caps, which are centrally symmetric to each other. If you distinguish the two caps, denote them by $\mathrm{Cap}^{+}_{\mathbf{z}}(\mathcal{P})$ and $\mathrm{Cap}^{-}_{\mathbf{z}}(\mathcal{P})$.

4. Main theorem

Lemma 4.1. *If an affine transformation L maps the parallelotope $\mathcal{P} \oplus S(\mathbf{z})$ to the DV cell $\mathcal{D} \oplus S(\mathbf{z}')$, where $\mathrm{L}(\mathbf{z}) = \mathbf{z}'$, then the affine transformation L maps the parallelotope $\mathcal{P}$ to the parallelotope $\mathcal{D}$.*

Proof. Because of the linearity, $\mathrm{L}(\mathbf{x} + \lambda\mathbf{z}) = \mathrm{L}(\mathbf{x}) + \lambda\mathrm{L}(\mathbf{z})$ for any $\mathbf{x} \in \mathcal{P}$, where $\mathrm{L}(\mathbf{x}) \in \mathrm{L}(\mathcal{P})$ and $\lambda \in \mathbb{R}$. So the Minkowski sum and the affinity are commutative. Applying the affinity L for the Minkowski sum

$$\mathrm{L}(\mathcal{P} \oplus \lambda\mathbf{z}) = \mathrm{L}(\mathcal{P}) \oplus \lambda\mathrm{L}(\mathbf{z}).$$

If $S(\mathbf{z}) = \{\lambda\mathbf{z} | 0 \leq \lambda \leq 1\}$ and $\mathrm{L}(\mathbf{z}) = \mathbf{z}'$, then using the notation $\mathrm{L}(\mathcal{P}) = \mathcal{D}$, $\mathcal{D}$ is a parallelotope for which $\mathrm{L}(\mathcal{P} \oplus S(\mathbf{z})) = \mathcal{D} \oplus S(\mathbf{z}')$. □

It is clear that the parallelotope $\mathcal{D}$ is not necessary a DV cell, but we prove that it is affine image of a DV cell. Consider an $(n-1)$-dimensional hyperplane H orthogonal to $\mathbf{z}'$ which contains the center of the DV cell $\mathcal{D} \oplus S(\mathbf{z}')$. Let $S(\mathbf{z}') = \{\lambda\mathbf{z}' | -\frac{1}{2} \leq \lambda \leq \frac{1}{2}\}$, i.e. let the center of the contracted parallelotope $\mathcal{D}$ coincide with the center of the DV cell $\mathcal{D} \oplus S(\mathbf{z}')$ and let any facet of $\mathrm{Cap}_{\mathbf{z}'}(\mathcal{D})$ be parallel to the according facet of $\mathrm{Cap}_{\mathbf{z}'}(\mathcal{D} \oplus S(\mathbf{z}'))$ for all pairs of facets. So if the facet F is a facet of $\mathrm{Cap}_{\mathbf{z}'}(\mathcal{D})$, then the facet $F + \frac{1}{2}\mathbf{z}'$ or $F - \frac{1}{2}\mathbf{z}'$ is a facet of $\mathrm{Cap}_{\mathbf{z}'}(\mathcal{D} \oplus S(\mathbf{z}'))$, too.

Lemma 4.2. *If $\mathcal{D} \oplus S(\mathbf{z}')$ is a DV cell, then there is an orthogonal affinity M with fixed hyperplane $H \perp \mathbf{z}'$ that $\mathrm{M}(\mathbf{t}) \perp \mathrm{M}(F)$ holds for a facet $F \in \mathrm{Cap}_{\mathbf{z}'}(\mathcal{D})$ and its relevant vector $\mathbf{t}$.*

Proof. Consider the facet $F+\frac{1}{2}\mathbf{z}'$ of $\mathrm{Cap}_{\mathbf{z}'}(\mathcal{D}\oplus S(\mathbf{z}'))$ and let $\mathbf{t}+\mathbf{z}'$ be the relevant vector of this facet $F+\frac{1}{2}\mathbf{z}'$. Let $\mathbf{s}^i$ be a basis of aff $\left(F+\frac{1}{2}\mathbf{z}'\right)$, where $i=1,\ldots,n-1$. In a fixed coordinate system, where $\mathbf{z}' = x\cdot\mathbf{e}_n$ and $H = [\mathbf{e}_1,\ldots\mathbf{e}_{n-1}]$, there are

$$\mathbf{t} = (t_1,\ldots t_{n-1},t_n),\quad \mathbf{t}+\mathbf{z}' = (t_1,\ldots t_{n-1},t_n+x),\quad \mathbf{s}^i = (s^i_1,\ldots s^i_{n-1},s^i_n).$$

Let M be an orthogonal affinity with fixed hyperplane H and $\mathrm{M}(\mathbf{e}_n) = \lambda\cdot\mathbf{e}_n$, where $\lambda^2 = 1+\frac{x}{t_n}$ and $t_n \neq 0$ because of $F \in \mathrm{Cap}_{\mathbf{z}'}(\mathcal{D})$. The parallelotope $\mathcal{D}\oplus S(\mathbf{z}')$ is a DV cell, so $\mathbf{t}+\mathbf{z}' \perp \mathbf{s}^i$, where $i = 1,\ldots,n-1$.

Thus the inner products of $\mathbf{t}$ and $\mathbf{s}^i$ are zero:

$$t_1\cdot s^i_1+\cdots+t_{n-1}\cdot s^i_{n-1}+(t_n+x)\cdot s^i_n = 0.$$

Because of the equality $\lambda^2 = 1+\frac{x}{t_n}$: $(t_n+x)\cdot s^i_n = \lambda^2 t_n\cdot s^i_n$. Using this equality

$$t_1\cdot s^i_1+\cdots+t_{n-1}\cdot s^i_{n-1}+\lambda^2 t_n\cdot s^i_n = 0.$$

If the inner product of two vectors is zero, then the two vectors are orthogonal, so

$$(t_1,\ldots t_{n-1},\lambda t_n) \perp (s^i_1,\ldots s^i_{n-1},\lambda s^i_n).$$

Thus $\mathrm{M}(\mathbf{t}) \perp \mathrm{M}(\mathbf{s}^i)$, where $i = 1,\ldots,n-1$.
Consequently $\mathrm{M}(\mathbf{t}) \perp \mathrm{M}(F)$. So the lemma is proved. □

Lemma 4.3. *If $\mathcal{D}\oplus S(\mathbf{z}')$ is a DV cell,* M *is an orthogonal affinity with fixed hyperplane $H \perp \mathbf{z}'$, $\mathrm{M}(\mathbf{t_1}) \perp \mathrm{M}(F_1)$ holds for a facet $F_1 \in \mathrm{Cap}_{\mathbf{z}'}(\mathcal{D})$ and its relevant vector $\mathbf{t_1}$, and the facets F_1 and F_i have a common belt, then $\mathrm{M}(\mathbf{t_i}) \perp \mathrm{M}(F_i)$ holds where $\mathbf{t_i}$ is the relevant vector of the facet F_i.*

Proof. At first we will prove that all belts cut the shadow boundary in at least $(n-2)$-dimensional face. The shadow boundary of a parallelotope consists of $(n-1)$ or $(n-2)$-dimensional closed faces and divides the parallelotope for two parts $\mathrm{Cap}^+_{\mathbf{z}'}(\mathcal{D})$ and centrally symmetric pair $\mathrm{Cap}^-_{\mathbf{z}'}(\mathcal{D})$ and the sets of the inner points of $\mathrm{Cap}^+_{\mathbf{z}'}(\mathcal{D})$ and $\mathrm{Cap}^-_{\mathbf{z}'}(\mathcal{D})$ are disjoint sets. So the maximal $(n-2)$-dimensional faces of the shadow boundary contain two facets $F_1 \in \mathrm{Cap}^+_{\mathbf{z}'}(\mathcal{D})$, $F_2 \in \mathrm{Cap}^-_{\mathbf{z}'}(\mathcal{D})$. In every belt if $F_1 \in \mathrm{Cap}^+_{\mathbf{z}'}(\mathcal{D})$, then $-F_1 \in \mathrm{Cap}^-_{\mathbf{z}'}(\mathcal{D})$, so a belt containing the facet F_1 has at least one point in the shadow boundary. Let $G \in \mathrm{sh}_{\mathbf{z}'}(\mathcal{D})$ be any maximal dimensional face of a belt. If the face G is a facet, then the statement is true. If G is not a facet, then two facets F_i of the belt contain the face G, where $F_i \notin \mathrm{sh}_{\mathbf{z}'}(\mathcal{D})$ because the face G is a maximal element. So $F_1 \in \mathrm{Cap}^+_{\mathbf{z}'}(\mathcal{D})$, $F_2 \in \mathrm{Cap}^-_{\mathbf{z}'}(\mathcal{D})$. In any belt the intersection $F_1 \cap F_2$ is an $(n-2)$-dimensional face and in this situation it belongs to the shadow boundary, so it is G.

Consider an arbitrary facet $\overline{F} \in \mathrm{sh}_{\mathbf{z}'}(\mathcal{D}\oplus S(\mathbf{z}'))$. This facet $\overline{F}$ is orthogonal to H and H contains the center of the facet $\overline{F}$. The contraction of this facet $\overline{F}$ is an $(n-1)$ or $(n-2)$-dimensional face of the parallelotope $\mathcal{D}$ of which the centers coincide with the center of the facet $\overline{F}$.

I. At first suppose that the contraction of the facet $\overline{F}$ is an $(n-2)$-dimensional face G of the parallelotope $\mathcal{D}$. So $G\oplus S(\mathbf{z}') = \overline{F}$. The face G determines a 4-belt of $\mathcal{D}$ otherwise an 8-belt would be in the DV cell $\mathcal{D}\oplus S(\mathbf{z}')$. The face G belongs to two facets F_1 and F_2 with relevant vectors $\mathbf{t}_1$ and $\mathbf{t}_2$. The relevant vector $\mathbf{t}$ of $\overline{F}$ and

G is equivalent. Evidently, relevant vectors of the facets F_1 and F_2 in the DV cell $\mathcal{D}\oplus S(\mathbf{z}')$ are $\mathbf{t}_1+\mathbf{z}'$ and $\mathbf{t}_2-\mathbf{z}'$, because in the case of a 6-belt $(\mathbf{t}_1+\mathbf{z}')+(\mathbf{t}_2-\mathbf{z}')=\mathbf{t}$, where $\mathbf{t}\in H$. So $\mathbf{t}_1+\mathbf{t}_2=\mathbf{t}$ holds. We prove that $\mathrm{M}(\mathbf{t}_2)\perp \mathrm{M}(F_2)$. Indeed, by the condition $\mathrm{M}(\mathbf{t}_1)\perp \mathrm{M}(F_1)$ and $\mathrm{M}(G)\subset \mathrm{M}(F_1)$, so the face $\mathrm{M}(G)$ is orthogonal to the vector $\mathrm{M}(\mathbf{t}_1)$. $G\subset \overline{F}$ and by the orthogonal affinity $\mathrm{M}(G)\subset \overline{F}$. On the other hand $\mathbf{t}\perp \overline{F}$, so $\mathbf{t}\perp \mathrm{M}(G)$. Consequently $[\mathrm{M}(\mathbf{t}_1),\mathbf{t}]\perp \mathrm{M}(G)$. By the linearity of the affine transformation $\mathrm{M}(\mathbf{t}_1)+\mathrm{M}(\mathbf{t}_2)=\mathrm{M}(\mathbf{t})=\mathbf{t}$, so $\mathrm{M}(\mathbf{t}_2)\perp \mathrm{M}(G)$.

The face G determines a 4-belt and it is centrally symmetric (Á. G. Horváth [8]), so the endpoint of the vector $\frac{\mathbf{t}}{2}$ is the center C of the face G. This center is in the hyperplane H. Because H is fixed hyperplane of the affinity, the center of the face $\mathrm{M}(G)$ is the point C, too. The midpoints of the relevant vectors $\mathbf{t},\mathbf{t}_1,\mathbf{t}_2$ are centers of the according faces. If K denotes the center of the facet $\mathrm{M}(F_1)$ and O denotes the center of the parallelotope $\mathrm{M}(\mathcal{D})$, then $\overrightarrow{OK}+\overrightarrow{KC}=\frac{\mathbf{t}}{2}$ and $\frac{\mathrm{M}(\mathbf{t}_1)}{2}=\overrightarrow{OK}\perp\overrightarrow{KC}$. So $\frac{\mathrm{M}(\mathbf{t}_2)}{2}=\overrightarrow{KC}\perp\frac{\mathrm{M}(\mathbf{t}_1)}{2}=\overrightarrow{K'C}$, where K' is the center of the facet $M(F_2)$. Summing up, $\mathrm{M}(\mathbf{t}_2)\perp \mathrm{M}(G)$ and $\mathrm{M}(\mathbf{t}_2)\perp\overrightarrow{K'C}$, so $\mathrm{M}(\mathbf{t}_2)\perp \mathrm{M}(F_2)$. Consequently, $\mathrm{M}(\mathbf{t}_i)\perp \mathrm{M}(F_i)$ holds in this 4-belt.

II. On the other hand, consider that the contraction of the facet $\overline{F}$ is an $(n-1)$-dimensional face. We will denote this facet by F. So the relevant vector $\mathbf{t}$ of F is orthogonal to the facet F. Study an arbitrary $(n-2)$-dimensional face G of the facet F. This face G determines a 4- or a 6-belt. In a 4 belt, by the condition, $\mathrm{M}(\mathbf{t}_1)\perp \mathrm{M}(F_1)$, where F_1 is a facet containing the face G. Consequently, in this situation $\mathrm{M}(\mathbf{t}_i)\perp \mathrm{M}(F_i)$ holds for every facet of this belt, too.

If the face G determines a 6-belt, then denote by F_1 and F_2 two facets neighboring with F in the 6-belt. The relevant vectors of the facets F_1 and F_2 in the DV cell $\mathcal{D}\oplus S(\mathbf{z}')$ are $\mathbf{t}_1+\mathbf{z}'$ and $\mathbf{t}_2-\mathbf{z}'$. So $(\mathbf{t}_1+\mathbf{z}')+(\mathbf{t}_2-\mathbf{z}')=\mathbf{t}$, where $\mathbf{t}\in H$. Thus $\mathbf{t}_1+\mathbf{t}_2=\mathbf{t}$ holds. By the condition $\mathrm{M}(\mathbf{t}_1)\perp \mathrm{M}(F_1)$. By the linearity of the affinity $\mathrm{M}(\mathbf{t}_1)+\mathrm{M}(\mathbf{t}_2)=\mathrm{M}(\mathbf{t})=\mathbf{t}$, so the relevant vectors $\mathbf{t}$, $\mathrm{M}(\mathbf{t}_1)$, $\mathrm{M}(\mathbf{t}_2)$ are in a 2-dimensional plane, which is orthogonal to the face $\mathrm{M}(G)$, because $\mathbf{t}\perp \mathrm{M}(F)$ and $\mathrm{M}(\mathbf{t}_1)\perp \mathrm{M}(F_1)$, so the intersection $\mathrm{M}(G)=\mathrm{M}(F)\cap \mathrm{M}(F_1)$ is orthogonal to the vectors $\mathbf{t}$ and $\mathrm{M}(\mathbf{t}_1)$. The projection of the parallelotope $\mathrm{M}(\mathcal{D})$ to the 2-dimensional plane in the direction $\mathrm{M}(G)$ is a centrally symmetric hexagon, in which the relevant vectors $\mathbf{t}$ and $\mathrm{M}(\mathbf{t}_1)$ are perpendicular bisectors of according edges of the hexagon. The circumcenter of a triangle is determined by two perpendicular bisectors, so $\mathrm{M}(\mathbf{t}_2)$ is perpendicular bisector of the third edge of the hexagon. On the other hand, $\mathrm{M}(\mathbf{t}_2)\perp \mathrm{M}(G)$, so $\mathrm{M}(\mathbf{t}_2)\perp \mathrm{M}(F_2)$.

Consequently, if in any 4-belt an arbitrary facet is orthogonal to its relevant vector, then for other facets of this belt the orthogonality holds, too. In a 6-belt some facet of the shadow boundary belongs to the 6-belt (otherwise 8-belt would be in $\mathcal{D}\oplus S(\mathbf{z}')$) so by the above if two facets are orthogonal to their relevant vectors then for other facets of this 6-belt the orthogonality holds, too. □

Lemma 4.4. *If $\mathcal{D}\oplus S(\mathbf{z}')$ is a DV cell, then there is an orthogonal affinity* M *that the parallelotope* $\mathrm{M}(\mathcal{D})$ *is a DV cell.*

Proof. Consider any coherent pairs of the facets of $\mathcal{D}$ and $\mathcal{D} \oplus S(\mathbf{z}')$. By lemma 4.2 there exists an orthogonal affinity M that $\mathrm{M}(\mathbf{t_1}) \perp \mathrm{M}(F_1)$ holds for a facet $F_1 \in \mathrm{Cap}_{\mathbf{z}'}(\mathcal{D})$ and its relevant vector $\mathbf{t_1}$. By lemma 4.3 in each belt containing this facet F_1 each facet is orthogonal to their relevant vectors. The surface of the parallelotope $\mathrm{M}(\mathcal{D})$ is facet-connected, i.e. to arbitrary two facets there is finite sequence of the facets, where the intersection of two adjacent facets is an $(n-2)$-dimensional face. So the orthogonality come down to every facet and their relevant vectors. Consequently, the parallelotope $\mathrm{M}(\mathcal{D})$ is a DV cell. □

First and last we proved the following theorem:

Theorem 4.5. *If the parallelotope $\mathcal{P} \oplus S(\mathbf{z})$ is the affine image of a DV cell $\mathcal{D} \oplus S(\mathbf{z}')$ then the parallelotope $\mathcal{P}$ is the affine image of a DV cell $\mathrm{M}(\mathcal{D})$, too.*

References

[1] Deza M., Grishukhin V., *Properties of parallelotopes equivalent to Voronoi's conjecture*, European Journal of Combinatorics, Vol. **25**, (2004), 517–533.

[2] Dirichlet G. L., *Über die Reduktion der positiven Quadratischen Formen mit drei unbestimmten ganzen Zahlen*, J. Reine und Angew. Math., Vol. **40**, (1850), 209–227.

[3] Dolbilin N. P., *Properties of Faces of Parallelohedra*, Tr Mat. Inst. Steklova, Vol. **266**, (2009), 112–126.

[4] Dutour M., Grishukhin V., Magazinov A., *On the sum of a parallelotope and a zonotope*, European Journal of Combinatorics, Vol. **42**, (2014), 49–73.

[5] Erdhal R. M., *Zonotopes, dicings and Voronoi's conjecture on parllelohedra*, European Journal of Combinatorics, **20**, (1999), 527–549.

[6] Grishukhin V. P., *Parallelotopes of non-zero width*, Sb. Math., (2004), 195 (**5**), 669–686.

[7] Grishukhin V. P. *Free and Nonfree Voronoi Polyhedra* (Russian), Matematicheskie Zametki **80**, (2006), 367–378, translated in Math. Notes **80**, (2006), 355–365.

[8] Horváth Á. G., *On the boundary of an extremal body*, Beiträge zur Algebra und Geometrie, Vol. **40**, No. 2., (1999), 331–342.

[9] Horváth Á. G., *On the connection between the projection and the extension of a parallelotope*, Monatsh. Math., **150**, (2007), 211–216.

[10] Martini H., *Shadow-boundaries of convex bodies*, Discrete Math., **155**, (1996), 161–172.

[11] McMullen P., *Space tiling zonotopes*, Mathematica, **22**, (1975), 202–211.

[12] McMullen P., *Convex bodies which tile space by translation*, Mathematica, **27**, (1980), 113–121.

[13] Magazinov A., *Voronoi's conjecture for extensions of Voronoi parallelohedra*, arXiv:1308.6225v2.

[14] Ordine A., *Proof of the Voronoi conjecture on parallelotopes in a new special case*, Ph.D. Thesis, Queen's University, Ontario, 2005.

[15] Venkov B. A., *On a class of Euclidean polytopes* (Russian), Vestnik Leningradskogo Univ., **9**, (1954), 11–31.

[16] Venkov B. A., *On projecting of parallelohedra* (Russian), Mat. Sbornik, **49**, (1959), 207–224.

[17] Voronoi G. F., *Nouvelles applications des parametres continus a la theorie des formes quadratiques*, J. Reine und Angew. Math., Vol. **134**, (1908), 198–287.

[18] Voronoi G. F., *Nouvelles applications des parametres continus a la theorie des formes quadratiques II.*, J. Reine und Angew. Math., Vol. **136**, (1909), 67–181.

[19] Zhitomirskii O. K., *Verschärfung eines Satzes von Voronoi*, Zhurnal Leningradskogo Math. Obschtchestva, **2**, (1929), 131–151.

Attila Végh, Department of Mathematics, Kecskemét College, H-6000 Kecskemét, Hungary,
E-mail address: `vegh.attila@gamf.kefo.hu`,

Studies of the University of Žilina
Mathematical Series
Vol. 27/2015, 87–96

HOW TO MAKE GEOMETRY MORE ACCESSIBLE TO STUDENTS

M. VOJTEKOVÁ, D. STACHOVÁ and V. ČMELKOVÁ

Abstract. Geometry is one of the oldest scientific disciplines. What exactly is its place in technical education in Slovakia today? The aim of this paper is to briefly review teaching of descriptive geometry at the University of Žilina and to describe our experience with the use of the GeoGebra system in classes to facilitate teaching of geometry, to make classes more engaging and lively, and to increase imagination and spatial orientation. In doing so, we compare traditional and modern teaching methods and tools, and dicuss their advantages and potential pitfalls.

Introduction

"Let no one ignorant of geometry enter." According to tradition, this phrase was engraved at the door of Plato's Academy, the school he established in Athens. What is the position of geometry in technical education today? Is geometry unnecessary for engineers? Should we get rid of geometry because it is too difficult for students? Can computer graphical programmes substitute geometrical thinking? There are many technical programmes at universities where geometry has been significantly reduced or completely removed in recent years and the future seems even worse. What can we, geometry teachers, do to improve the situation? How can we make geometry more engaging for students? In this paper, we try to answer some of these question.

1. History of teaching of geometry at the University of Žilina

University of Žilina in Žilina was originally founded as Railway University in Prague by separating from the Czech Technical University in Prague. After relocating to Žilina as the University of Transport (VŠD), the university consisted of three faculties – Faculty of Operations and Economics of Transport (PED), Faculty of Mechanical and Electrical Engineering (SET), and Faculty of Military (VF). Faculty PED expanded teaching in technical, economical, and telecommunications programmes and was thus renamed in 1997 to Faculty of Operations and Economics of Transport and Communications (FPEDAS).

Received December 22, 2014.
2000 *Mathematics Subject Classification.* Primary 97G80.
Key words and phrases. Descriptive geometry, GeoGebra, Teaching.
Supported by Visegrad Fund small grant 11420082.

Descriptive geometry was part of the core curriculum from the inception of the university. In the 1960s, descriptive geometry was taught at the Faculty of Electrical Engineering as a one-semester course in the extent 4–4, i.e. 4 lectures and 4 tutorials weekly, later as 3–3. At the Faculty of Civil Engineering, descriptive geometry classes spanned 5 semesters of full-time and 4 semesters of part-time studies. Students from this era took altogether between 171 and 226 hours of descriptive geometry in the form of lectures and tutorials.

In the 1970s, the total number of hours was reduced to between 80 and 180, and the course spanned at most 3 semesters. Later in 1980s, the extent was further reduced when the 3-semester form of the course was taught only in Civil Engineering part-time programmes, whereas in the Electrical Engineering programmes the course was removed altogether, and in other programmes the course was taught as 2–2 or 1–2 which reduced the total number of hours further to between 60 and 90.

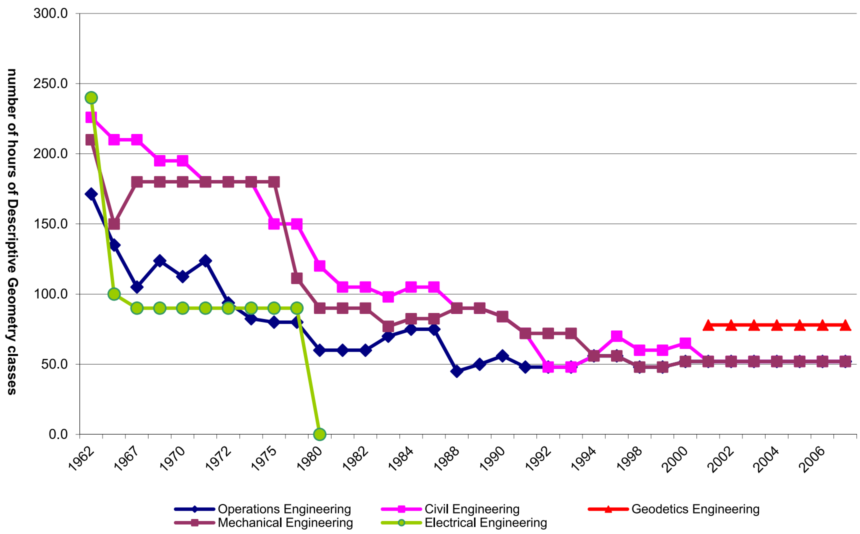

Figure 1. The annual number of hours of classes of descriptive geometry taught at the current faculties of the University of Žilina. Source: archives of the University of Žilina.

In the 1990, the university finished establishing all of the current faculties, however descriptive (resp. constructive, or engineering) geometry was taught only at four of them (Civil, Mechanical, PEDAS, and Faculty of Special Engineering). Even at present, descriptive (constructive, engineering) geometry is taught only at these faculties and constructive geometry is taught at the Faculty of Humanities in general education programmes in combination with mathematics. In the 1990s, the total extent of the course was between 48 and 84 hours which in most cases was taught in one semester (two semesters only at the Faculty of Mechanical Engineering in full-time programmes). Since 2000, the extent has been 52 hours (1 semester) with the exception of Geodetics Engineering where it is 78 hours (2 semesters).

Opinions regarding the form of grading also changed over the years. While until 1980 the course was graded based on a final examination, possibly including tutorial grades. At present, the course is more increasingly graded only based on tutorials. This change diminished the importance of the course in the curriculum, and more importantly, it reduced the engagement and preparation of students for the classes. The situation has been further exacerbated by the fact that the course has over the years been some times mandatory, and other times optional (in particular, in Civil Engineering programmes) and in many programmes the course was cancelled altogether.

The space which descriptive geometry used to occupy in the curriculum was naturally overtaken by courses focusing on applying the newly developping information technologies. Initially technical drawing was added to geometry, later the two subjects were taught separately, but the original content of the course was not retained. Later (after 1990) new courses were developped such as Computer-aided construction, Technical writing, Engineering simulation using MATLAB, CAD I. and CAD II. systems, Computer-aided construction projects, Computer graphics, Computer geometry, and courses on Geographical Information Systems, which are taught in selected programmes. Most of the programmes, however, do not teach pure geometry.

A detailed summary of course hours obtained from archives of the University of Žilina are shown in Fig. 1. The chart incorporates data from all available course listings published in "Študijné programy a informácie" since 1962 until present.

2. Methods and tools used in teaching geometry

For many years the main tools used in teaching descriptive geometry were chalk and blackboard. The teacher used a compass, ruler, and sharp chalk to draft constructions on a blackboard. Lectures and tutorials were physically challenging for the teacher. When grading homeworks and student projects the graphical aspect of the work was paramount. A mature graphical ability was expected from students both on a paper and on a blackboard. This made descriptive geometry difficult for many students, and it was a common practice to have the homeworks made by professional drafters (civil or mechanical engineers) for money, in order to get a good grade. Sometimes such formalities overshadowed the content. On the positive side, the use of spatial models in teaching (projections of lines, planes, spatial bodies in Monge's projection, surface maps, etc.) helped students develop spatial orientation.

The 1980s meant a change in teaching practice when the use of overhead projectors became commonplace. The teacher could prepare drafts on a transparency ahead of time which were then presented to students via the projector, and the blackboard was only used to explain particular steps. The projector, however, was often not functional, transparencies were poorly made, and markers commonly dry. If the teacher used only transparencies, students could do no more than literarly transcribe the content of transparencies (without having time to understand them), since the teacher would generally go faster through the material as it was no longer necessary to draft on the blackboard alongside the students. Many of, mostly older, geometry teachers would stick with the tried-and-tested method of blackboard and chalk. The use of transparencies and projectors however meant that the teacher was able to present several solutions to the same problem and discuss different possible approaches, since the material could be prepared ahead of time and reused across different course offerings.

The "age of computer" also affected teaching of descriptive geometry. Handmade transparencies were first substituted by computer text and illustrations prepared using simple graphical software. Many teachers of geometry made their own drawing programmes on first personal computers. At the University of Transport and Communications Jozef Kateřiňák pioneered this approach, and already in the 1970 used an HP computer for solving problems from descriptive geometry. Later, Václav Medek and Jozef Zámožík [5] made further developments and in 1991 published a book "Osobný počítač a geometria" (Personal computer and geometry), which demonstrated solutions of geometric problems on a personal computer (PMD, ZX-Spectrum, and PC-type 16-bit computers). The use of personal computers and plotters for teaching in the 1990 at the University of Transport and Communications is connected with the name Jaroslav Husarčík, who, among other things, designed an algorithm to plot a curve given by an implicit equation [4]. The algorithm was at the time more efficient than any then-available mathematical software. He further wrote customisable drawing software accompanied by libraries for drawing planar curves, spatial curves, and surfaces (Fig. 2).

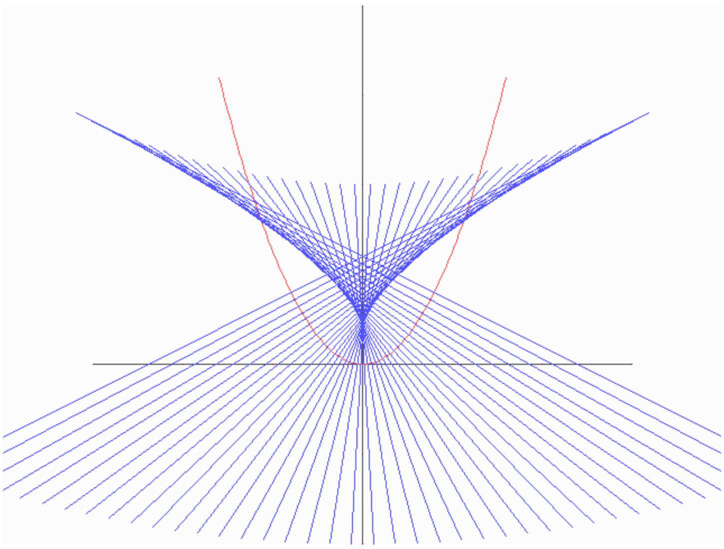

Figure 2. Evolute of parabola as the envelope of parabola normals.

The increased use of computers in classrooms and the availability of laptop computers used by students leads us to the next stage of development of teaching tools for descriptive geometry. Today's generation of students grew up using computers (via computer games). It is thus natural to use computers for teaching; for us this means namely PowerPoint slides and GeoGebra applets (which we discuss below).

3. Geogebra

GeoGebra is an interactive geometry, algebra, statistics and calculus application, aimed to facilitate learning and teaching mathematics and sciences for students of all levels (from primary school to university). Its creator, Markus Hohenwarter, started the project in 2001 at the University of Salzburg, continuing it at Florida Atlantic University (2006–2008), Florida State University (2008–2009), and now at the University of Linz together with the help of a small group of assistants and open-source developers and translators all around the world.

GeoGebra is a freely distributable general-purpose mathematical software that can be utilized in many fields of mathematics education. It is currently available in more than 50 languages and offers a very user-friendly interface. The programme was originally designed to be used for solving Euclidean geometry problems. It allows, for instance, drawing basic geometric objects: points, segments, rays, lines, and other objects such as a midpoints of segments, axes of segments, intersections of objects, lines perpendicular or parallel to other lines. There are tools to construct angles, regular polygons, circles, conics and to use various transformations (rotations, translations, axial symmetries, etc.) and to measure object areas and distances. GeoGebra later expanded into other fields of mathematics including mathematical analysis, algebra, statistics, tabular calculations (e.g. analysis of graphs of functions, probabilistic calculations, linear regression, etc.). All geometrical objects represented in GeoGebra can be expressed analytically as algebraic formulae. The system supports adding text labels and annotations using TeX-like scripting language (without the need of installing the TeX system). Another useful feature of the programme is the ability to produce animations. The programme also allows enriching the drawing plane with scrollbars, buttons, checkboxes and text areas. Another advantage of GeoGebra is the possibility to export the constructions (as PDF, Postscipt, or bitmap files), and the possibility to produce applets in an HTML format so that students can use them without having to install GeoGebra. The HTML applets can be uploaded to the GeoGebra Tube website and are freely available to anyone. Beginner users can acquaint themselves with the program in its installation-free online version GeoGebra Start.

4. How to use Geogebra in the teaching process

GeoGebra is for a teacher a useful tool for producing complex drawings for use in classrooms. What we, the teachers of descriptive geometry, appreciate most about GeoGebra is its dynamic nature; the possibility to create and then repeat the construction step by step. It is convenient to have the option of hiding auxiliary

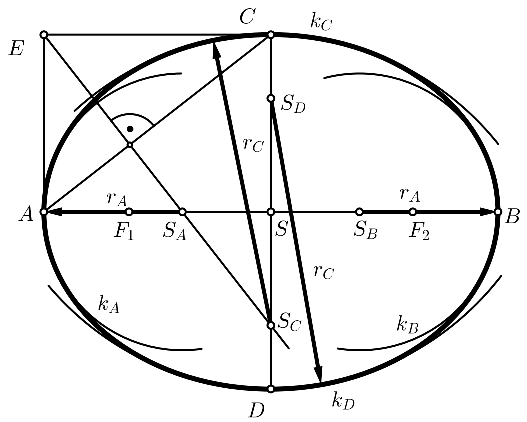

Figure 3. Construction of osculating circles of ellipse.

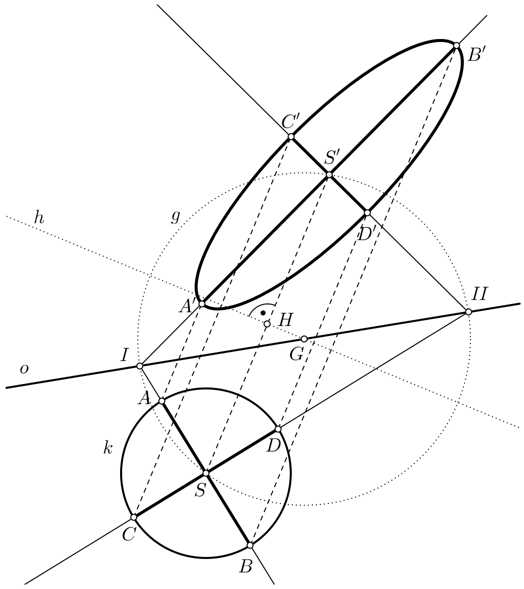

Figure 4. Circle and its image in the axial affinity.

lines, the possibility to pause the dynamic applets at any point, to move frame-by-frame back and forward as needed. This is useful not only in a lecture but also for students working at home without teacher's presence. Students can follow the construction on a computer and with its help do their homework. Students can use the GeoGebra Tube webpage to find elementary constructions that are needed (e.g. constructions of polygons, axial symmetry, etc.). Students are furthermore given the option to explore the examples by modifying the objects displayed in the drawing plane and thus acquire a better understanding of the given topic.

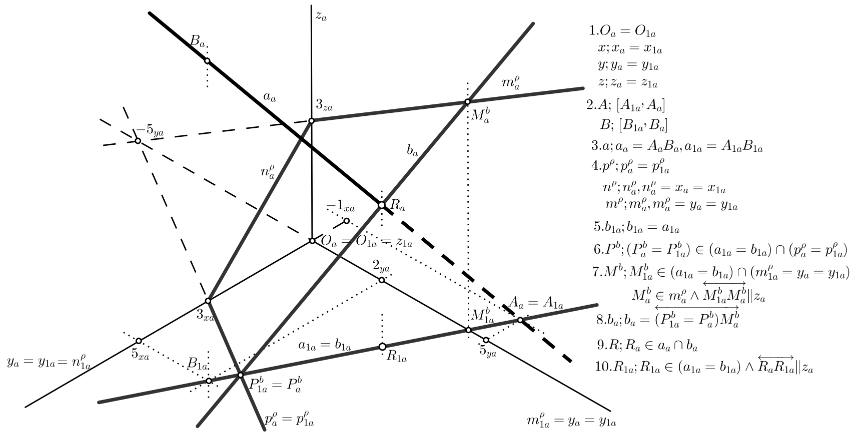

Figure 5. Axonometric view of the intersection of a line and a plane.

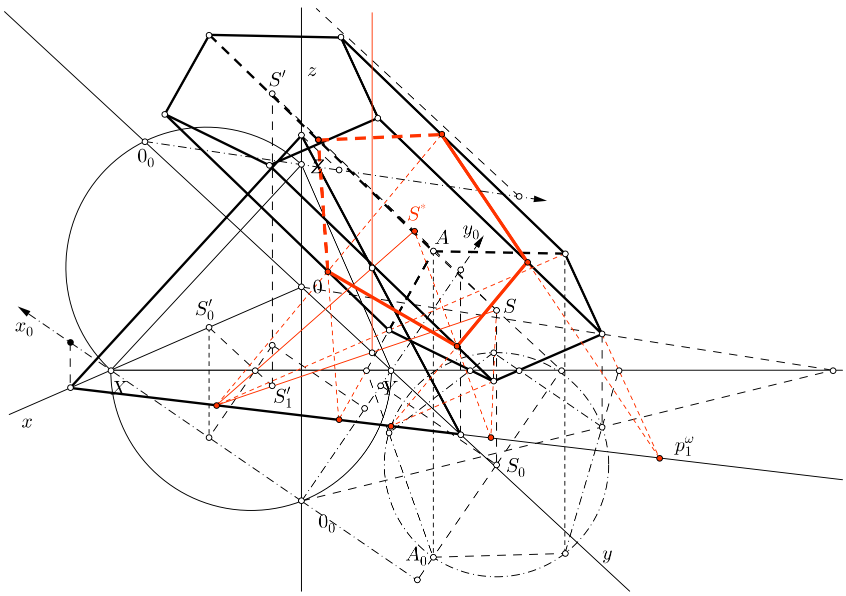

Figure 6. Orthogonal axonometric view of the plane section of a pentagonal prism.

For our course, we have developped a number of applets for students to help them better understand the principles of planar and spatial transformations, applets producing basic constructions of conics: ellipse (Fig. 3), hyperbola and parabola, applets constructing objects in axial affinity (Fig. 4) and collineation, and applets constructing objects using the Monge mapping method and the orthogonal axonometry method (Fig. 5 and Fig. 6, respectively).

GeoGebra also plays an important role in teaching point symmetries in cartography (Fig. 8), since it allows to depict complex constructions neatly by splitting the construction into simpler steps which greatly increases understanding.

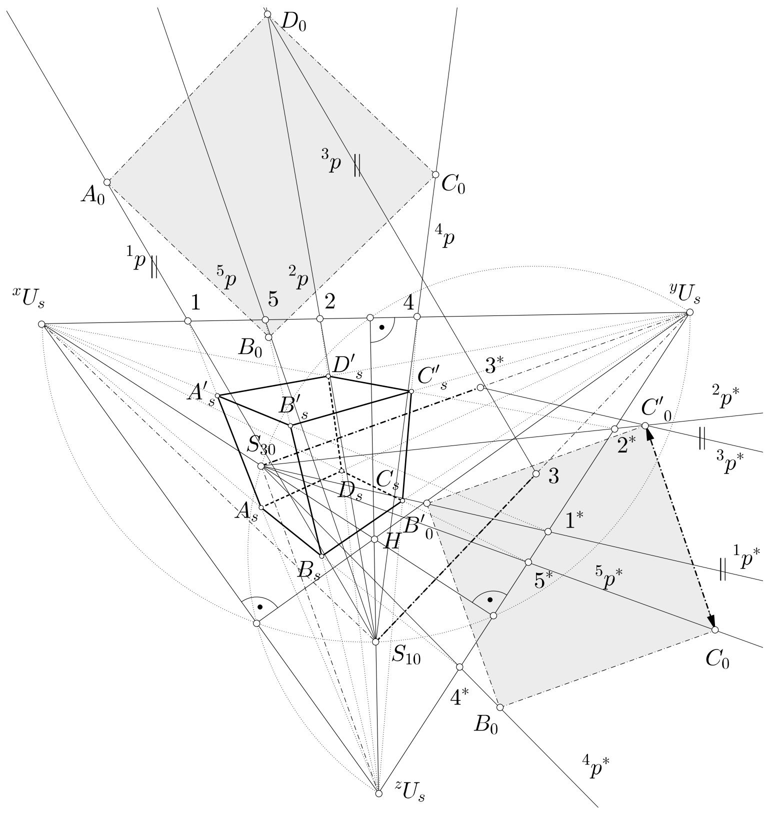

Figure 7. Reconstruction of rotated top- and side-views of an image of a box.

Among students with difficulties in learning geometry there are sometimes those who have interest in geometry while also wanting to create something new, not only do the homework. Fig. 9 shows a work of such a student – using the Method of intersection to create an axonometric view of an object formed from two orthographic projections of the object.

5. Conclusion

The goal of this article was to describe the history and the present state of teaching of descriptive geometry at the University of Žilina. We believe that geometry has

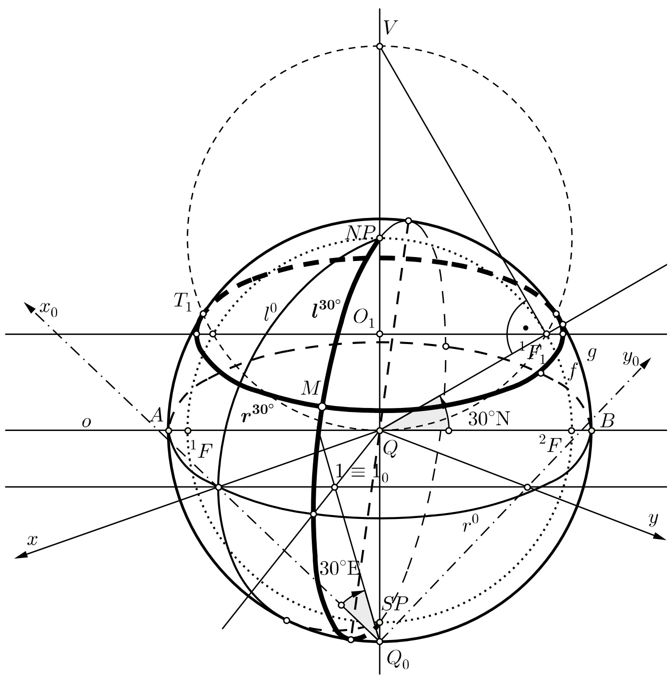

Figure 8. Cartographic projection of a point on a sphere with coordinates 30°N 30°E.

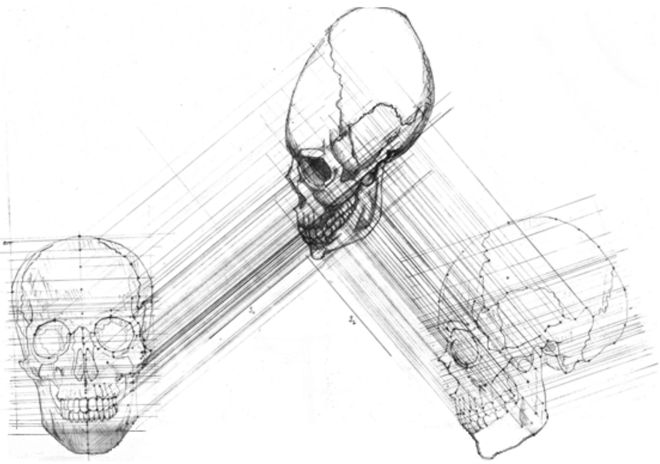

Figure 9. Axonometric view of the skull..

its place in technical education and there are means to modernize its teaching such as the use of the GeoGebra system. GeoGebra applets can be used to facilitate the teaching process as well as assist students in self-study. Its dynamic nature, accuracy and clarity of presentation are its key useful features. Students appreciate availability, repeatability and comprehensibility of GeoGebra constructions and consider them very useful. But we must be careful not to completely replace geometrical thinking with these modern tools. Methods of visualization are interesting for students, they improve imagination, but there is always the danger that learning geometry gets reduced to “watching movies”. It is a task for the teacher to find appropriate forms of use of computer drawings tools in teaching in order to enrich the teaching process but leave room for imagination.

References

[1] Čmelková V., *The aid of GeoGebra to teach and learn descriptive geometry at the Faculty of Operation and Economics of Transport and Communications at the University of Žilina in Žilina, Slovakia*, In: Proceedings of the 16th International Conference on Geometry and Graphics, Universität Innsbruck, Innsbruck University Press, 2014, pp. 18–24.

[2] Čmelková V., *Cvičenia z geometrie*, Žilina, University of Žilina, 2008.

[3] Čmelková V., *GeoGebra a LaTeX v podpore výučby geometrie na Fakulte prevádzky a ekonomiky dopravy a spojov Žilinskej univerzity v Žiline*, In: Zborník sympózia o počítačovej geometrii SCG'2013, Bratislava, Slovak Technical University, 2013, pp. 50–56.

[4] Husarčík J., *Algorithm for Computer-aided Drawing the Curve* $F(x, y) = 0$. In: Proceedings of Seminars on Computational Geometry, 1991/1992, MtF STU Trnava, SjF STU Bratislava.

[5] Kateřiňák J., *Úlohy z deskriptívnej geometrie s použitím počítačovej techniky*, VŠD Žilina, Alfa Bratislava, 1978.

[6] Stachová D., *Dejiny a perspektívy vyučovania deskriptívnej geometrie na ŽU v Žiline*, In: Zborník príspevkov z konferencie Deskriptívna geometria na Slovensku včera a dnes, Žilina, FPEDAS, University of Žilina in Žilina, 2014, pp. 50–60.

[7] Stachová D., *Metódy zobrazovania* (1. ed.), Žilina, University of Žilina, 2014.

[8] GeoGebra, *About GeoGebra*, Info, `http://www.geogebra.org/cms/sk/info` (October 2th, 2014).

M. Vojteková, Univerzitná 1, 010 26 Žilina, Slovakia,
E-mail address: `maria.vojtekova@fpedas.uniza.sk`

D. Stachová, Univerzitná 1, 010 26 Žilina, Slovakia,
E-mail address: `darina.stachova@fhv.uniza.sk`

V. Čmelková, Univerzitná 1, 010 26 Žilina, Slovakia,
E-mail address: `viera.cmelkova@fpedas.uniza.sk`

Manuscript submission

Volumes of our journal are prepared using LaTeX format of TeX. Authors are encouraged to use the following preamble in the LaTeX source file

```
\documentclass[twoside]{univzil}
\usepackage[english]{babel}
            %% use english and your language respectively
\usepackage[T1]{fontenc}
\usepackage[utf8]{inputenc} %% use only UTF-8 encoding
\usepackage{amsmath}
\usepackage{amscd,amssymb,amsfonts}
\usepackage{graphicx}       %% for include pictures *.jpg.*.png, *.pdf
\usepackage[pdftex,unicode,bookmarks=false]{hyperref}
            %% for e-mail and url adress
```

Figures in articles should be prepared either with the TeX package or included as `.jpg` files (recommended), `.png` or `.pdf` files. To insert printing files (recommended) use the following commands

```
\begin{figure}[ht]
\includegraphics[width=3.5cm]{pict01.jpg}
\caption{Example 2}      \label{picture2}
\end{figure}
```

Do not use nonstandard fonts. If nonstandard macros or styles are used, corresponding style files must be enclosed.
See file `sample.tex` for example. You can find all files (`univzil.sty`, `amsmath.sty`, `amssymb.sty`, ..., `graphicx.sty` and `sample.tex`) at

`http://fpedas.uniza.sk` or `http://frcatel.fri.uniza.sk/studies`.

To submit a paper, a diskette or CD containing a LaTeX2e source text with corresponding PDF or PS file should be addressed to any member of the editorial board Submitting by e-mail is also acceptable. A short abstract summarizing the article, the AMS Mathematical Subject Classification 2000 (`http://www.ams.org/msc`), a list of key words and phrases, references, and the address of the author (e-mail address as well) should be included in the article. All papers will be refereed.
In special cases we can accept a paper without in non-electronic form. However, in such cases retyping of the article could significantly delay its publication.
The author will obtain 30 offprints of this article. Annual subscription rate: 8 €.
Bank: Všeobecná úverová banka, a.s., Mlynské Nivy 1, 829 90 Bratislava 25. Swift code of bank: `SUBA␣SK␣BX`, bank account: `7034-28529-432`, sort code: `0200`.
Subscription inquiries should be sent to: `Studies Žilina-Mathematical series`, `University of Žilina`, `Univerzitná 1, 010 26 Žilina`, `Slovakia`.

CONTENTS

Visegrad Fund
www.visegradfund.org

Studies of the University of Žilina • Mathematical series
Faculty of Operation and Economics of Transport and Communications, University of Žilina,
Univerzitná 1, 010 26 Žilina, Slovakia
phone: +42141 5133250, fax: +42141 5651499, e-mail: studies@fpedas.uniza.sk,
electronic edition: `http://fpedas.uniza.sk` or `http://frcatel.fri.uniza.sk/studies`
Typeset using LaTeX2e, Printed by: EDIS – Žilina University publisher

ISSN 1336–149X